uOttawa

L'Université canadienne
Canada's university

FACULTÉ DES ÉTUDES SUPÉRIEURES ET POSTOCTORALES

uOttawa

L'Université canadienne
Canada's university

FACULTY OF GRADUATE AND POSDOCTORAL STUDIES

Andrew Hoang Ha
AUTEUR DE LA THÈSE / AUTHOR OF THESIS

M.Sc. (Biochemistry)
GRADE / DEGREE

Department of Biochemistry, Microbiology and Immunology
FACULTÉ, ÉCOLE, DÉPARTEMENT / FACULTY, SCHOOL, DEPARTMENT

Wnt/β-Catenin Signaling in Development of the Ciliary Margin in the Muring Eye
TITRE DE LA THÈSE / TITLE OF THESIS

Valerie Wallace
DIRECTEUR (DIRECTRICE) DE LA THÈSE / THESIS SUPERVISOR

CO-DIRECTEUR (CO-DIRECTRICE) DE LA THÈSE / THESIS CO-SUPERVISOR

Robin Parks

Catherine Tsilfidis

Gary W. Slater
Le Doyen de la Faculté des études supérieures et postdoctorales / Dean of the Faculty of Graduate and Postdoctoral Studies

Wnt/β-catenin Signaling in Development of the Ciliary Margin in the Murine Eye

By
Andrew Ha

Thesis submitted to the
Faculty of Graduate and Postdoctoral Studies
In partial fulfillment of the requirements
For the degree of M.Sc.

Department of Biochemistry, Microbiology and Immunology
Human and Molecular Genetics
Faculty of Medicine
University of Ottawa

Your file Votre référence
ISBN: 978-0-494-73833-7
Our file Notre référence
ISBN: 978-0-494-73833-7

ABSTRACT

The ciliary body (CB) of the vertebrate eye is located in the peripheral region of the retina and is involved in lens accommodation and production of aqueous humor. The CB develops from the ciliary margin (CM) where non-neural epithelial tissue differentiates from the neural ectoderm during embryonic development. The CM/CB represents an interesting area of study since the pigmented layer of the CM is reported to accommodate a pool of adult retinal stem cells. In fish and amphibians, these stem cells facilitate retinal growth and replenishment although this has yet to be observed in the mammalian retina. Previous studies have reported that the canonical Wnt signaling pathway has a role in development of the CM. Activation of this pathway both *in vitro* and *in vivo* resulted in an increase of CM markers at the expense of neural retinal markers and also resulted in an inhibition of neurogenesis in the retina. In this study, I show a preliminary screen of genes that play a role in Wnt mediated development of the CM. Using microarray analysis, quantitative real-time PCR, and *in situ* hybridization, I have identified candidate Wnt target genes in addition to known effectors of Wnt signaling in CM development. Additionally, I have begun a preliminary investigation to elucidate the role of the CM marker, *Msx1,* as a potential Wnt effector in CM development by showing that expression of this gene results in the downregulation of several bHLH transcription factors that are required for retinal neurogenesis. These findings provide some insights in how CM development is regulated by effectors of Wnt signaling.

ACKNOWLEDGEMENTS

I would first like to thank my supervisor, Dr. Valerie Wallace for providing me the opportunity to pursue my graduate studies in her lab. I am grateful for her guidance, encouragement and enthusiasm for my project and the pursuit of knowledge. Thanks are also extended to my committee members, Drs. Alan Mears and Lynn Megeney for providing me with advice and suggestions. I would also like to thank Dr. Carolina Perez-Iratxeta for collaborations. Sincere gratitude is also owed to past and current members of the Wallace lab including Chantal, Brian, Dana, Shawn, Matt, Randy, Charles, Sherry, Yaping as well as summer and honours students for making the lab a positive and always eventful environment to work in. Finally, I would like to sincerely thank my friends and family for their never-ending support in obtaining my Masters degree.

TABLE OF CONTENTS

Page

LIST OF ABBREVIATIONS

APC	adenomatous polyposis coli
BMP	bone morphogenic protein
BrdU	Bromodeoxyuridine
CaMKII	calcium/calmodulin dependent protein kinase II
CDRD	context-dependent regulatory domain
CNS	central nervous system
CB	ciliary body
CM	ciliary margin
CMZ	ciliary marginal zone
CRD	cysteine-rich domain
FEVR	familial exudative vitreoretinopathy
GSK	glycogen synthesis kinase
HMG	high mobility group
IHC	immunohistochemistry
INL	inner nuclear layer
IPE	iris pigmented epithelium
ISH	in situ hybridization
JNK	Jun amino (N)-terminal kinase
LDL	low-density lipoprotein
LEF	lymphoid enhancer-binding factor
LRP	low-density lipoprotein receptor-related protein
NDP	Norrie disease protein
nPCE	non-pigmented ciliary epithelium
NR	neural retina
ONL	outer nuclear layer
PCE	pigmented ciliary epithelium
PCP	planar cell polarity
PKC	protein kinase C

RGC	retinal ganglion cell
RPC	retinal precursor cell
RPE	retinal pigmented epithelium
RSC	retinal stem cells
Q-PCR	quantitative polymerase chain reaction
TCF	T-cell specific transcription factor

LIST OF FIGURES

Page

LIST OF TABLES

1.0 Introduction

The development of the central nervous system (CNS) from immature neuroepithelial cells is regulated by a number of cellular processes. These processes include patterning of the CNS, where distinct anatomical and functional regions are defined, determination of cell fate and number in a developing structure and establishment of the complex net of neuronal connections of the CNS. The vertebrate retina serves as an excellent model in which to study these cellular processes with advantages that include easy accessibility for manipulation, as well as containing a small number of well-characterized neuronal subtypes.

1.1 Ocular Development

1.1.1 Early Eye Development

Retinal development in the mouse begins in early embryogenesis and extends into the postnatal period (reviewed by Smith, 2002). Formation of the optic cup begins at approximately embryonic day 8 (E8) (Fig. 1). At this stage, the optic vesicles appear as evaginations of neuroepithelial tissue from the diencephalon and maintain contact with the brain via the optic stalks (Smith, 2002). By E9-E10, the optic vesicles contact the surface ectoderm, at which point the ectoderm and vesicle layers thicken. This thickening of tissue on the lateral wall of the optic vesicle forms the presumptive neural retina and the surface ectoderm gives rise to the lens placode (Pei and Rhodin, 1970). At this point the development of a number of eye structures occurs simultaneously (Smith, 2002). Upon contact with the surface ectoderm at E10, the optic vesicle begins to invaginate, leading to formation of the optic cup. The inner and outer neuroepithelial layers of the optic cup

Figure 1. Eye morphogenesis. The optic vesicle is formed by the evagination of the forebrain. It grows laterally to make contact with the head ectoderm, and induces the formation of the lens placode. Through invagination, the lens placode forms the lens, while the optic vesicle forms the optic cup. As the optic cup differentiates, the inner layer forms the retina, and the outer layer forms the retinal pigmented epithelium. Figure used with copyright permission from (McNeill et al., 2007)

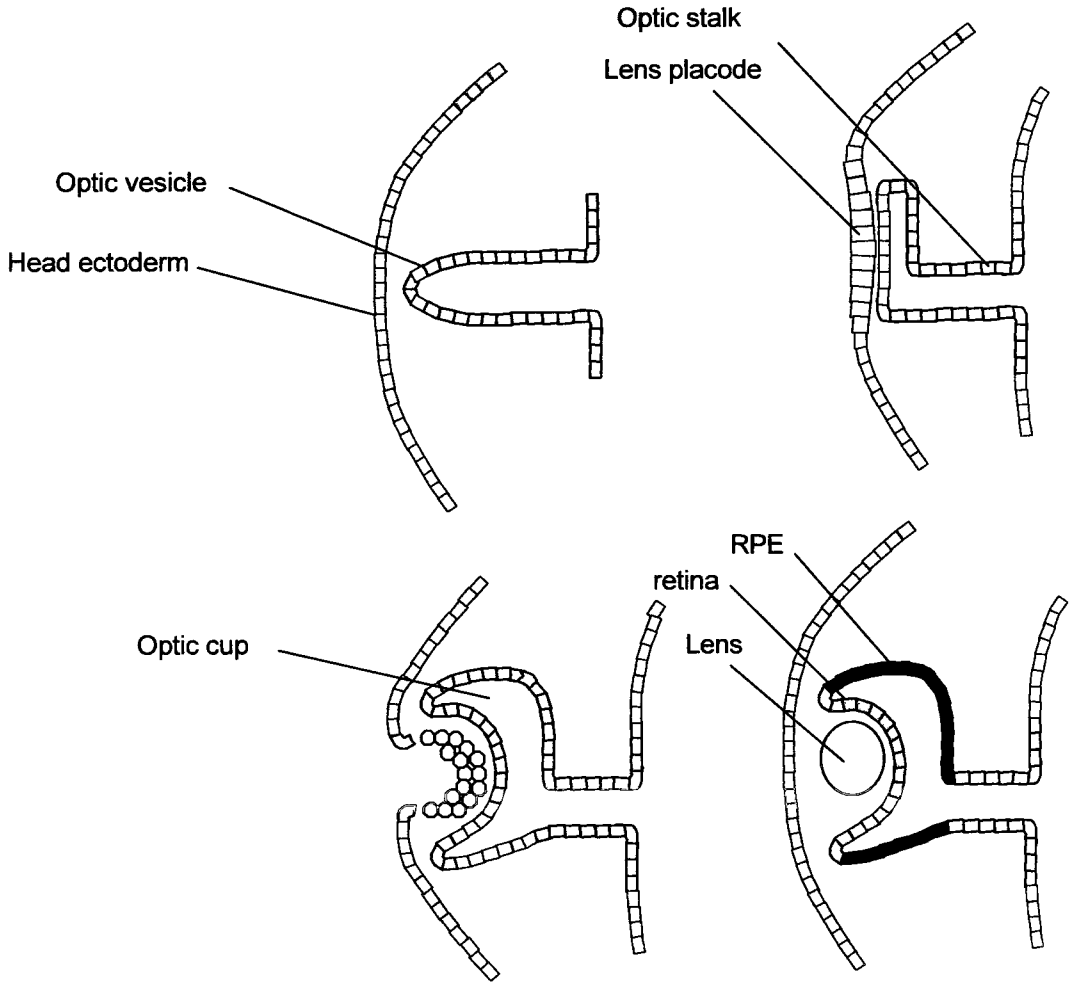
Optic stalk
Lens placode
Optic vesicle
Head ectoderm
RPE
retina
Optic cup
Lens

develop into distinct structures; the outer layer forms the retinal pigment epithelium (RPE) and the inner layer develops into the neural retina (Smith, 2002). The lens placode invaginates, first forming the lens pit and then the lens vesicle, which pinches off from the surface ectoderm by E11 (Smith, 2002). The hollow lens vesicle becomes filled with the growth of lens fibers in a posterior-anterior direction from the lens epithelium. The optic stalk, which connects the developing optic cup to the brain, remains open, and is invaded by E12 with hyaloid arteries and axons of retinal ganglion cells (RGC) to form the optic nerve (reviewed by Jean et al., 1998). The development of ocular tissues from E12 to birth, such as the cornea, iris, ciliary body and eyelid, is facilitated by the differentiation of the surface ectoderm as well as an invasion of cranial paraxial mesoderm and mesenchymal cells from the neural crest (Jean et al., 1998; Smith, 2002).

1.1.2 Neural Retina Development

Development of the neural retina from the inner neuroepithelial layer of the optic cup involves a series of cellular events that include proliferation, differentiation and cell fate specification. The mature vertebrate retina is composed of six distinct neuronal cell types; RGCs, amacrine cells, bipolar cells, horizontal cells, cone and rod photoreceptors, as well as Müller glia (reviewed by Dyer and Cepko, 2001). The nuclei of these cells are arranged in three distinct layers of the neural retina (Fig. 2). The outer nuclear layer (ONL) consists of the rod and cone photoreceptors, the inner nuclear layer (INL) is made up of amacrine, bipolar, horizontal and Müller glia cell bodies, and the RGC layer consists of ganglion cells and displaced amacrine cells. The three layers are each separated by plexiform layers that contain axons and dendrites.

Figure 2. Histology of the mature mammalian retina. The retina is composed of three cellular layers. The ganglion cell layer is composed of ganglion cells and displaced amacrine cells, the inner nuclear layer consists of amacrine, bipolar, horizontal and Müller glia cell bodies and the outer nuclear layer contains rod and cone photoreceptors. The layers are separated by plexiform layers that consist of axons and dendrites. The arrow indicates the path of light as it passes through the retina. Figure used with copyright permission from (McNeill et al., 2007)

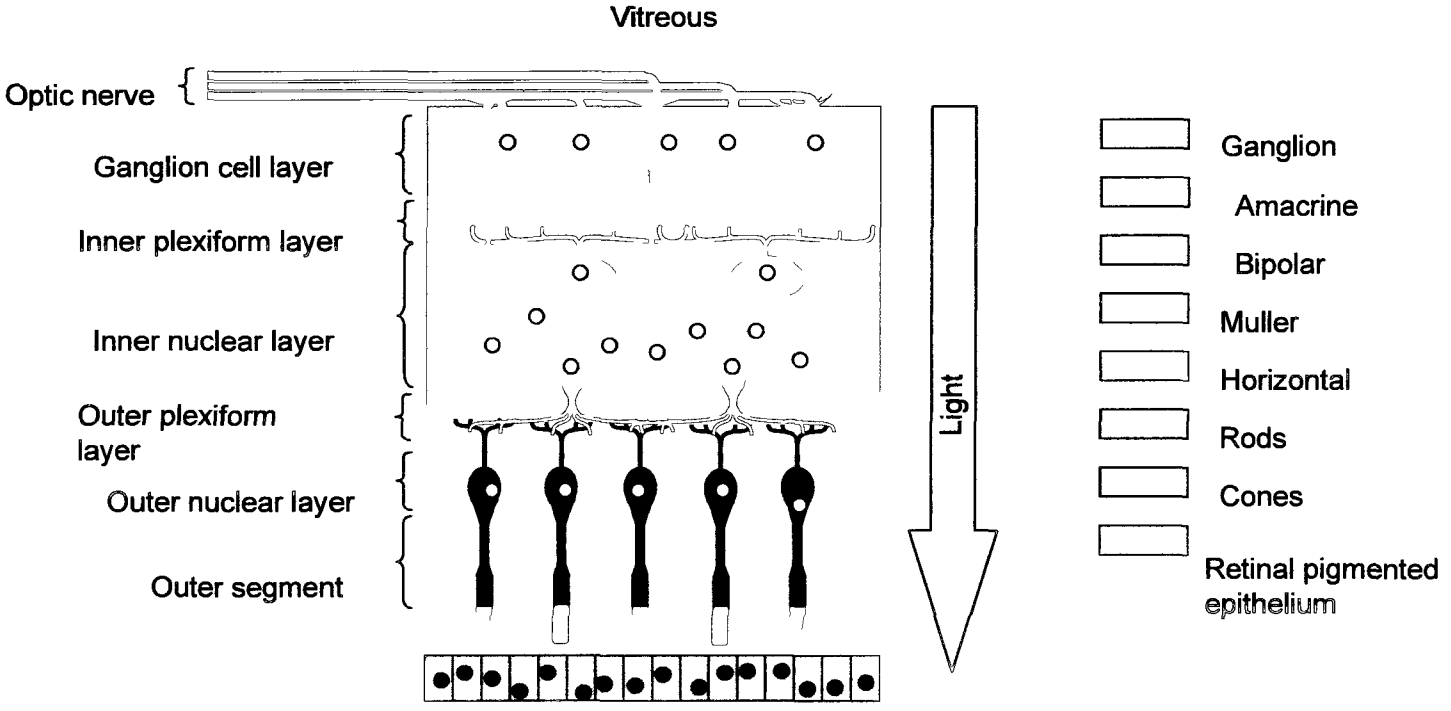
Vitreous
Optic nerve
Ganglion cell layer
Inner plexiform layer
Inner nuclear layer
Outer plexiform layer
Outer nuclear layer
Outer segment
Light
Ganglion
Amacrine
Bipolar
Muller
Horizontal
Rods
Cones
Retinal pigmented epithelium

1.1.3 Retinal Neurogenesis

Development of the neural retina is similar to other regions of the CNS where the timing of the generation of each subset of cell types is highly conserved (Dyer and Cepko, 2001). The birthorder of cells in the mammalian retina was established by using the concept of birthdating, the point at which a neuronal precursor exits the cell cycle for subsequent neuronal differentiation. There are two major waves of retina histogenesis (Fig. 3). The first wave begins during embryonic development in which RGCs, horizontal, cone photoreceptor and half of the amacrine cells are generated and this wave is followed by a second postnatal wave during which the bipolar, Müller glia and remaining amacrine cells are generated. Rod photoreceptors are generated throughout retinal histogenesis (Young, 1985). Lineage-tracing studies have shown that retinal precursor cells (RPC) are multipotent. A single progenitor cell has the potential to differentiate into different retinal cell types including neurons and glia (Cepko et al., 1996; Young, 1985). However, heterochronic mixing studies have shown that a progenitor cell is only able to differentiate into a limited number of cell types at a particular developmental age (reviewed by Livesey and Cepko, 2001). Work by Cepko and colleagues have established a retinal competence model to associate the multipotentiality of RPCs with the temporal development of the different cell types of the retina. The competence model proposes that RPCs progress irreversibly through a series of competence states in which they are able to produce a restricted subset of retinal cell types (reviewed by Cepko et al., 1996). Progression through these competence states is regulated by cell-intrinsic and -extrinsic factors that control the maintenance of competence and the initiation of cellular differentiation into a particular cell fate (Livesey and Cepko, 2001).

Figure 3. Retinal development. (A) The competence model of retinal cell-fate determination, which illustrates the progression of the RPC through different competence states in which they can produce a subset of retinal cell types. (B) The generally conserved order of birth of the seven cell types that comprise the mature retina. Figure used with copyright permission from (McNeill et al., 2007)

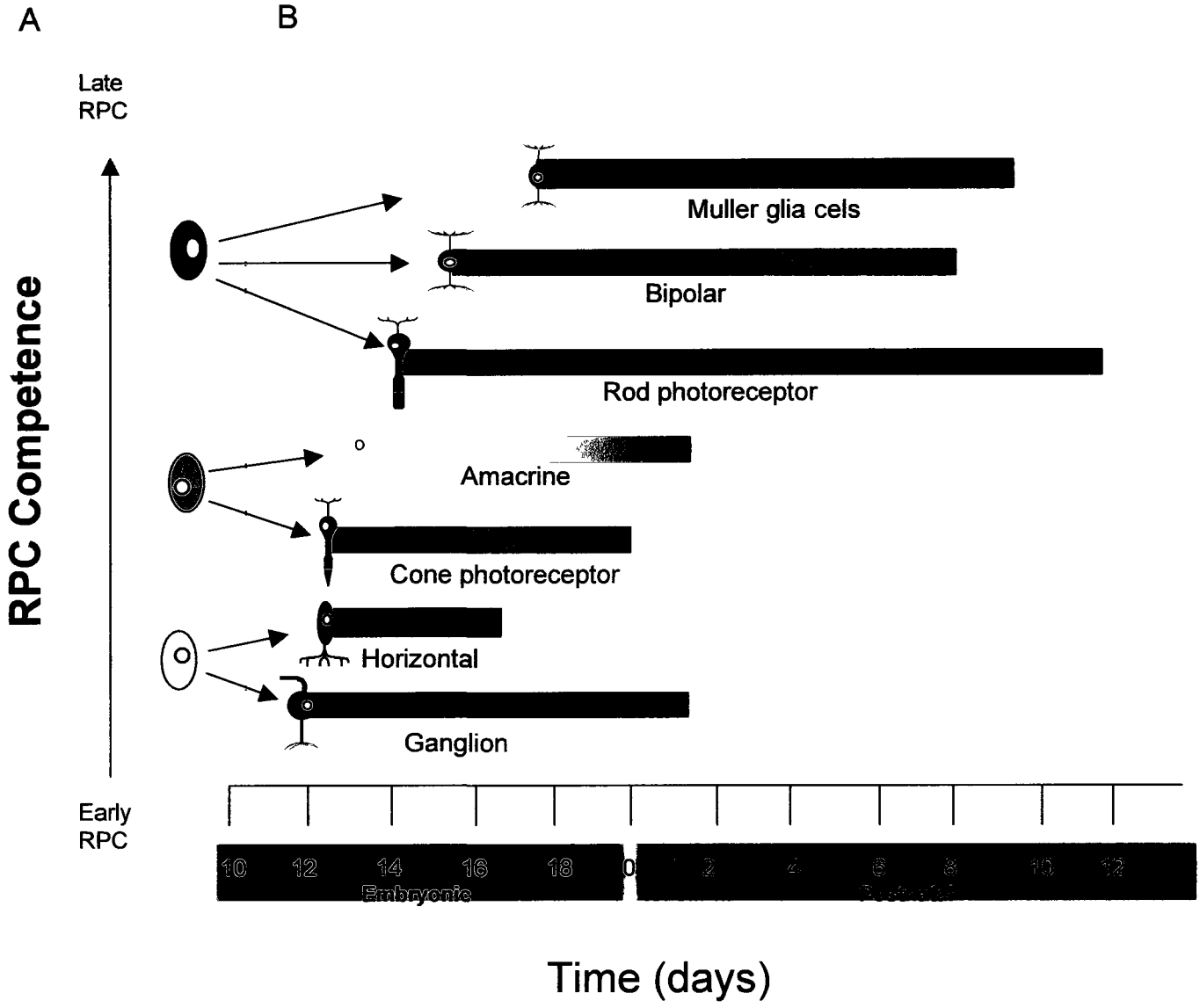
A
B
Late
RPC
RPC Competence
Muller glia cels
Bipolar
Rod photoreceptor
Amacrine
Cone photoreceptor
Horizontal
Ganglion
Early
RPC
10
12
14
16
18
0
2
4
6
8
10
12
Embryonic
Time (days)

1.1.4 Peripheral Optic Cup Development

Although the entire optic cup originates from the neuroepithelium, the peripheral and central regions develop into distinctly different structures. The central or posterior region is composed of the neural retina and the peripheral or anterior region of the optic cup develops into what is known as the ciliary margin (CM), which differentiates distally into the iris and proximally into the ciliary body (CB). As the iris and CB are non-neural components of the eye, development of the CM is unique in that it is an example of non-neural tissue having a neuroepithelial origin. This is a rare occurrence in vertebrate development, and the mechanisms that regulate this phenomenon are generally unknown.

1.1.5 Ciliary margin development

The CM differentiates and develops into the two non-neural epithelial layers of the iris and CB. The distal-most region becomes the iris pigmented epithelium (IPE), while more proximally, the inner layer of the CM becomes the non-pigmented ciliary epithelium (nPCE) and the outer layer develops into the pigmented ciliary epithelium (PCE) (reviewed by Beebe, 1986). Development of the CM becomes distinct from the neural retina at E12.5 with the expression of CM-specific genes *Msx1*, *Otx1*, *Tmsb4* and *Tgfb1i4* exclusively in this region of the optic cup (Martinez-Morales et al., 2001; Monaghan et al., 1991; Thut et al., 2001). By E14.5, the CM morphologically differentiates from the neural retina by elongating and extending distally to support invading periocular mesenchymal cells that will form the stroma of the iris and CB (reviewed by Gould et al., 2004). This differentiation becomes more distinct by E16.5 and at post-natal times P2-P4, the iris and CB are clearly

distinguishable from the retina (Gould et al., 2004) and by three weeks after birth, have completed development (reviewed by Thumann, 2001).

1.1.6 Iris and ciliary body development

The anterior segment of the mammalian eye consists of the cornea, lens, ciliary body, iris, trabecular meshwork and canal of Schlemm. Proper development of these structures is critical for normal eye function, as developmental abnormalities of any of these components can result in a number of eye diseases, such as glaucoma (Civan and Macknight, 2004). As previously mentioned, the CM in the developing eye differentiates into two structures, the proximal CB and the distal iris (Fig. 4). The CB can be sub-divided into two regions; the posterior pars plana and the anterior pars plicata. These two components each have contrasting physical characteristics; the pars plana is flat whereas the pars plicata is folded into finger-like ciliary processes consisting of a stroma and epithelium (reviewed by Beebe, 1986). The ciliary epithelium that spans both of these two regions of the CB is made up of two epithelial layers, the PCE which is continuous with the RPE and the nPCE that is continuous with the retina (Beebe, 1986). Aqueous humour is produced in the nPCE and flows through the pupil into the anterior chamber where it bathes the cornea and lens. The humour drains from the eye through the trabecular meshwork and canal of Schlemm, which are located at the junction between the cornea and iris. This balance between secretion and drainage of the aqueous humour determines the intraocular pressure, and an imbalance in this pressure can lead to several ailments of the eye (reviewed by Nassr et al., 2009).

Figure 4. Anterior segment of the adult mammalian eye. The ciliary body (CB) is divided into the flat pars plana and pars placata containing the finger-like ciliary processes. The ciliary epithelium that spans both of these two regions of the CB is made up of two epithelial layers, the pigmented ciliary epithelium (PCE) (brown) which is continuous with the retinal pigmented epithelium (RPE) and the non-pigmented ciliary epithelium (nPCE) (purple) that is continuous with the neural retina (NR). The iris pigmented epithelium (IPE) consists of two layers and is continuous with the ciliary epithelium. Aqueous humor is secreted from the nPCE and drains from the anterior chamber at the canal of Schlemm and trabecular meshwork. Figure adapted from Liu, 2007

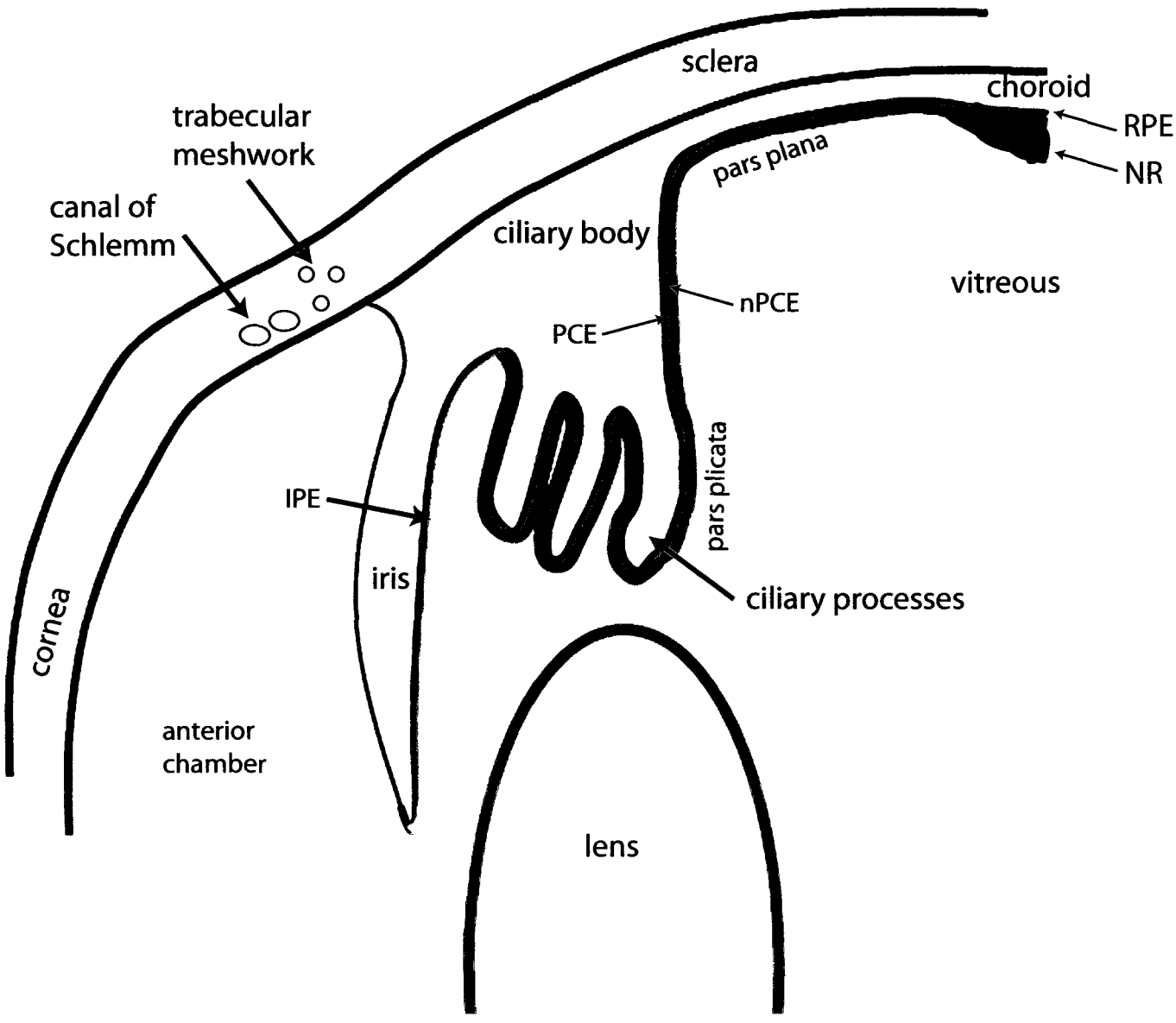
sclera
choroid
RPE
NR
trabecular
meshwork
canal of
Schlemm
pars plana
ciliary body
vitreous
nPCE
PCE
IPE
pars plicata
iris
ciliary processes
cornea
anterior
chamber
lens

The iris is located anterior to the CB and surrounds the anterior surface of the lens in a radial pattern. The anterior region of the iris is made up of stroma and connective tissue. The posterior region of the iris consists of sphincter and smooth muscle which control the diameter of the pupil in response to light. The iris smooth muscle develops from the optic cup, and is thus one of the few examples of smooth muscle derivation from the neuroepithelium (reviewed by Thumann, 2001). The region between the iris and cornea is composed of connective tissue of the trabecular meshwork, one of the areas where aqueous humour drains from the anterior chamber of the eye. The iris and CB stroma develop from invading mesenchymal cells of the cranial mesoderm and neural crest (Smith, 2002).

1.1.7 Ciliary Margin vs. Ciliary Maginal Zone

The development and growth of the eyes of lower vertebrates, such as fish and amphibians, differs from that of higher vertebrates, including mammals. Unlike eyes from higher vertebrates, which cease development in the adult stage of the organism, the eyes of fish and amphibians continue to grow throughout the lifespan of the organism (reviewed by Harris and Perron, 1998). This growth is facilitated by the ciliary marginal zone (CMZ) that is located at the far periphery of the eye, and is thus topologically analogous to the CM/CB of the eye in mammals (reviewed by Perron and Harris, 2000). Previous studies have shown that a pool of undifferentiated retinal stem cells (RSC) is located at the extreme periphery of the CMZ and as the organism ages, generate new neurons that are added to the periphery of the eye (reviewed by Harris and Perron, 1998). These cells remain in the eye throughout the

lifespan of the organism, resulting in retinal growth at the peripheral edges. Bromodeoxyuridine (BrdU) or tritiated thymidine labelling studies have shown that new neurons are added to the retina in a ring-like pattern, similar to those seen in a tree (reviewed by Harris and Perron, 1998). The spaces between the labelled rings give an indication of the growth rate of the eye during a particular time of development. Gene profiling studies have revealed that the CMZ is divided into several developmental zones, from peripheral to central: the specification zone, the proneural and neurogenic zone, the cellular determination zone and the differentiation zone (reviewed by Harris and Perron, 1998). The cells in each of these zones have a distinct proliferation and differentiation capacity, and gene marker expression (reviewed by Harris and Perron, 1998).

While the existence of an active CMZ has only been described in fish and amphibians, there is evidence that other vertebrates also contain pools of cells that resemble the CMZ (reviewed by Kubota et al., 2002). Studies on the retinal margin of post-hatch chick shows the existence of progenitor cells that resemble those found in the CMZ that are able to proliferate and differentiate into mature neurons (Fischer and Reh, 2000). A comparative study on other vertebrates suggests that the presence of a CMZ diminishes as vertebrate evolution progresses since the CMZ of a quail is highly reduced and is completly absent in mice (Kubota et al., 2002).

Although higher vertebrates lack a CMZ that facilitates retinal growth throughout their lifespan, it has been shown that cells harvested from the CB of adult humans, monkeys and rodents have been able to proliferate and differentiate into neurospheres and mature neurons when grown in culture (Ahmad et al., 2000; Fischer et al., 2001; Tropepe et al.,

2000). This observation suggests that the localization of cells with retinal stem cell potential to peripheral regions of the eye is conserved throughout evolution, although the ability of these stem cells to actively contribute to retinal growth is diminished in higher vertebrates. The presence of these retinal stem cells in the adult CB makes understanding the development of the CM of particular interest for research as manipulation of these cells can lead to possible methods of treatment for various eye diseases.

1.2 Signaling Factors in Ciliary Body Development

The temporal and spatial regulation of the complex cellular processes involved in CB development requires instructional cues from secreted proteins and signaling cascades. To date, complete knowledge of the mechanisms that mediate the development of the anterior segment structures of the eye is limited, however, a number of cell intrinsic and extrinsic factors have been implicated in the development of these structures. The transcription factors *Otx1* and *Lmx1b* are required for both CM and iris development, as these structures fail to develop in mouse mutants for these genes (Acampora et al., 1996; Pressman et al., 2000). Extracellular factors, such as lens-derived signals, have also been shown to be required in CB development (Beebe, 1986; Thut et al., 2001). The bone morphogenic protein (BMP) signaling pathway has also been implicated in this process, as inhibition of BMP activity through the overexpression of the BMP antagonist Noggin, abrogates CB development in transgenic mice (Zhao et al., 2002). The restriction of *Notch2* and *Jagged* expression to the CM also implicates a role for the Notch signaling pathway in CM development (Bao and Cepko, 1997), although this has yet to be formally demonstrated. Finally, the canonical, β-catenin-dependent, Wnt signaling pathway has been shown to play a role in the specification

and development of the CM (Cho and Cepko, 2006; Liu et al., 2003; Liu et al., 2006; Liu et al., 2007) which will be elaborated further in section 1.2.7.

1.2.1 Wnt signaling

The Wnt signaling pathway has been shown to be involved in a number of cellular processes, including proliferation, specification, polarity, apoptosis and stem cell maintenance (reviewed by Ciani and Salinas, 2005). The first Wnt gene was identified as mouse *Int*, a proto-oncogene that was activated by the integration of a mouse mammary tumour virus (Nusse and Varmus, 1982). It was later found that the *Drosophila melanogaster* segment polarity gene *wingless* (*wg*) was the orthologue of *Int1* (Rijsewijk et al., 1987). Therefore *Int1* was changed to *Wnt1* as an amalgamation of *Wg* and *Int*. To date, there have been at least 19 mammalian *Wnt* genes identified with each isoform having unique functions and expression patterns during development (Nusse, 2009). There are numerous methods in which Wnt genes can be classified; one common method is based on their ability to induce transformation of the mouse mammary epithelial cell line C57MG. In this case, *Wnt1*, *Wnt2*, *Wnt3*, *Wnt3a* and *Wnt7a* have all been found to exhibit potent transformation ability in C57MG cells. Conversely, the Wnt members that either induced an intermediate level of transformation or did not induce transformation in C57MG cells include *Wnt2*, *Wnt4*, *Wnt5a*, *Wnt5b*, *Wnt6*, *Wnt7b* and *Wnt11* (reviewed by Smalley and Dale, 1999). Another method used to classify Wnts is the *Xenopus* axis duplication assay (Wodarz and Nusse, 1998). In this method, Wnt genes are divided into two classes based on their ability to cause duplication of the embryonic axis in *Xenopus* embryos. The Xwnt-8

class of Wnt proteins were able to induce duplication while the Xwnt-5a was not (reviewed by Nusse, 2009; Wodarz and Nusse, 1998).

1.2.2 Wnt proteins

Wnts are secreted glycoproteins that share a conserved pattern of 23 cysteine residues, an N-terminal signal sequence and several N-glycosylation sites (reviewed by Miller, 2002). The size of Wnt proteins varies from 350-400 amino acids (Miller, 2002). Wnts undergo a number of post-translational modifications. The first is the addition of a palmitate group to Cys77 that is responsible for the signaling activity of the protein (Willert et al., 2003). The second lipid modification is the addition of palmitoleic acid to a conserved serine residue, Ser209. This modification is required for correct intracellular targeting and secretion (Takada et al., 2006). Additionally, some Wnt proteins are glycosylated in the endoplasmic reticulum. Although the purpose of this glycosylation is unknown, it is suggested that this modification may be important for the proper secretion of Wnts (Hausmann et al., 2007). Purifying Wnt proteins for more extensive study has generally proven to be difficult due to their hydrophobicity (Burrus and McMahon, 1995), however biologically active Wnt1 (Bradley and Brown, 1995) and Wnt3a (Shibamoto et al., 1998) proteins have been shown to accumulate in culture medium of transfected cells.

1.2.3 Functions of Wnt signaling

While the focus of Wnt signaling was initially on cancer research, Wnt signaling is now implicated in a number of cellular processes including proliferation, specification,

polarity, apoptosis, axon guidance, neurite growth and stem cell maintenance (reviewed by Ciani and Salinas, 2005; Reya et al., 2003; Wodarz and Nusse, 1998). Aberrant function of the Wnt pathway is also responsible for a number of retinal diseases, including familial exudative vitreoretinopathy (FEVR), congenital hypertrophy or hyperplasia of the RPE, retinal coloboma, and retinitis pigmentosa (reviewed by de Iongh et al., 2006).

1.2.4 Wnt signaling pathways

Wnt proteins transduce an intracellular signal in at least 3 ways (Fig. 5): canonical Wnt/β-catenin, planar cell polarity (PCP) and the Wnt/$Ca2^+$ pathways (reviewed by Ciani and Salinas, 2005). In the canonical Wnt/β-catenin pathway, a Wnt protein binds to its membrane receptor Frizzled (Fzd), leading to activation of the intracellular protein Dishevelled (Dvl). Active Dvl, in turn, leads to the inhibition of the Axin/APC/GSK-3β protein complex, which normally phosphorylates and ubiquinates intracellular β-catenin, targeting it for proteosomal degredation (Ciani and Salinas, 2005). Inactivation of the GSK-3β complex promotes the cytoplasmic accumulation and nuclear translocation of β-catenin where it interacts with T-cell specific transcription factor (TCF) and lymphoid enhancer-binding factor (LEF) to transactivate target genes (Ciani and Salinas, 2005). The planar cell polarity pathway involves an activated Fzd signaling to Dvl, which in turn activates the GTPases RhoA, Rac1 and c-Jun amino (N)-terminal kinase (JNK). Activity of the PCP pathway is thought to regulate changes in cell and tissue polarity, as well as dendritic arborization (Ciani and Salinas, 2005). The Wnt/$Ca2^+$ pathway is the other non-canonical

Figure 5. Wnt signaling pathway. Wnt signaling is initiated with the binding of a Wnt protein to its transmembrane receptor frizzled (Frz), leading to activation of one of three main branches of the Wnt signaling pathway. (a) Canonical signaling pathway, where the inhibition of the Axin/APC/GSK-3β destruction complex leads to an accumulation of β-catenin that is able to translocate into the nucleus and regulate transcription. (b) Planar cell polarity (PCP) pathway, where activation of Rho GTPases, Rho, and Rac results in changes to the cytoskeleton. (c) Wnt or calcium pathway, where an increase in intracellular calcium activates protein kinase C (PCK) and calcium or calmodulin-dependent protein kinase II (CaMKII) to regulate cell fate and movement. Figure used with copyright permission from (Cwinn et al., 2010).

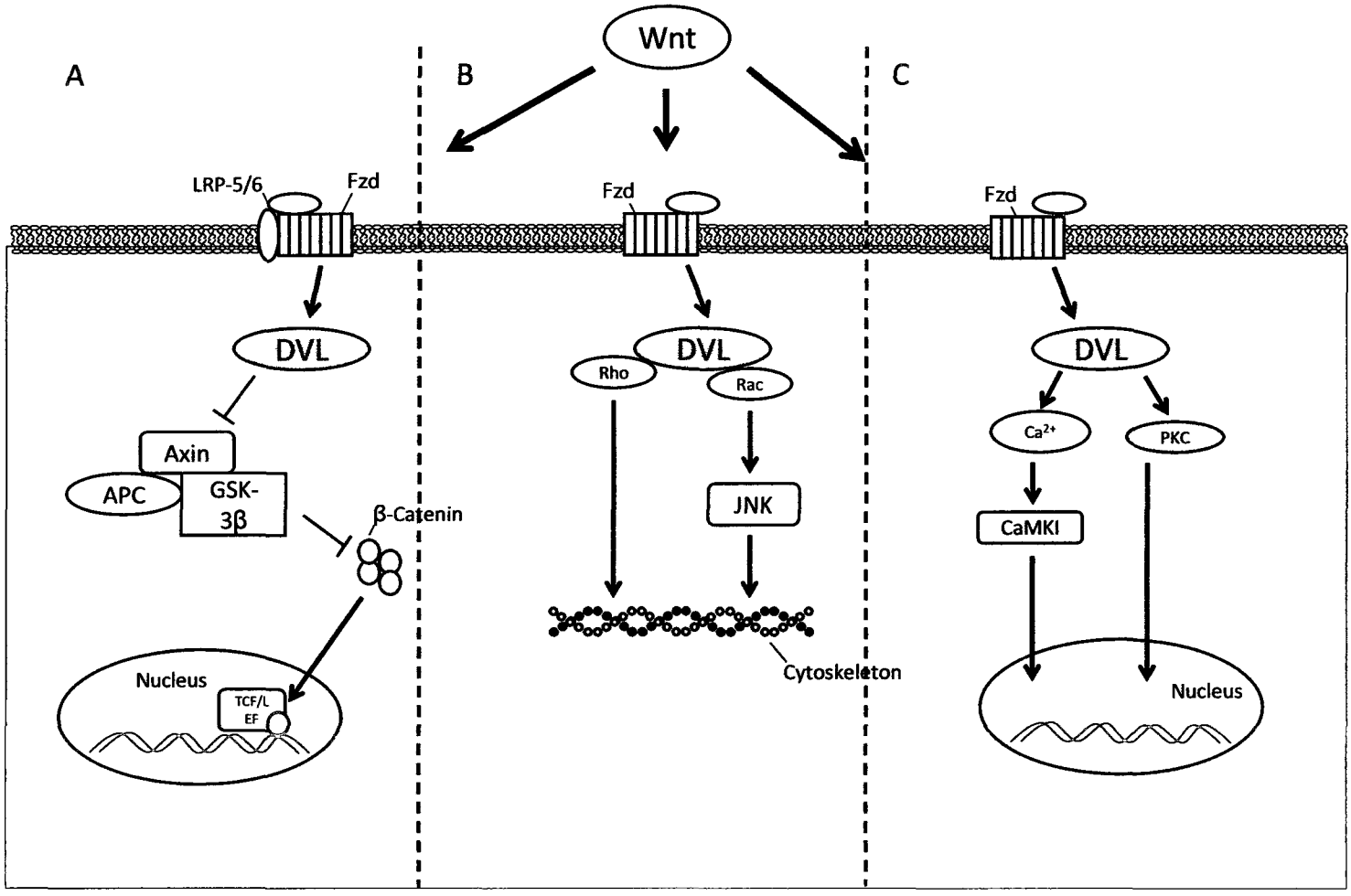
A
B
C
Wnt
LRP-5/6
Fzd
Fzd
Fzd
DVL
DVL
DVL
Rho
Rac
Axin
APC
GSK-3β
β-Catenin
JNK
Ca2+
PKC
CaMKI
Nucleus
TCF/LEF
Cytoskeleton
Nucleus

cascade where signals from an activated Dvl induce the release of intracellular calcium and activation of protein kinase C (PKC) and calcium/calmodulin dependent protein kinase II (CaMKII). This form of Wnt signaling has been found to regulate cell fate determination in *Xenopus* and cell movement and migration during gastrulation and heart development (Ciani and Salinas, 2005).

1.2.5 Components of the canonical Wnt signaling cascade

As noted above, the canonical Wnt pathway is composed of a number of receptors and intracellular proteins, each with its own important function in mediating canonical Wnt signaling.

Frizzled genes encode seven-pass transmembrane proteins that act as receptors for secreted Wnt proteins (Bhanot et al., 1996). To date, 12 Fzd proteins have been identified in mice and humans (Nusse, 2009). All Fzd proteins share the same structural composition: a signal peptide sequence at the N-terminus, an extracellular domain of approximately 120 amino acids that contains a cysteine-rich domain (CRD) made up of 10 conserved cysteine residues, the seven-pass transmembrane region and a cytoplasmic domain (reviewed by Wodarz and Nusse, 1998). Wnt-Fzd binding specificities are generally poorly characterized at this time as there is evidence that individual Wnt protein are capable of binding to numerous Fzd receptors and individual Fzd receptors are capable of binding to more than one Wnt protein (Wodarz and Nusse, 1998), although specificity may come from the context dependent availability of Wnt ligands and the *in vitro* aspect of these binding assays may have revealed more permissive binding specificities than are present *in vivo*. In addition to

Fzd, Wnt proteins have been shown to bind to the low-density lipoprotein receptor-related protein (LRP) co-receptors LRP5 and LRP6 (reviewed by Logan and Nusse, 2004). These co-receptors are single-pass transmembrane proteins that belong to the low-density lipoprotein (LDL) receptor family (Tamai et al., 2000). Studies have shown that LRP5 and LRP6 binding is exclusive to the canonical Wnt pathway and is essential for proper signaling (reviewed by Li and Bu, 2005).

The intracellular protein β-catenin serves as a vital effector of canonical Wnt signaling. β-catenin is composed of a central domain containing 12 armadillo repeats that harbour the interaction domains for E-cadherin, APC, and TCF (Klingensmith and Nusse, 1994; Willert and Nusse, 1998). The N-terminal region contains serine-threonine residues that can be phosphorylated by GSK-3β for proteosomal degradation (reviewed by Brembeck et al., 2006). The C-terminal region functions as a transcriptional activation domain (reviewed by Willert and Nusse, 1998). Manipulation of β-catenin is the most common method to activate the canonical Wnt pathway (reviewed by Brembeck et al., 2006). Techniques range from ectopically expressing β-catenin to functionally preventing GSK-3β-mediated phosphorylation,which prevents its degradation (reviewed by Logan and Nusse, 2004). Additionally, GSK-3β activity can be inhibited pharmacologically with GSK3 inhibitor, including Lithium (Li^+), thus activating canonical Wnt signaling (Klein and Melton, 1996). β-catenin also serves an additional Wnt independent role in cell adhesion through association with E-cadherin and α-catenin at the plasma membrane (reviewed by Nelson and Nusse, 2004), however it is believed that these two pools of β-catenin remain functionally independent from another (Willert and Nusse, 1998).

TCF/LEF transcription factors are important effectors of canonical Wnt signaling by serving as the binding mediators between β-catenin and the promoters of Wnt target genes. Although β-catenin contains strong transcriptional activation domains within its N- and C-terminus, it is unable to bind to DNA independently to activate target genes; therefore, TCF and LEF are required for this function. In mammals, there are 4 TCF/LEF members that have been identified: TCF1, LEF1, TCF3, and TCF4 (Korinek et al., 1998; Travis et al., 1991; van de Wetering et al., 1991). TCF/LEF transcription factors are composed of an N-terminal β-catenin binding domain, a context-dependent regulatory domain (CDRD) and a C-terminal DNA-binding domain called the high mobility group (HMG box) (reviewed by Lustig and Behrens, 2003). While generally known as transcriptional activators, the composition of the CDRD determines whether LCF/LEF also acts as a transcriptional repressor (Brannon et al., 1997). In some TCF/LEFs, an alternatively spliced exon in this region results in a repressor function by facilitating the binding of the pleiotropic repressor Groucho (Cavallo et al., 1998). All TCF/LEFs bind to the consensus sequence CCTTTGWW on Wnt target genes (van Beest et al., 2000). Knowledge of this consensus motif has led to the development of several reporter constructs that are used to monitor canonical Wnt activity (reviewed by Barolo, 2006).

1.2.6 Wnt antagonists and agonists

A number of extracellular Wnt inhibitors have been identified. Secreted-frizzled-related protein (Sfrp) binds to both Wnt proteins and Fzd receptors, preventing a Wnt-Fzd interaction (reviewed by Wodarz and Nusse, 1998). To date 6 Sfrps have been identified in

the mouse (Nusse, 2009), and knockout studies resulted in a mild or absent mutant phenotype (Bodine et al., 2004; Leaf et al., 2006; Satoh et al., 2006), suggesting that these genes may be functionally redundant. Although Sfrps are predominately known to antagonize Wnt signaling, recent studies have revealed additional functions of this protein such as influencing axon guidance, and interfering with BMP signaling (reviewed by Bovolenta et al., 2008). Wnt inhibitory protein (Wif) functions as another antagonist by binding to Wnt proteins, preventing them from interacting with Fzd (reviewed by Miller, 2002). As both Sfrps and Wifs prevent Wnt proteins from binding to Fzd, they act as antagonists for both canonical and non-canonical Wnt signaling. The Dickkopf (Dkk) family of proteins form a tertiary complex between their receptor Kremen and LRP5/6 (Bafico et al., 2001; Mao et al., 2002). As Wnt proteins are unable to bind to LRP5/6 in this scenario, Dkk is considered to be an antagonist of canonical Wnt signaling (reviewed by Zorn, 2001). Similar to Dkk, Wise acts as another canonical Wnt antagonist by binding to LRP6 preventing Wnt proteins from binding to its co-receptor (Itasaki et al., 2003).

Finally, there is a precedent for Fzd activation via non-Wnt ligands. The secreted protein Norrin or Norrie disease protein (NDP) shares no homology with Wnt proteins, yet it has been shown to be a Wnt agonist by binding to Fzd4 and LRP5/6 to activate the canonical signaling pathway (Xu et al., 2004). Norrin has been shown to regulate vascularisation in the developing retina (Rehm et al., 2002) and mutations in Norrin and Fzd4 have been implicated in congenital blindness in humans including Norrie's disease, FEVR and Coates disease (Riveiro-Alvarez et al., 2005).

1.2.7 Wnt signaling in eye development

A number of Wnt proteins are expressed in the mouse retina during development including Wnt1, Wnt3, Wnt5a, Wnt5b, Wnt7b, and Wnt13 (Wnt2b) (Liu et al., 2003). Additionally, Mfzd3, Mfzd4, Mfzd6 and Mfzd7 were also found to be expressed in the mouse retina (Liu et al., 2003). The function of Wnt signaling in retinal development has proven to be a controversial topic. Previous studies have provided conflicting evidence of Wnts acting as potential regulators during eye development in different species. In *Xenopus*, canonical Wnt signaling promotes progenitor cells to adopt a neural identity (Van Raay et al., 2005). In contrast, studies in zebrafish, chick and mouse have shown that increasing levels of canonical Wnt activity in the eye inhibits neuronal differentiation (Cho and Cepko, 2006; Kubo et al., 2003; Liu et al., 2006; Liu et al., 2007; Yamaguchi et al., 2005). Another area of controversy concerns the proliferative effects of Wnt signaling in the eye. Ectopic expression of Wnt2b was shown to increase the proliferation of chick CMZ-derived progenitor cells and the growth of chick retinal explants in culture (Kubo et al., 2003; Kubo et al., 2005). Also, inhibiting canonical Wnt signaling reduces proliferation in the *Xenopus* retina (Van Raay et al., 2005). In contrast, ectopic activation of β-catenin in chick and mouse resulted in reduced proliferation in the retina (Cho and Cepko, 2006; Liu et al., 2007). In addition to having an effect on neuronal differentiation and precursor proliferation, studies have implicated canonical Wnt signaling in regulating development of the CB. Studies using TCF reporter mice have shown active Wnt signaling within the CM during development (Liu et al., 2006; Liu et al., 2007). Expression profiling has shown that *Wnt2b* is expressed in the RPE overlying the CM in mouse (Liu et al., 2003), and other components of the canonical Wnt pathway are expressed in the CM region of various species (Cho and

Cepko, 2006; Liu et al., 2006; Van Raay et al., 2005). Studies in the chick have shown that activating the canonical Wnt pathway, either through ectopic expression of *Wnt2b* or constitutively active β-catenin, inhibits neuronal differentiation and promotes the development of the CM, CB and iris (Cho and Cepko, 2006; Kubo et al., 2003). This anti-neurogenic activity is also observed in the mouse eye. Supplementing mouse embryonic retinal explants with Li^+, a well characterized activator of canonical Wnt signaling (Klein and Melton, 1996), resulted in ectopic expression of CM marker genes and an expansion of the CM (Liu et al., 2006). This effect of canonical Wnt signaling in mice was also observed *in vivo*, in which a transgenic mouse model harbouring a constitutively active β-catenin allele resulted in a cell autonomous expansion of the CM that coincided with a reduction of the neural retina during embryogenesis (Liu et al., 2007). Thus, work in the mouse and chick systems suggest a role for canonical Wnt signaling in CM development. A model for Wnt specification of the CB can be developed where Wnt/β-catenin signaling acts to inhibit neurogenesis and proliferation in the mammalian retina however, the downstream effectors of this signaling cascade have yet to be characterized.

1.3 Msx1

Evidence that the gain-of-function for β-catenin results in transdifferentiation of the neural retina to the CB is supported by the β-catenin mediated induction of several known Wnt target genes that are normally expressed in the CM and excluded from the neural retina, including *Msx1* (Liu et al., 2007). Vertebrate muscle segment homeobox (Msx) genes are vertebrate homologs of the *Drosophila* segment homeobox gene (Davidson, 1995) and belong to a family of transcriptional repressors that are involved in neuronal differentiation

(Bendall and Abate-Shen, 2000). There are three members of the Msx gene family; *Msx1* and *Msx2* have nearly identical homeodomains (Ekker et al., 1997) and are expressed in overlapping patterns of many developing systems including limb and tooth buds, craniofacial processes and adjacent cells in the dorsal neural tube and neural crest (Davidson, 1995) whereas *Msx3* is expressed exclusively in the neural tube (Shimeld et al., 1996). Msx genes are effectors of the Bmp, Wnt and Fgf signaling pathways (reviewed by Ramos and Robert, 2005) and are expressed in the eye during development with *Msx1* expressed after formation of the optic cup in the CM while *Msx2* is expressed in the optic vesicle and later in the neural retina (Monaghan et al., 1991). Therefore, Msx1 may represent a Wnt target gene important for mediating the effect of Wnt/β-catenin signaling in promoting CM development.

1.4 Rationale, hypothesis and research objectives

Wnt signaling is involved in the development of the boundary between the non-neural CB and iris from neuroepithelium (Liu et al., 2007). Wnt signaling has also been implicated in a similar boundary formation in the brain where the neural ectoderm gives rise to the choroid plexus, a cuboidal secretory epithelium that has similar morphological characteristics to the ciliary epithelium in the retina (Grove et al., 1998). Such a phenomenon of non-neural structures having a neural tissue origin is rare in mammalian development. Therefore, elucidating the role of the Wnt/β-catenin signaling pathway during the development of the CB may provide insights into the molecular mechanisms involved in

boundary formation and the development of secretory epithelia. Therefore, this thesis tests the following hypothesis:

Wnt/β-catenin induction of target genes promotes the specification of the CM

Objective 1: Identify candidate target genes of the Wnt/β-catenin pathway in retinal progenitor cells using microarray analysis.

To identify novel candidates of Wnt/β-catenin signaling in the retina, we performed a comparative microarray analysis using a retinal explant culture system that facilitated manipulating the activity of the Wnt/β-catenin pathway. Bioinformatic analysis was used to identify candidate Wnt/β-catenin signaling targets with conserved TCF/LEF binding sites. Selected genes were then investigated for changes in gene expression in response to Wnt pathway activation using Li^+ treated retinal explants and transgenic mice with constitutive β-catenin activation.

Objective 2: Functional analysis of Msx1 in retinal development.

If putative Wnt target genes are identified in the microarray analysis, determining their functional roles in development of the CM would be the next step in elucidating the role of Wnt signaling in eye development. Among these putative Wnt targets that were identified in the microarray analysis was Msx1. Although Msx1 is a known CM marker, little is known regarding its role in CM development. The role of Msx1 in CM development was investigated by ectopically expressing *Msx1* in RPCs and determined its effect on gene expression and proliferation using ISH, Q-PCR and dissociated cell culture analyses.

2.0 Methods and Materials

2.1 Retinal Explant Culture

CD1 wild-type mice (obtained from Jackson Laboratories Bar Harbor, Maine) were time-mated to generate E14.5 embryos, with day 0 of gestation designated by the presence of the vaginal plug. The eyes were harvested from the embryos and dissected in CO_2-independent medium to remove the RPE while leaving the lens intact. The retina was then transferred to ethanol sterilized, 13 mm polycarbonate filters (Nucleopore) with the vitreal face of the retina oriented downwards on the filter. The retinal explants were cultured at 8% CO_2 and 37°C in 500 µl serum-free retinal explant medium (1:1 F12/Dulbecco's Modified Eagle's Medium, transferrin (100 mg/ml), insulin (10 µg/ml), bovine serum albumin (BSA Fraction V: 100 mg/ml), putrescine (16 µg/ml), progesterone (60 ng/ml), sodium selenite (40 ng/ml) and gentamycin (25 µg/ml)) (Wang et al., 2005).

2.1.1 Treatment with lithium

The Wnt/ β-catenin signaling pathway was activated by supplementing the retinal explant medium with 20 mM LiCl for 24 hours. Control explants were treated with 20 mM NaCl. Following culture, the explants were harvested for RNA extraction followed by Q-PCR (see section 2.2) or microarray analysis (see section 2.3).

2.1.2 Msx1 electroporation in retinal explants

Electroporation was performed as described previously (Matsuda and Cepko, 2004). Briefly, E14.5 eyeglobes with the RPE removed were placed, with the lens attached, in groups of 2 or 3 in a 2 mm gap cuvette (VWR) with 100 µl of 0.5-1 µg/µl Msx1/pCMV-SPORT6 (Open Biosystems) in endotoxin free TE buffer. Visualization of the electroporated regions of the explants was accomplished by co-transfection of the plasmid DNA with pUB-GFP (a kind gift from Takahiko Matsuda) in a 10:1 ratio. Control electroporations used a 10:1 ratio of empty SPORT6:pUB-GFP at the concentrations outlined above. The retinas were electroporated using a BTX Harvard Apparatus ECM 830 set to the following parameters: 5 pulses at 30V each with a 50 ms duration in intervals of 900 ms. Following electroporation, the retinas were detached from the lens and flattened onto the polycarbonate filters and cultured as described above (section 2.1) for 72 hours. The explants were then processed for Q-PCR, ISH and IHC.

2.2 RNA extraction, cDNA synthesis, and Q-PCR

RNA was harvested from retinal explants using Trizol (Invitrogen). Briefly, groups of 2 or 3 retinal explants were placed in 1 ml of Trizol and sonicated using a VCX 600 Vibra-Cell Ultrasonic processor (Sonics and Materials Inc.) set at 5 pulses (8-10 seconds each) with an amplitude of 35%. RNA extraction was then completed according to the manufacturer's instructions. cDNA was synthesized from 2 µg of total RNA using random hexamers (Invitrogen) and M-MLV reverse transcriptase (Invitrogen) following the manufacturer's protocols. Quantitative PCR was performed using 1 µl of cDNA with SYBR® Green JumpStart Taq ReadyMix for High Throughput QPCR master mix (Sigma) using the manufacturer's instructions with the exception that the total reaction volume was

scaled down to 25 µl. Primer pairs were designed, using Primer3 software, with 100% homology to the target sequence and confirmed using a BLAST search (National Center for Biotechnology). The primers were designed with a melting temperature of 58-59 °C. Amplicon sizes generated by the primer pairs ranged from 100-200 bp. Sequences of the primer pairs used are listed in Appendix A. The PCR reaction was performed using a Stratagene Mx3000P with the following cycling parameters: 94 °C for 3 min, followed by 40 cycles of 94 °C for 30 s, annealing at 58 °C for 30 s and extension at 72 °C for 1 min. Changes in gene expression were quantified using the $2^{\Delta Ct}$ method (Bustin, 2002; Radonic et al., 2004) and normalized to the house-keeping genes 18S and GAPDH. To standardize the transfection efficiency in electroporated retinal explants, the data was normalized to GFP. All reactions were performed in triplicate in 3 independent experiments. Statistical significance of the reported changes in gene expression was determined using the student's t-test.

2.3 Microarray Analysis

Two sets of eight retinal explants were cultured in either NaCl or LiCl for 24 hours under conditions outlined above (see section 2.1.1). Each set of explants was pooled together and total RNA was extracted using an RNeasy Mini kit (Qiagen) to obtain approximately 10-15 ug of total RNA. The RNA obtained from each explant set was then divided into two equal amounts in order to perform a dye-flipped array analysis. The dye flipped analysis involves two arrays where the sample-dye combination used in one array is swapped in the second array. The experiment was performed twice to obtain 2 biological

replicates each with a technical sub-replicate (dye-flip) for a total of 4 microarray analyses summarized below:

Array 1		Array 2		Array 3		Array 4	
Li-1-Cy5	Na-1-Cy3	Li-1-Cy3	Na-1-Cy5	Li-2-Cy5	Na-2-Cy3	Li-2-Cy3	Na-2-Cy5

The microarray analysis was performed on MEEBO 38.5k arrays obtained from Microarrays Inc (Huntsville, AL, USA). The cDNA synthesis, labeling and microarray hybridization was performed using the 3DNA Array 900 Cy3/Cy5 kit (Genisphere, Hatfield, PA, USA) following manufacturer's instructions. The microarray was scanned using a Scan Array Express scanner and analyzed using the Pro Scan Array Express (Perkin Elmer) software package.

2.4 Computational screening for genes with conserved TCF/LEF binding sites

The differentially expressed genes identified from the microarray analysis were mapped within the genome using genomic coordinates from their corresponding mRNAs from the RefSeq database (NCBI). Regions spanning 5 kb upstream of the transcriptional start site to 1 kb downstream from the transcriptional stop site for each gene were searched for TCF binding sites by matching a sliding window to the binding site sequence CTTTGWW. Matches were filtered by their degree of phylogenetic conservation using the conservation scores phastCons (Siepel et al., 2005) available at the UCSC genome browser (Karolchik et al., 2003). These conservation scores are generated from a multiple alignment of 16 vertebrate genomes to the mouse genome (Kent et al., 2003; Schwartz et al., 2003). For each match, we computed the average conservation score. Genes with TCF matches that had

an average score greater than 0.7 (out of a possible 1) were identified as potential Wnt targets.

2.5 Transgenic Mice

Transgenic mice were maintained and crossed as previously described (Liu et al., 2007). The *α-Cre* (obtained from P. Gruss (Marquardt et al., 2001)) and *Catnb*$^{+/lox(ex3)}$ (Harada et al., 1999) transgenic mouse lines were maintained on a C57BL/6 background and the *TCF/Lef-LacZ* mouse line (obtained from D. Dufort (Mohamed et al., 2004)) was maintained on a CD1 background. The *α-Cre* mice were crossed with the *TCF/Lef-LacZ* mice to create the *α-Cre;TCF/Lef-LacZ* mouse line. Heterozygous *α-Cre;TCF/Lef-LacZ* mice were crossed with the *Catnb*$^{+/lox(ex3)}$ mice to generate *α-Cre;Catnb*$^{+/lox(ex3)}$ or *α-Cre;Catnb*$^{+/lox(ex3)}$*;TCF/Lef-LacZ* genotypes and were designated as CatnbΔex3 mutant mice. Littermates with *α-Cre;Catnb*$^{+/+}$ or *α-Cre;Catnb*$^{+/+}$*;TCF/Lef-LacZ* genotypes were designated as control or wild-type (WT) mice. Genotyping for the transgenic mice was performed by PCR using the following primer pairs (5' → 3'):

α-Cre

(F) ATGCTTCTGTCCGTTTGCCG

(R) CCTGTTTTGCAGGTTCAGCG

TCF/Lef-LacZ

(F) CAGTGGCGTCTGGCGGAAAACCTC

(R) AAACAGGCGGCAGTAAGGCGGTCGG

Catnb$^{+/lox(ex3)}$

(F) GACACCGCTGCGTGGACAATG

(R) GTGGCTGACAGCAGCTTTTCTG

For analysis, E14.5 embryo heads were harvested and fixed in 4% paraformaldehyde phosphate buffer overnight and washed in PBS. Heads were then transferred to a 30% sucrose/PBS solution overnight and embedded in 1:1 Optimal cutting temperature/ 30% sucrose/PBS mixture for cryosectioning into horizontal sections.

2.6 In Situ Hybridization

ISH was performed as previously described (Dakubo et al., 2003; Jensen and Wallace, 1997; Wallace and Raff, 1999). The antisense riboprobes used for ISH include *Cyclin D1* (a kind gift from Gordon Peters, London Research Institute, London, UK), and *Msx1* (a kind gift from Yi-Hsin Liu, Keck School of Medicine, USA). All other riboprobes used in this study were designed using PCR primers listed in Appendix B. Briefly, the primers were used to produce a 500-800 bp amplicon of the appropriate gene and subcloned into the pGEM®-T Easy Vector (Promega). The insert + vector construct was then sequenced to confirm the identity of the transcript and orientation of the amplicon in the plasmid. Anti-sense DIG-labeled probes were then produced by linearizing the vector with the appropriate restriction enzyme and synthesized using T7 or SP6 RNA polymerase.

Cryosections were cut at 12 μm and dried for 1-5 hours at room temperature. The riboprobes were denatured in hybridization solution (1:1000) (Appendix 3) at 65 °C for at least 10 min and followed by vortexing. The denatured riboprobe/hybridization solution

(150-200 µl) was directly applied to the sections, sealed with a coverslip, and incubated at 65 °C overnight in a humidified box containing Whatman filter paper soaked with wetting buffer (Appendix C). The sections were then washed in wash buffer (Appendix C) 3 times at 65 °C with agitation followed by 2 washes in 1x MABT (Appendix C) at room temperature. The slides were transferred to blocking solution (Appendix C) for 1 hour at room temperature followed by an overnight incubation with anti-digoxigenin (1:1500) (Roche) in blocking solution at 4 °C. The sections were washed 4-5 times in 1x MABT for 20 min each followed by 2 washes in pre-stain buffer (Appendix C) for 15 min each. Finally, the sections were incubated in staining buffer (Appendix C) for 1-8 hours for colour development. Images were analyzed using a Zeiss Axioplan2 microscope and captured with an Axiocam camera (Carl Zeiss Inc) at 20X (0.8 N.A). Images were processed with Adobe Photoshop® CS2.

2.7 Single Cell Dissociation and Immunohistochemistry for Ki-67

Msx1 electroporated explants were cultured as described above (see section 2.1.2). The explants were then incubated in Ca^{2+}/Mg^{2+} free PBS with 0.125% trypsin (Sigma) for 10-15 min at 37 °C. Trypsin was inactivated by adding a solution of 20% FBS/DMEM and DNase (0.04%). Explants were dissociated into a single-cell suspension by titurating with a pipette 8-10 times. Cells were collected by centrifuging at 1000 g for 5 min and resuspended in DMEM/0.04% insulin to at a final density of 1 x 10^7 cells/ml. The resuspended cells were plated onto Superfrost slides (Sigma) in 15 µl aliquots and allowed to adhere for 45 min at 37°C. The cells were then fixed using 4% paraformaldehyde phosphate buffer for 5 min and washed (3 times for 5 min) with PBS.

Immunohistochemistry for Ki-67 was performed as previously described (Dakubo et al, 2003; Jensen and Wallace, 1997, Wallace and Raff, 1999). Briefly, the dissociated cells were microwave treated in 1x sodium citrate for 5-10 min to unmask antigens. Cells were washed in PBS and blocked with 20% sheep serum/TBLS with 0.3% Triton X-100 for 1 hour in a humidified box containing Whatmann paper soaked with PBS. Cells were then incubated in the primary antibodies mouse monoclonal anti-Ki-67 (1:400) (BD Biosciences) and rabbit polyclonal anti-GFP (1:1000) (Molecular Probes) in blocking solution overnight at 4 °C. Cells were washed in PBS and incubated with the secondary antibodies goat anti-rabbit IgG FITC (1:400) (Molecular Probes) and goat anti-mouse IgG Cy3 (1:000) (Molecular probes) in blocking solution for 45 min at room temperature in a humidified box then washed in PBS. Hoechst staining was used to visualize nuclei. Controls using uncomplimentary antibodies were performed to determine whether the double staining was not due to cross reactivity of antibodies. Fluorescent images were analyzed using a Zeiss Axiocam HRm microscope and captured with an Axioimager M1 camera (Carl Zeiss Inc) at 20X (0.8 N.A). Images were processed with Adobe Photoshop® CS2.

2.8 X-gal staining for detection of β-galactosidase activity

X-gal staining was performed as previously described (Dufort et al., 1998; Liu et al., 2003; Wallace and Raff, 1999). Briefly, embryonic tissue designated for X-gal staining was fixed in 4% paraformaldehyde for 15 min prior to embedding for cryosectioning. Cryosections were cut at 12 μm and dried at room temperature for 2-6 hours. Sections were immersed in PBS for 5 min and incubated in LacZ staining buffer overnight at room

temperature in the dark. Sections were then washed with PBS and mounted using glycerol/PBS (1:1).

3.0 Results

3.1 Microarray Analysis of Li^+-treated retinal explants to identify novel candidate Wnt/β-catenin Target Genes in the Murine Retina

The CM and neural retina originate from neuroepithelium, yet the CM develops into the CB and iris, two non-neural structures. This unique occurrence of non-neural tissue developing from neuroepithelium has yet to be fully understood at the molecular level. The canonical Wnt pathway has been implicated in CM specification during eye development; however knowledge of Wnt target genes in this developing system remains limited. To identify possible target genes of Wnt signaling, a microarray analysis was performed to identify genes that are differentially expressed when β-catenin signaling is activated. The analysis was performed using an *in vitro* retinal explant system in which Li^+ treatment ectopically activated Wnt/β-catenin signaling.

3.1.1 Quantitative analysis of Li^+-induced changes in gene expression in retinal explants

Li^+ inhibits the activity of GSK-3β (Klein and Melton, 1996) and is used to activate Wnt/β-signaling pharmacologically. Previous work in our laboratory showed that culturing embryonic retinal explants for 24 hours in the presence of Li^+ results in increased expression of CM-specific genes (Liu et al., 2007). The *in vitro* retinal explant system is ideal for a microarray analysis as it provided a sufficient quantity of RNA, therefore, an amplification step was not required prior to the microarray analysis. To determine whether the retinal

explant system was suitable for microarray, known CM markers were tested by Q-PCR in Li^+-treated explants that were previously reported (Liu et al, 2007). Retinal explants (E14) were cultured for 24h in the presence of Li^+ or Na (control) and harvested for Q-PCR analysis. Gene expression was examined in 3 independent experiments performed in triplicate in which 3-4 explants were pooled for each sample. Primer efficiency was tested on RNA from E14 retinas. The observed cycle-threshold (CT) values of analyzed genes were normalized to the averaged expression of the housekeeping genes Glyceraldehyde 3-phosphate dehydrogenase (GAPDH) and 18S ribosomal RNA before fold changes were calculated. The expression of the CM marker, *Msx1,* was significantly increased in Li^+-treated explants compared with control explants. Expression of *Bmp4*, a gene that was previously shown to be essential in CM development (Zhao et al., 2002), was also increased in Li^+-treated explants (Fig. 6a), however, the expression of *Otx1*, another CM marker did not change with Li^+ treatment, in contrast to previously observed results (Fig.6a) (Liu et al., 2007). In contrast to the up-regulation of CM markers following Li^+ treatment, the expression of neural retinal markers *Crx* and *Math3* was downregulated in Li^+-treated explants (Fig. 6b), consistent with the effects of Li^+ in promoting CM, while inhibiting neural retina development that have been reported previously (Liu et al., 2006; Liu et al., 2007). One exception was the expression of Pax6, which was reported to be downregulated by Li^+ (Liu et al., 2007), but which was unchanged in this experimental series (Fig. 6b). Based on these data Li^+-cultured retinal explants were selected as a model for microarray analysis to identify novel β-catenin target genes in CM development.

Figure 6. Q-PCR analysis in gene expression in Li^+-treated retinal explants.
Quantitative RT-PCR (normalized to GAPDH and 18S) was performed for the indicated genes on RNA extracted from retinal explants cultured under control conditions (Na^+) or in the presence of Li^+ for 24 h. A total of 3 separate experiments were performed in triplicate (n=3). Results are presented as mean fold change of (a) up-regulated or (b) down-regulated genes. Data is presented by mean fold change in Li^+ compared with NaCl-treated controls ± S.D. *$p<0.05$.

A

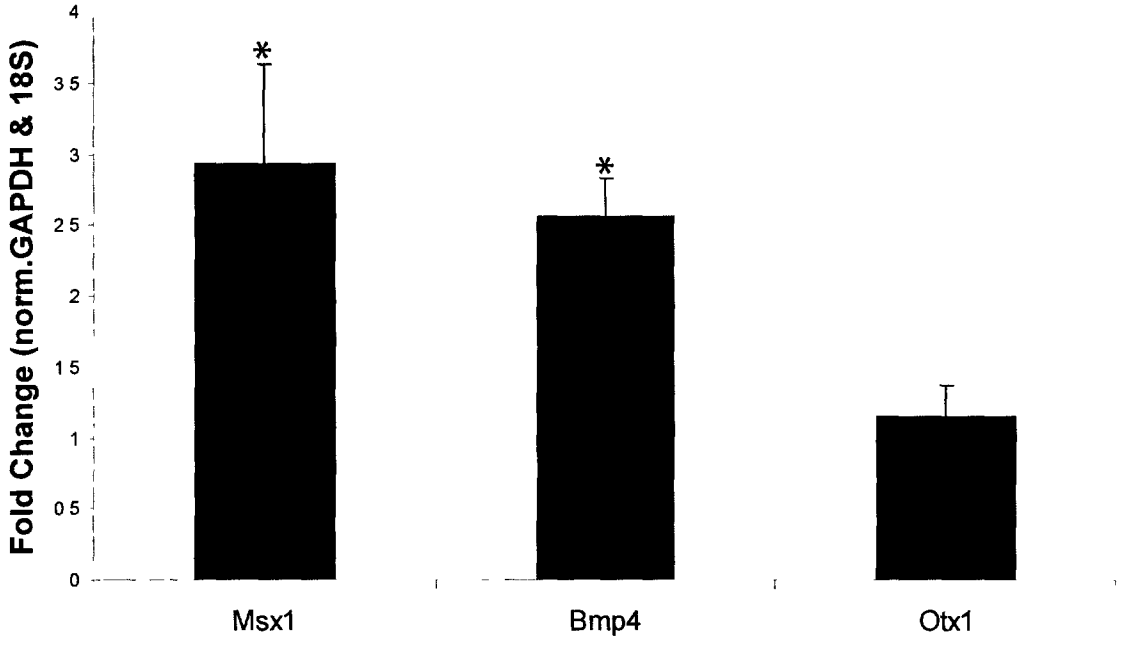
Fold Change (norm.GAPDH & 18S)
4
3 5
3
2 5
2
1 5
1
0 5
0
*
*
Msx1
Bmp4
Otx1

B

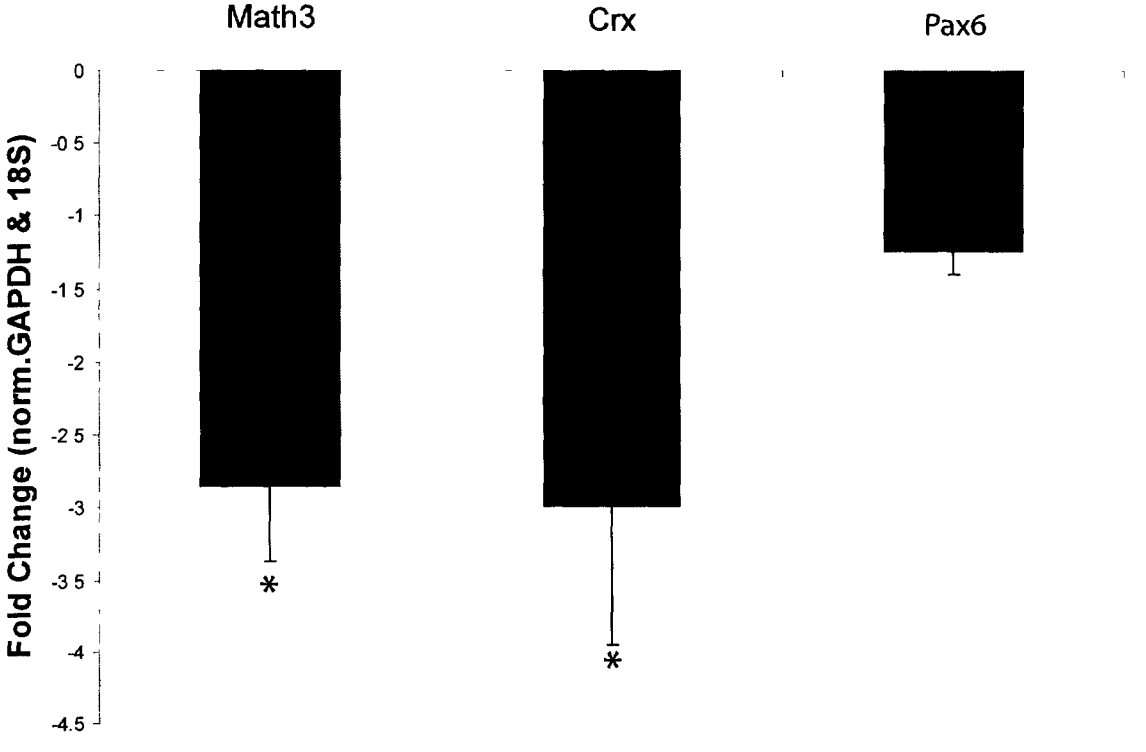
Math3
Crx
Pax6
Fold Change (norm.GAPDH & 18S)
0
-0 5
-1
-1 5
-2
-2 5
-3
-3 5
-4
-4 5
*
*

3.1.2 Microarray analysis of Li^+-modulated genes

To perform the microarray analysis, RNA from pooled control and Li^+-treated retinal explants (n = 8 for Li^+ and control, respectively) from two separate experiments was analyzed on a MEEBO 38.5k array containing 35,000 probe sets corresponding to the mouse transcriptome. Previous work from our laboratory determined that LacZ-reporter activity in Li^+-treated retinal explants from TCF-LacZ reporter mice peaked at 24 hours and then decreased by 48 hours (Liu et al., 2006). Therefore, retinal explants were cultured for 24 hours corresponding to the peak of β-catenin-dependent reporter gene activation. In each experiment the pooled RNA was divided into two equal samples allowing for the use of dye-flipped arrays. The microarray analysis was performed on MEEBO 38.k arrays using a 3DNA Array 900 kit from Genisphere. Using a 2-fold change in expression in 3 out of 4 arrays as the filtering cutoff criteria, a total of 904 genes were found to be differentially expressed in the Li^+-treated explants. Among these, 435 genes were found to be upregulated (Appendix D) and 469 genes were downregulated (Appendix E). A preliminary analysis of the microarray hits using the gene annotation program GoStat identified a number of functional classes of upregulated genes including those involved in programmed cell death, cell differentiation and cell cycle control (Table 1). The functional groups containing annotated genes that were downregulated included genes involved in chromatin architecture and nervous system development (Table 2). As GoStat was able to identify gene-ontology groups that are highly represented within the microarray data, this suggests that treating retinal explants with Li^+ results in a significant change in expression of genes that may be involved in retinal development. The expression of CB marker genes that we have previously observed, such as *Msx1* and *Otx1,* as well as known Wnt target genes, *Axin2* and

Table 1. Functional Groups of upregulated genes from microarray analysis

Functional Group	Programmed Cell Death	Cell Differentiation	Sensory Perception	Cell Cycle Arrest	G-protein Coupled Receptor Activity
Genes	1200009f10rik, Actc1, Apaf1, Atf5, Bax, Cdkn1a, Ckap2, Col18a1, Ddit3, Eda2r, Eef1a2, Elmo1, Gas2, Krt18, Lrdd, Lrp1, Gmt, Msx1, Nme5, Perp, Pmaip1, Raet1b, Sgk, Tbrg4, Tcf7, Tnfrsf12a, Traf3, Traf4, Trp53inp1, Tsc22d3, Mat3,	1200009f10rik, Acsl6, Actc1, Adcyap1r1, Apaf1, Atf5, Axin2, Bax, Capn3, Cdc25b, Cdkn1a, Chrdl1, Ckap2, Col18a1, Cugbp1, Cxcl4, Ddit3, Eda2r, Eef1a2, Elmo1, Epha2, Ephb1, Fyn, Gas2, Hs1bp3, Ifrd1, Klf1, Klf10, Krt18, Lhx3, Lor, Lrdd, Lrp1, Lrp4, Mgmt, Mlf1, Msx1, Mt3, Nav1, Nme5, Ntrk2, Perp, Pmaip1, Ptk7, Raet1b, Serpine2, Sgk, Traf3, Tbrg4, Tcf7, Tnfrsf12a, Traf4, Trp53inp1, Tsc22d3, Unc45a, Zmat3	Fyn, Olfr247	Ak1, Cdkn1a, Cgref1, Ddit3, Gas2, Sesn2, Trp53inp1	Adcyap1r1, Celsr2, Olfr247, P2ry2, Slc19a2, Sstr3

Functional Group	Rhosdopsin-like Receptor Activity	Neurological system process	Nucleotide binding	Anatomical structure development	Transmembrane receptor activity	Cell Cycle
Genes	Olfr247, P2ry2, Slc19a2, Sstr3	Cldn11, Fyn, Lynx1, Ntrk2, Olfr247, Sncb	Actc1, Afg3l1, Ak1, Apaf1, Ascc3l1, Aurka, B230120h23rik, Cars, Cdc42bpg, Cry2, Cugbp1, Cyb5r1, Ddx11, Ddx19b, Dus4l, Ears2, Eef1a2, Ehd4, Eif4a2, Epha2, Ephb1, Fyn, Gne, Gsg2, Gspt2, Hnrpdl, Iars, Mapkapk3, Med12, Mthfd1, Mthfd1l, Nav1, Nme5, Ntrk2, Orc1l, Pkn3, Plk2, Rad51, Rap2a, Rap2b, Rbm19, Rbm38, Recql, Rhod, Sdha, Sgk, Smc5, Tbrg4, Tubb6, Zrsr2	Acsl6, Actc1, Adamts1, Anxa2, Apaf1, Axin2, Baiap2, Bax, Capn3, Cd81, Celsr2, Chrdl1, Cldn11, Col18a1, Cxcl4, Cyr61, Epha2, Ephb1, Fyn, Gas2, Hoxa3, Hoxd9, Hs1bp3, Ifrd1, Ift88, Klf1, Klf10, Lhx3, Lor, Lrp4, Luc7l, Mlf1, Msx1, Mt3, Myl6b, Nav1, Ntrk2, Odz4, Otx1, Pdgfa, Ppan, Ptk7, Serpine1, Serpine2, Tcf7, Tnfrsf12a, Traf4, Vcl, Unc45a, Ung, Zmat3	Adcyap1r1, Celsr2, Epha2, Ephb1, Ntrk2, Olfr247, P2ry2, Plxna1, Ptk7, Slc19a2, Sstr3	Ak1, Axin2, Aaurka, B230120h23rik, Btg3, Ccnb1, Ccng1, Cdc25b, Cdkn1a, Cgref1, Ckap2, Ddit3, Ddx11, Gas2, Gsg2, Gspt2, Mlf1, Pdgfa, Plk2, Rad51, Sesn2, Sgol2, Trp53inp1, Ube2c

Table 2. Functional Groups of genes downregulated in microarray analysis.

Functional Group	Chromatin architecture	Receptor activity	Protein complex	G-protein coupled receptor activity
Gene	Actl6b, Cbx6, Hist1h1c, Hist1h2ba, Hist1h2bb, Hist1h2bf, Hist1h2bh, Hist1h2bj, Hist1h2bk, Hist1h2bl, Hist1h2bm, Hist1h2bn, Hist1h2bp, Hist3h2ba, Hist1h3a, Hist1h3b, Hist1h3c, Hist1h3i, Hist1h4a, Hist1h4b, Hist1h4c, Hist1h4d, Hist1h4f, Hist1h4h, Hist1h4i, Hist1h4k, Hist1h4m, Suv420h2	Chrna3, Darc, Fcer1g, Impg2, Irx6, Loxl2, Msr2, Nrp1, P2ry5, Sco1	Actl6b, Apc2, Ap1s2, Chm, Chrna3, Crx, Cox4i2, Dnaic1, Dcx, Fcer1g, Gnb3, Gng2, Gng3, Gngt2, Hes6, Heyl, Hist1h1c, Hist1h2aa, Hist1h2ba, Hist1h2bb, Hist1h2bf, Hist1h2bj, Hist1h2bh, Hist1h2bk, Hist1h2bl, Hist1h2bm, Hist1h2bn, Hist1h2bp, Hist1h3a, Hist1h3b, Hist1h3c, Hist1h3i, Hist1h4b, Hist1h4a, Hist1h4c, Hist1h4d, Hist1h4f, Hist1h4h, Hist1h4i, Hist1h4k, Hist1h4m, Hist3h2ba, Irf9, Irx2, Jazf1, Kctd8, Klc3, Maz, Mbd2, Mtap2, Mxd1, Mmxd3, Myt1, Pnck, Ppm1b, Pou4f3, Prkar2b, Ptf1a, Sox8, Tcf19,	Darc, Irx6, P2ry5,

Functional Group	Nervous System development	DNA binding	Transmembrane receptor activity	Signal transducer activity
Gene	Ascl1, Chrna3, Dll3, Dab1, Dcx, Dok4, Dpysl2, Etv1, Gap43, Gli1, Hes6, Id4, Insc, Klhl1, Llgl1, Mtap2, Myt1, Ndrg2, Neurod4, Nrp1, Pex7, Pmp22, Pou4f3, Ptf1a, Serinc5, Sept4, Sox8, Stmn3, Tagln3, Tiam1	Abtb1, Ascl1, Cdkn2c, Crx, Dbp, Etv1, Gli1, Hbp1, Hes6, Heyl, Hist1h1c, Hist1h2aa, Hist1h2ba, Hist1h2bb, Hist1h2bf, Hist1h2bh, Hist1h2bj, Hist1h2bk, Hist1h2bl, Hist1h2bm, Hist1h2bn, Hist1h2bp, Hist1h3a, Hist1h3b, Hist1h3c, Hist1h3i, Hist1h4a, Hist1h4b, Hist1h4c, Hist1h4d, Hist1h4f, Hist1h4h, Hist1h4i, Hist1h4k, Hist1h4m, Hist3h2ba, Irf9, Irx2, Irx6, Isl1, Isl2, Maz, Mbd2, Mxd1, Mxd3, Mycl1, Myt1, Neil3, Neurod4, Nfatc4, Nrl, Plagl1, Pou4f3, Prdm1, Ptf1a, Safb2, Spg3a, Sox8, St18, Tcea2, Tcf19, Xpa, Zfp521, Zfp593, Zfp524	Darc, Fcer1g, Irx6, Loxl2, Msr2, Nrp1, P2ry5, Sco1	Adcyap1, Araf, Chrna3, Darc, Dok4, Fcer1g, Gnb3, Gng2, Gng3, Gngt2, Impg2, Irx6, Khdrbs2, Loxl2, Msr2, Nrp1, P2ry5, Rgs4, Rgs10, Sco1, Tiam1

Wif1 were also altered on the microarray. The altered expression of known Wnt targets and CM markers suggests that the Li^+ treatment was increasing Wnt signaling.

3.1.3 Bioinformatics Screen to identify candidate Wnt/β-catenin target genes from the microarray analysis

Although Li^+ is a well known activator of canonical β-catenin signaling (Klein and Melton, 1996), it also mediates other effects in cells raising the possibility that some of the differentially expressed genes identified in this study were not related to β-catenin activity (Quiroz et al., 2004). To prioritize the list of candidate genes for potential Wnt/β-catenin targets, the microarray results were mined for genes that contain a consensus TCF binding site. Consensus TCF-binding sites (CCTTTGWW) (Roose and Clevers, 1999) are highly conserved and are generally clustered in groups of 1-4 binding sites located up to 1kb upstream from the transcriptional start site (Gustavson et al., 2004; Jho et al., 2002; Lee et al., 2007). Therefore, we screened the list of differentially expressed genes in Li^+-treated retinal explants for genes that contained a TCF-binding site in the interval from 5kb upstream of the transcriptional start site to 1kb downstream of the transcriptional stop site. This analysis reduced the number of differentially expressed genes from 904 to 677 (Fig. 7), corresponding to 306 upregulated (Appendix F) and 371 downregulated (Appendix G) genes. To refine this list of candidate genes, the results were filtered for genes that contain a TCF-binding site with a conservation value higher than 0.7 out of a possible 1. This value was calculated using an alignment of the mouse genome to 16 vertebrate genomes with

Figure 7. Prioritizing of microarray results. The initial microarray results showed a total of 907 genes that were differentially expressed in Li^+-treated compared with control retinal explants. Filtering the data for genes that contained a consensus TCF binding site (CCTTTGWW) located in a region 5kb upstream to 1kb downstream of the transcriptional start site reduced the number of array hits to 677. To further filter the data, genes with putative TCF binding sites that had a conservation value of >0.7 (out of a possible 1) were identified. This resulted in the final number of 260 differentially expressed genes identified from the microarray data. Numbers below the stated amount of genes identified represent the breakdown of upregulated and downregulated genes.

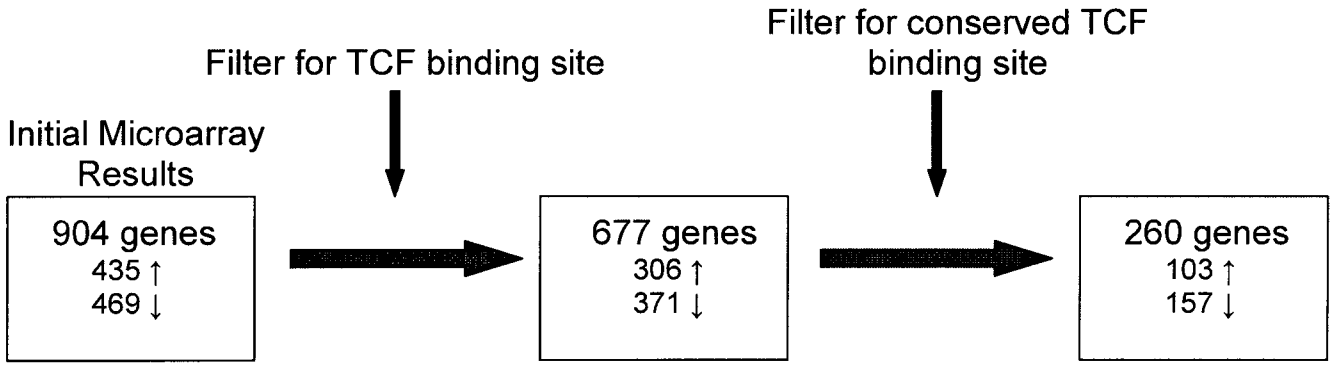
Initial Microarray Results
904 genes
435 ↑
469 ↓
Filter for TCF binding site
677 genes
306 ↑
371 ↓
Filter for conserved TCF binding site
260 genes
103 ↑
157 ↓

completed sequences from the UCSC genome browser (Karolchik et al., 2003). The alignment was done by generating pairwise alignments for each species using blastz. A multiple alignment was then constructed from the pairwise alignments using multiz. Predictions of conserved elements were then obtained by running phastCons on the multiple alignments with the most-conserved option. This final screen reduced the number of candidate targets to 260 genes (Fig. 7). The list of prioritized genes is reported in Appendix H and I. The known Wnt targets *Wif1* and *Axin2,* as well as CB markers *Msx1* and *Otx1* are represented in this final filtered list of genes, indicating that this approach is able to enrich for known Wnt target genes.

3.1.4 Validation of putative Wnt targets from microarray analysis

To facilitate the validation of candidate Wnt target genes identified in the bioformatic screen, genes with conserved TCF binding sites were analyzed using GoStat to identify their functional annotation (Tables 3 and 4). Genes were selected for validation based on their function; prioritizing genes involved in neurogenesis, cell proliferation and differentiation. Additionally, differentially expressed genes that exhibited a high fold-change, contained numerous TCF-binding sites or that were known Wnt target genes in other tissues, were also selected for further expression analysis. The prioritized list is summarized in Table 5. The first method of validation was performed by Q-PCR using two sources of RNA to measure gene expression. The first source was derived from Li^+-treated retinal explants, prepared as described in the previous section. The second source was derived from transgenic mice with conditional activation of β-catenin in the retina (Liu et al., 2006). These mice were

Table 3. Functional Groups of upregulated genes from microarray analysis with highly conserved TCF binding sites.

Functional Group	Genes
Pattern Specification	Axin2, Celsr2, Cyr61, Hoxa3, Hoxd9, Lrp4, Otx1
Cellular Proliferation	Axin2, Col18a1, Gspt2, Hoxa3, Msx1, Pdgfa, Sco1, Tcf7, Ube2c,
Embryonic Morphogenesis	Celsr2, Lrp4, Msx1, Otx1, Ptk7, Tcf7
Regulation of Apoptosis	Atf5, Col18a1, Msx1, Raet1b, Tcf7, Traf4, Trp53inp1, Tsc22d3
Cellular Differentiation	Atf5, Axin2, Cdc25b, Col18a1, Elmo1, Epha2, Fyn, Klf10, Lrp4, Mlf1, Msx1, Ptk7, Raet1b, Sco1, Serpine2, Tcf7, Traf4, Trp53inp1, Tsc22d3,
Cell Cycle Regulation	Aurka, Axin2, Btg3, Cdc25b, Gspt2, Mlf1, Pdgfa, Plk2, Sesn2, Trp53inp1, Ube2c
Protein-tyrosine Kinase Activity	Epha2, Fyn, Ptk7, Sco1, Wif1
Wnt Receptor Signaling Pathway	Axin2, Celsr2, Lrp4, Tcf7, Wif1

Table 4. Functional Groups of genes downregulated in microarray analysis with highly conserved TCF binding sites.

Functional Group	Chromatin architecture	Protein complex	Transcriptional Regulation
Genes	Hist1h4k, Hist1h4m, Hist1h2aa, Hist1h2ba, Hist1h2bb, Hist1h2bf, Hist1h2bh, Hist1h2bj, Hist1h2bn, Hist1h2bp, Hist1h3a, Hist1h3b, Hist1h3c, Hist1h3i, Hist1h4a, Hist1h4b, Hist1h4c, Hist1h4d, Hist1h4f, Hist1h4h, Hist1h4i	Apc2, Ap1s2, Chm, Cox4i2, Dcx, Fcer1g, Gng2, Gng3, Hes6, Hist1h2aa, Hist1h2ba, Hist1h2bb, Hist1h2bf, Hist1h2bh, Hist1h2bj, Hist1h2bn, Hist1h2bp, Hist1h3a, Hist1h3b, Hist1h3c, Hist1h3i, Hist1h4a, Hist1h4b, Hist1h4c, Hist1h4d, Hist1h4f, Hist1h4h, Hist1h4i, Hist1h4k, Hist1h4m, Irf9, Irx2, Mtap2, Mxd1, Mxd3, Myt1, Pou4f3, Prkar2b, Ptf1a, Tcf19	Abtb1, Ascl1, Dbp, Etv1, Hbp1, Hes6, Id2, Id3, Irf9, Irx2, Isl1, Isl2, Khdrbs2, Mxd1, Mxd3, Mycl1, Myt1, Nfatc4, Neurod4, Pou4f3, Prdm1, Ptf1a, Rdbp, St18, Tcf19, Zfp524, Zfp521, Zfp593, Zfp68, Zfp91

Functional Group	Nervous System development	DNA binding	Transmembrane receptor activity	Signal transducer activity
Genes	Ascl1, Dab1, Dcx, Dpysl2, Etv1, Hes6, Klhl1, Mtap2, Myt1, Ndrg2, Neurod4, Pex7, Pou4f3, Ptf1a	Abtb1, Ascl1, Dbp, Etv1, Hbp1, Hes6, Hist1h2aa, Hist1h2ba, Hist1h2bb, Hist1h2bf, Hist1h2bh, Hist1h2bj, Hist1h2bn, Hist1h2bp, Hist1h3a, Hist1h3b, Hist1h3c, Hist1h3i, Hist1h4b, Hist1h4c, Hist1h4a, Hist1h4d, Hist1h4f, Hist1h4h, Hist1h4i, Hist1h4k, Hist1h4m, Irf9, Irx2, Isl1, Isl2, Mxd1, Mxd3, Mycl1, Myt1, Neurod4, Nfatc4, Prdm1, Pou4f3, Ptf1a, St18, Tcf19, Zfp521, Zfp524, Zfp593, Zfp91	Fcer1g, Loxl2, P2ry5,	Adcyap1, Araf, Fcer1g, Gng2, Gng3, Khdrbs2, Loxl2, P2ry5, Pnrc1, Rgs4

Table 5. Genes selected for microarray validation.

	Fold change on microarray (M stdev)	# TCF-binding sites
Wnt targets		
Wnt inhibitory factor 1 (*Wif1*)	29.22 (3.15)	1
Axin2	2.81 (0.95)	4
CM markers		
Msh homeobox 1 (*Msx1*)	2.34 (0.73)	3
Orthodenticle 1(*Otx1*)	1.82 (1.00)	7
Neurogenesis		
Eph receptor A2 (*Epha2*)	8.36 (3.20)	1
Ephrin A3 (*Efna3*)	1.71 (0.67)	1
Synaptotagmin 13 (*Syt13*)	-11.02 (2.33)	6
Prickle-like 1 (*Prickle1*)	-6.10 (0.88)	1
N-myc downstream regulated gene 2 (*Ndrg2*)	-2.84 (1.21)	2
Cell Cycle		
Cyclin-dependent kinase inhibitor 1A (*Cdkn1a*/p21)	22.78 (1.29)	3
Differentiation		
Serpin peptidase inhibitor, clade E, member 2 (*Serpine2*)	25.12 (1.52)	1
Kruppel-like factor 10 (*Klf10*)	3.43 (0.21)	1
Cell division cycle 25 homolog B (*Cdc25b*)	1.86 (0.29)	1
Limb expression 1 (*Lix1*)	2.54 (0.25)	4
Cell Signaling		
Tumor necrosis factor receptor super family 19 (*Tnfrsf19/Troy*)	20.85 (2.89)	2
Mediator complex subunit 12 (*Med12*)	1.99 (0.36)	3

generated by crossing *α-Cre-GFP* transgenic mice, where Cre activity in the peripheral retina is driven by a regulatory element of Pax6 (Marquardt et al., 2001), with β-catenin transgenic mice (*Catnb*$^{+/lox\,(ex3)}$), where exon3 of β-catenin is flanked by lox-P sites (Harada et al., 1999). This cross produces offspring (*α-Cre;Catnb*$^{+/lox\,(ex3)}$, referred to subsequently as CatnbΔex3 mutant mice), in which the GSK-3β phosphorylation site in exon3 of β-catenin is removed by Cre-mediated excision, resulting in a constitutively active form of β-catenin (Liu et al., 2007). In this validation, gene expression was quantified in 3 independent experiments performed in triplicate in which 2-4 whole eyes from CatnbΔex3 mutant embryos (E14) were pooled together for each sample. Non-mutant littermates (*α-Cre;Catnb*$^{+/+}$) were used as control. Primer efficiency was determined using E14 wild-type retinas and observed CT changes were normalized to both GAPDH and 18S. *Wif1*, *Axin2*, *Tnfrsf19* and *Cdkn1a* (p21), all genes that were upregulated on the microarray were confirmed to be upregulated in Li^+-treated explants and mutant mouse samples (Fig. 8). With the exception of *Wif1, Axin2* and p21, the fold changes of expression in the explants and transgenic mice were generally lower than what was observed in the microarray analysis (Fig. 8). *Efna3* and *Serpine2* were significantly increased (Fig. 8), and *Syt13* and *Ndrg2* decreased (Fig. 9) in the explants, however no significant changes in expression were detected in the mutant retina for these genes, whereas *Lix1* was upregulated in the mutant retina, but not the explants (Fig. 8). In contrast, *Epha2* and *Med12*, which were upregulated in the microarray, were not changed in explants or mutant tissue (Fig. 10). Interestingly, *Prickle1*, *Klf10*, and *Cdc25b* were validated in the retinal explants, however the observed changes in gene expression in mutant tissue were opposite from what was reported from the microarray (Fig. 10), although these changes were not statistically significant. In general,

Figure 8. Q-PCR validation of gene expression in Li^+-treated retinal explants and CatnbΔex3 mutant eyes of upregulated genes. Quantitative RT-PCR (normalized to GAPDH and 18S) was performed using RNA extracted from Li^+-treated retinal explants and whole eyes from E14 CatnbΔex3 mutant mice. A total of 3 independent experiments were performed in triplicate (n=3). Numbers in parenthesis indicate the fold change reported from the microarray analysis. Results are expressed as mean fold change in Li^+ compared with NaCl-treated explants and CatnbΔex3 with littermate eyes ± S.D. *$p<0.05$.

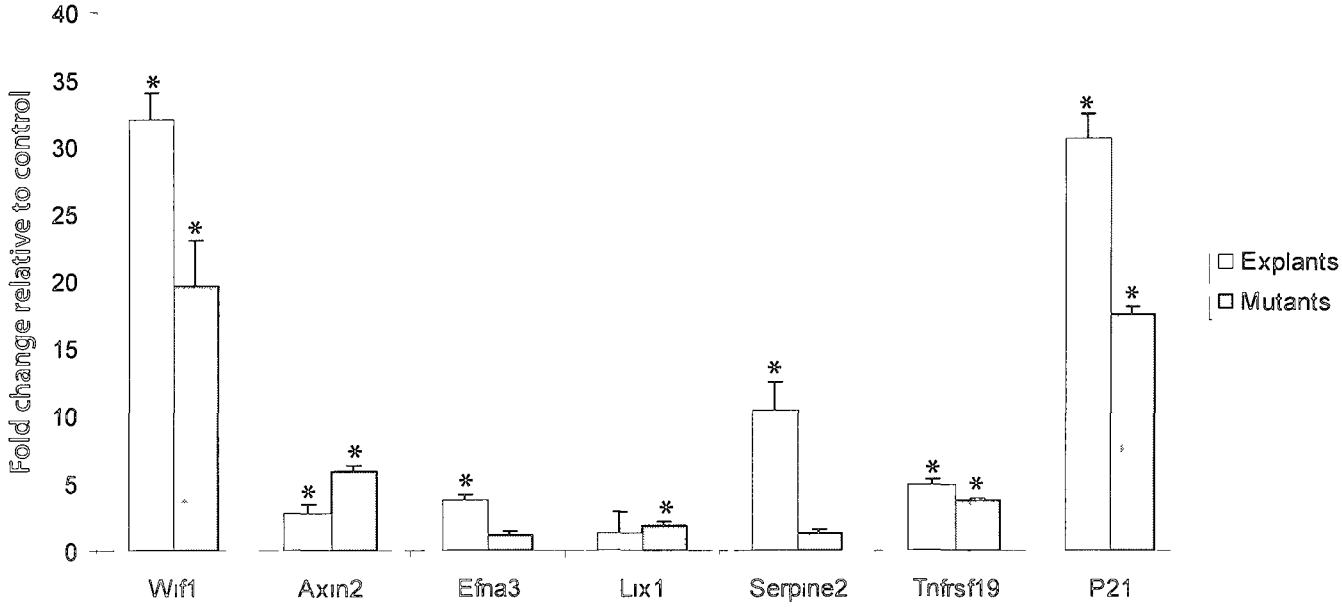
40
35
30
25
20
15
10
5
0
Fold change relative to control
Explants
Mutants
Wif1
Axin2
Efna3
Lix1
Serpine2
Tnfrsf19
P21

Figure 9. Q-PCR validation of gene expression in Li^+-treated retinal explants and CatnbΔex3 mutant eyes of downregulated genes. Quantitative RT-PCR (normalized to GAPDH and 18S) was performed using RNA extracted from Li^+-treated retinal explants and whole eyes from E14 CatnbΔex3 mutant mice. A total of 3 independent experiments were performed in triplicate (n=3). Numbers in parenthesis indicate the fold change reported from the microarray analysis. Results are expressed as mean fold change in Li^+ compared with NaCl-treated explants and CatnbΔex3 with littermate eyes ± S.D. *$p<0.05$.

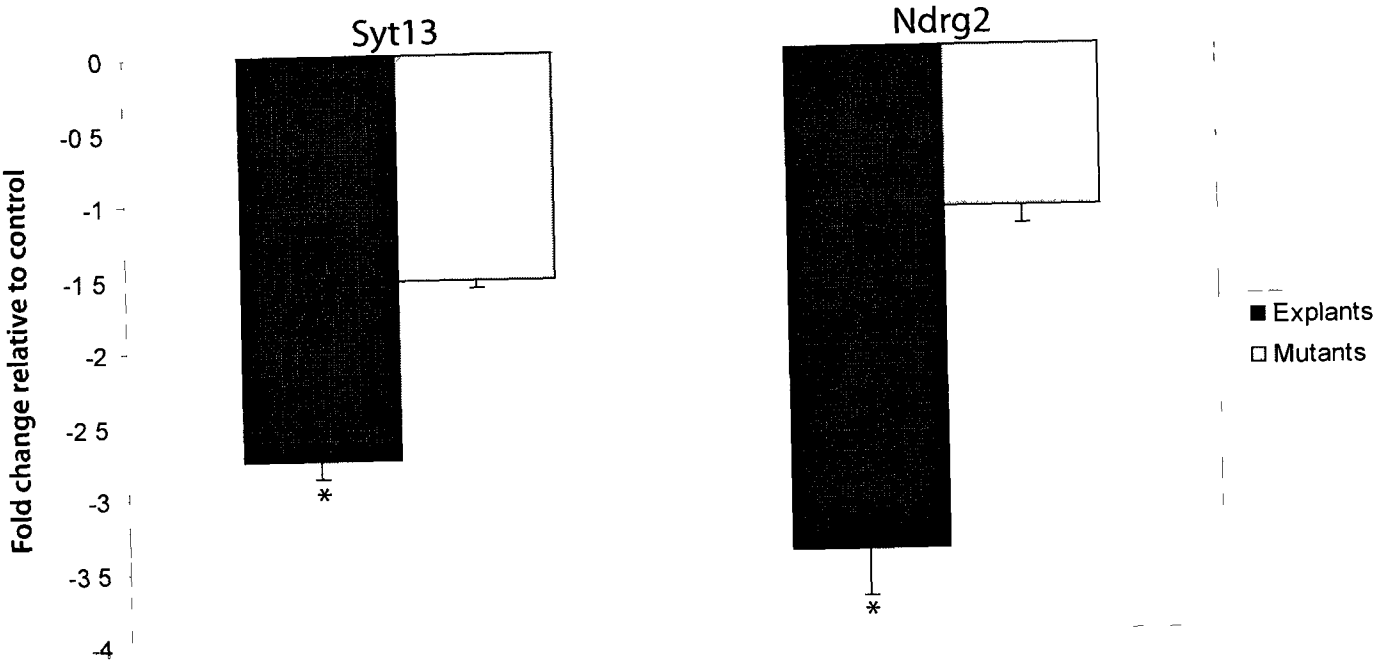
Syt13
Ndrg2
Fold change relative to control
0
-0 5
-1
-1 5
-2
-2 5
-3
-3 5
-4
*
*
Explants
Mutants

Figure 10. Q-PCR analysis of gene expression in Li^+-treated retinal explants and CatnbΔex3 mutant eyes of non-validated genes. Quantitative RT-PCR (normalized to GAPDH and 18S) was performed using RNA extracted from Li^+-treated retinal explants and whole eyes from E14 CatnbΔex3 mutant mice. A total of 3 independent experiments were performed in triplicate (n=3). Numbers in parenthesis indicate the fold change reported from the microarray analysis. Results are expressed as mean fold change in Li^+ compared with NaCl-treated explants and CatnbΔex3 with littermate eyes ± S.D.

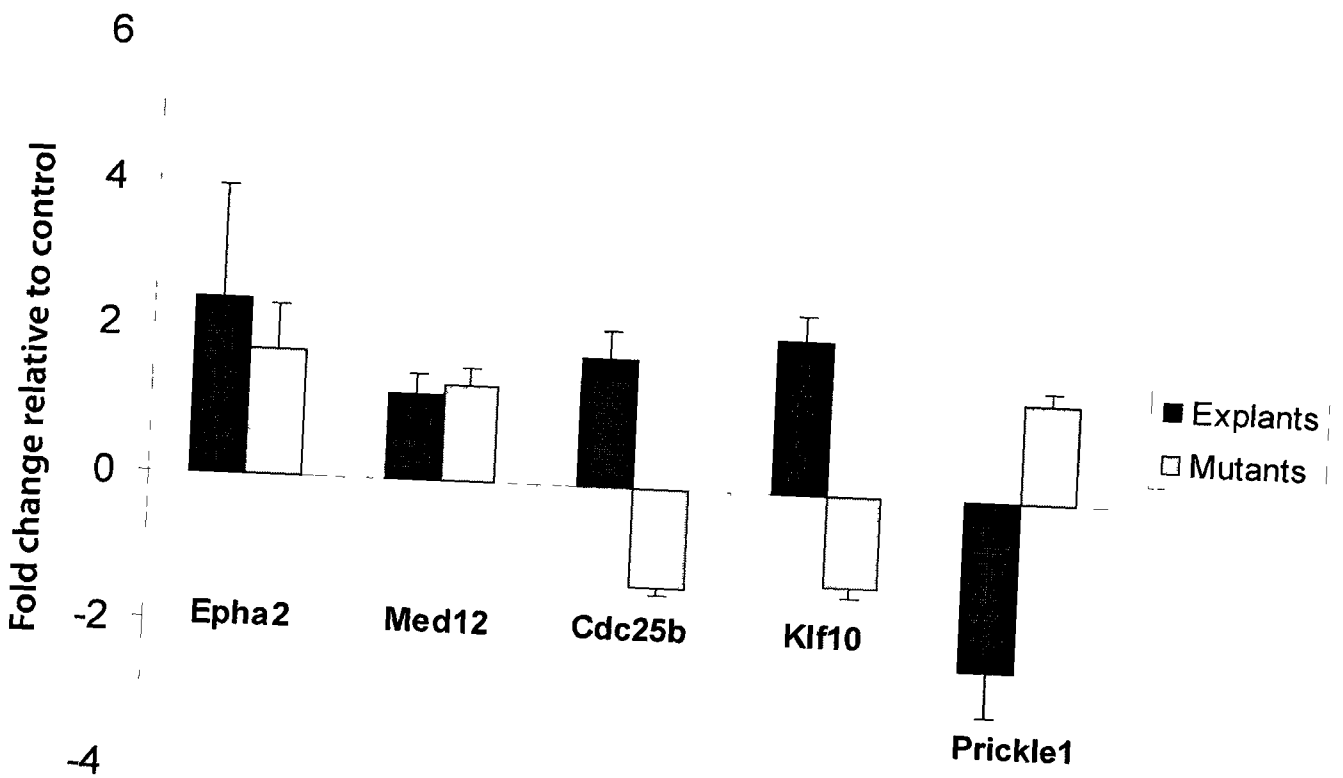
6
4
2
0
-2
-4
Fold change relative to control
Epha2
Med12
Cdc25b
Klf10
Prickle1
Explants
Mutants

the Q-PCR analysis of Li^+-treated explants was consistent with the results of the microarray analysis. However, the changes in gene expression were more consistent in the explants compared with the retinal tissue from the mutant mice, which could be related to reduced sensitivity because of the presence of wild-type retinal tissue in this mouse model.

To investigate whether differentially expressed genes identified in the bioinformatic analysis are expressed in the CM, and whether their expression was associated with increased β-catenin activity, the expression profile of candidate genes was assessed by *in situ* hybridization (ISH) on serial retinal sections of control and mutant mice. In the mutant mice, the conditional activation of β-catenin results in an increase in TCF-LacZ reporter activity and an expansion of the CM, as shown by the increased domain of the CM markers as previously reported (Liu et al., 2007). Mice that were *α-Cre;Catnb*$^{+/lox(ex3)}$ or *α-Cre;Catnb*$^{+/lox(ex3)}$*;TCF/Lef-LacZ* were designated as CatnbΔex3 mutant mice while littermates that were *α-Cre;Catnb*$^{+/+}$ or *α-Cre;Catnb*$^{+/+}$*;TCF/Lef-LacZ* were designated as control or wild-type (WT) mice. ISH for *Cdkn1a*(p21), *Tnfrsf19*, and *Wif1*, genes that were up-regulated in the microarray (Fig. 8), revealed that these genes are expressed in the expanded CM in the mutant eye, as their expression patterns overlapped with that of the CM marker *Msx1* and the region with increased β-gal activity (Fig. 11 and 12). It was also noted that the increased expression was restricted to the mutant region of the retina and excluded from the neural retina, which is marked by CyclinD1 expression (Fig. 11 and 12). It should be noted, however, that expression of these genes were not detected in the wild-type CM (Fig 11 and 12). *Syt13*, was expressed in the neural retina, but not the expanded CM in the retinas of mutant mice (Fig 13), which is consistent with the downregulation of this gene in the microarray analysis (Fig. 9). ISH for *Lix1* and *Med12* has offered an explanation on why

Figure 11. ISH analyses of *Cdkn1a* and *Tnfrsf19* expression in CatnbΔex3 mutant retinas. Serial horizontal retinal sections from E14.5 wild-type littermates (a-e) and CatnbΔex3 mutant mice (f-j), were processed for β-gal staining (a, f) and ISH *CyclinD1* (b, g), *Msx1* (c, h), *Cdkn1a* (d, i), and *Tnfrsf19* (e, j). Mice were crossed with TCF-LacZ reporter mice to monitor Wnt/β-catenin activity. In regions were Wnt signaling is activated, shown by β-gal activity (f), the expansion of expression of the microarray candidate genes *Cdkn1a* (i) and *Tnfrsf19* (j) is within the expanded CM region as shown by *Msx1* (h) and separate from the neural retina, shown by *CyclinD1* (g). Inset in (a) is a higher magnification view of the CM region where Wnt signaling is active. Arrows in (i) and (j) indicate expanded CM region on temporal side of eye not seen in (f-h) due to uneven generation of retinal sections during cryosectioning. Dotted line indicates expanded CM region. Scale bar: 100μm.

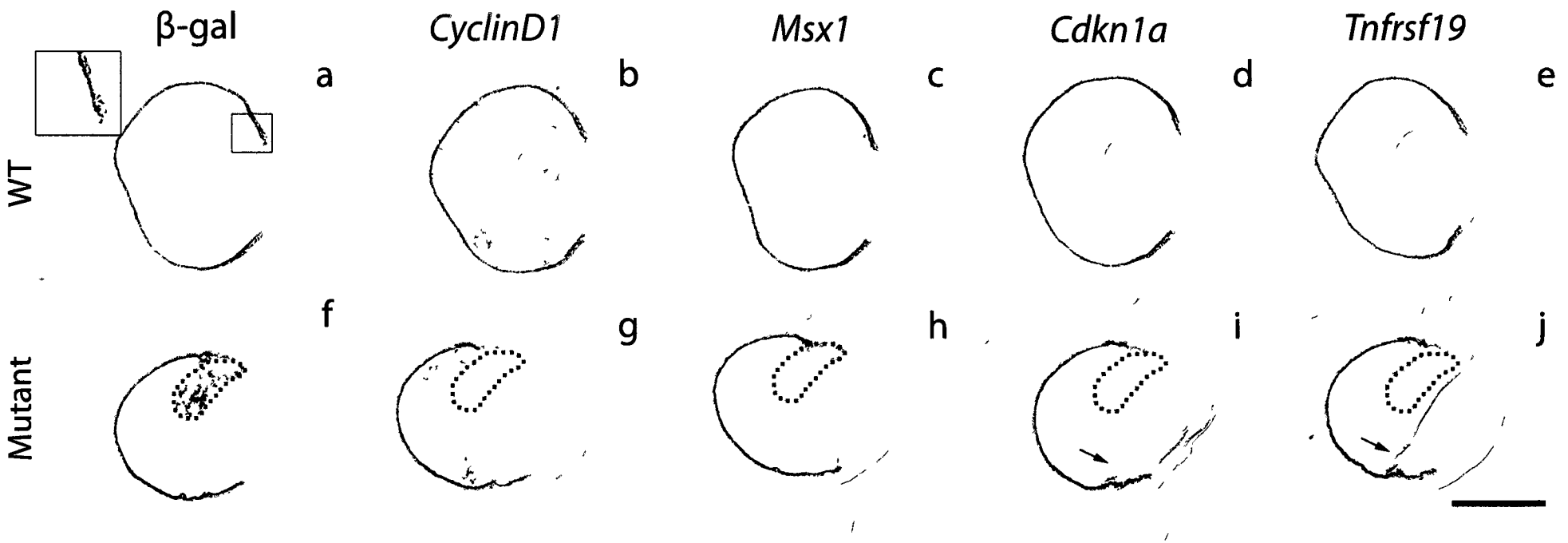
β-gal
CyclinD1
Msx1
Cdkn1a
Tnfrsf19
a
b
c
d
e
WT
f
g
h
i
j
Mutant
E14

Figure 12. ISH analysis of *Wif1* expression in CatnbΔex3 mutant eyes. Serial horizontal retinal sections from E14.5 wild-type littermates (a-c) and CatnbΔex3 mutant mice (d-f), were processed for β-gal staining (a, d), and ISH for *Wif1* (b, e), and *CyclinD1* (c, f). In regions were Wnt signaling is activated, shown by β-gal activity (d), the expansion of expression of the Wnt target *Wif1* (e) is in the same region where Wnt signaling is activated, shown by β-gal activity (d) and is separate from that of the neural retina as shown by *CyclinD1* (f). Dotted line indicates expanded CM region. Scale bar: 100μm.

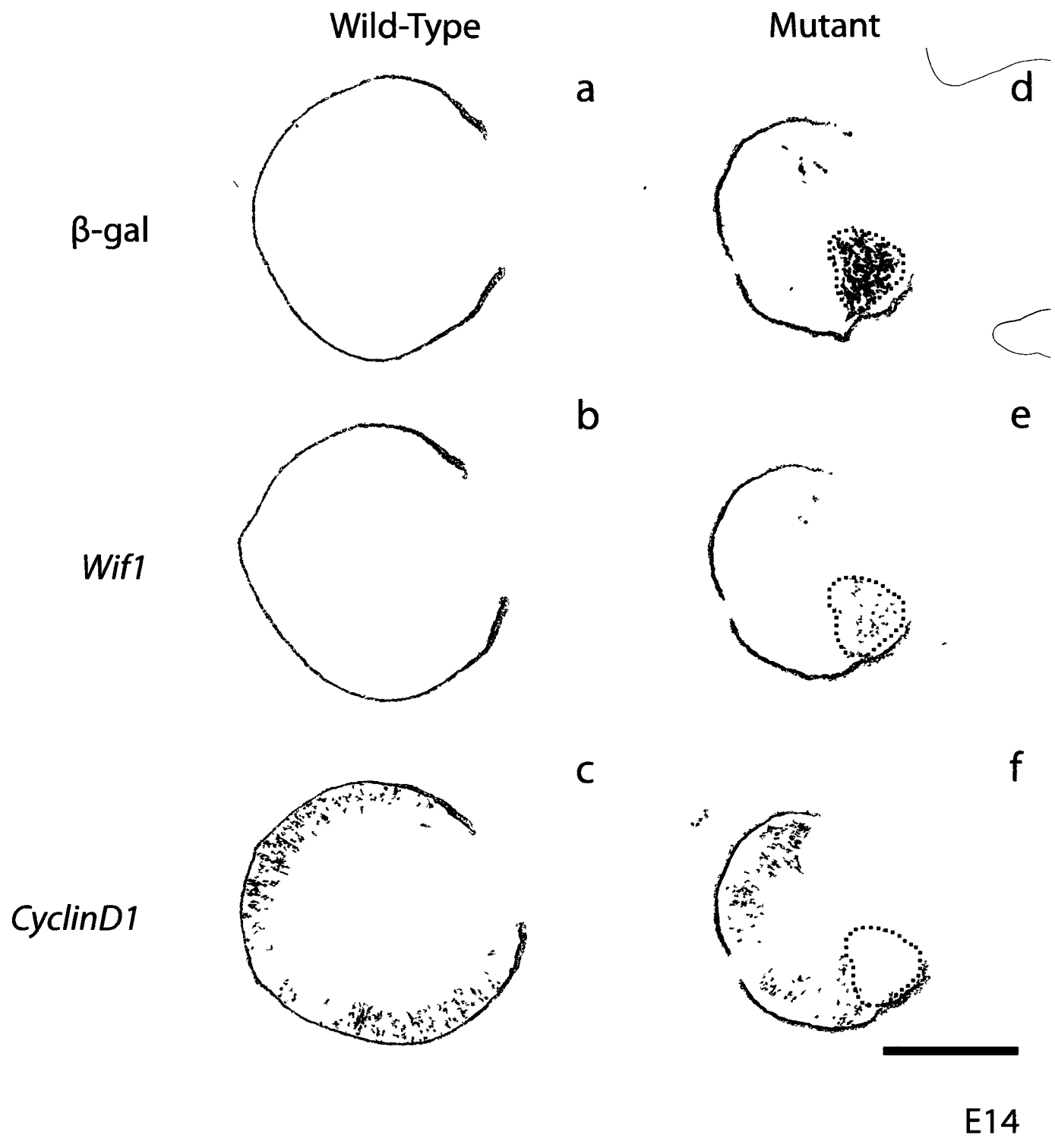
Wild-Type
Mutant
β-gal
Wif1
CyclinD1
a
b
c
d
e
f
E14

Figure 13. ISH analysis of Syt13 expression in CatnbΔex3 mutant eyes. Serial horizontal retinal sections from E14.5 wild-type littermates (a, b) and CatnbΔex3 mutant mice (c, d) were processed by ISH for mRNA of *Msx1* (a, d) and *Syt13* (b, d). *Syt13* was expressed in the neural retina (d) but not in the expanded CM region shown by *Msx1* (c). Dotted line indicates expanded CM region. Scale bar: 100μm.

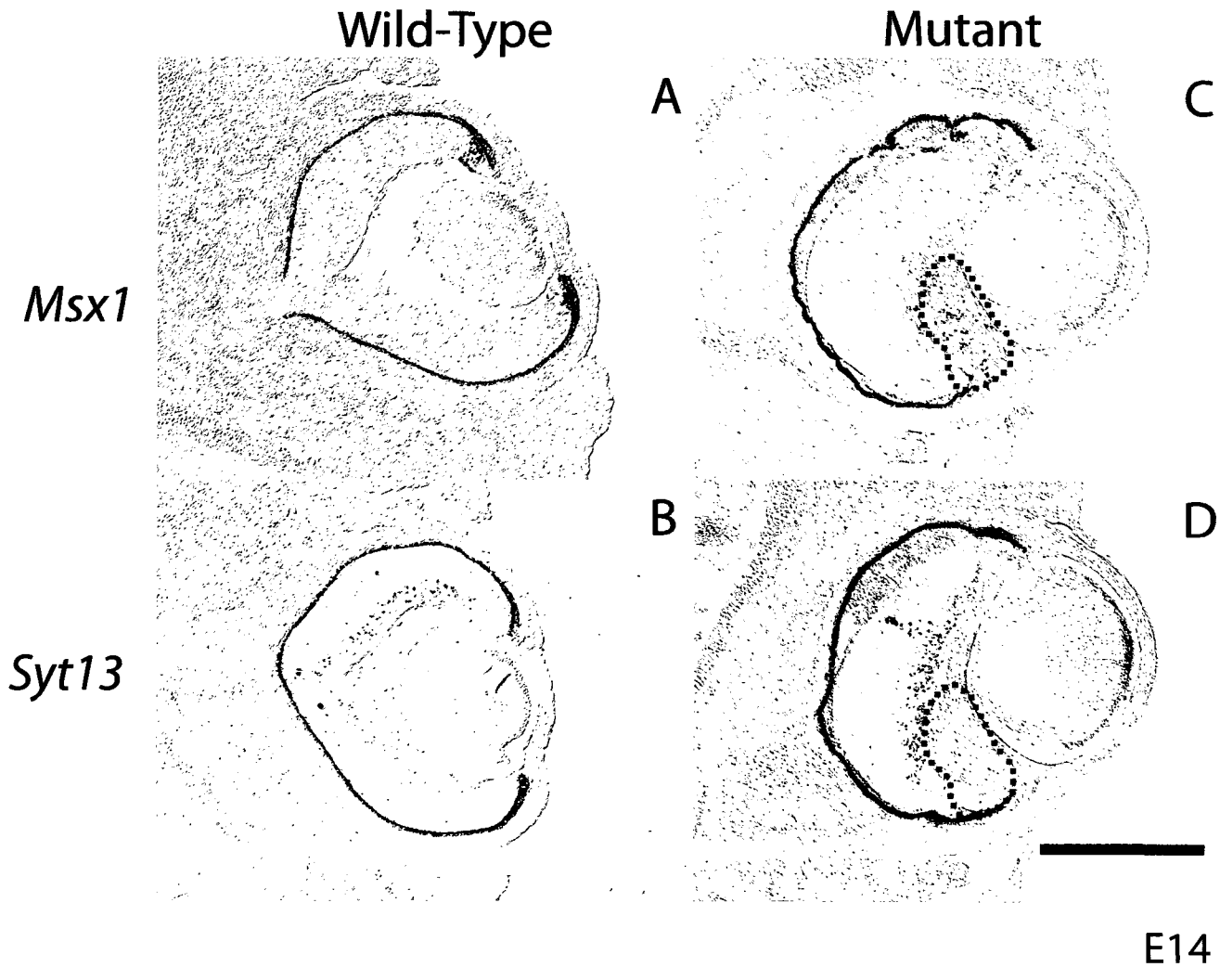
Wild-Type
Mutant
Msx1
Syt13
A
B
C
D
E14

these two genes were not validated by Q-PCR analysis of mutant mouse retinal tissue, *Med12* expression was ubiquitous in the retinas of both wild-type and mutant mice and although *Lix1* expression was observed in regions surrounding the eye, it was undetectable in the retina (Fig. 14). A summary of the candidate gene validation is shown in Table 6.

The expression of the collagen gene *Col9a1* and amino acid transporter *Slc7a8* has been shown to be enriched in the developing CM (Kubota et al., 2004; Thut et al., 2001), however, their expression has not previously been linked with activity of the canonical Wnt pathway. The microarray analysis identified a number of *Col* and *Slc* isoforms that harbor conserved TCF binding sites within their promoter regions and these genes were upregulated with Li^+-treatment (Appendix 8). Therefore, we selected the following genes for further characterization as possible Wnt signaling target genes in the developing CM: *Col6a1, Col18a1, Slc7a3, Slc7a7, and Slc44a2.* Unfortunately, Q-PCR analysis of these genes showed that the expression of these genes did not significantly change upon Li^+ treatment as reported from the microarray (Fig. 15). Although *Col18a1* expression did not change by Q-PCR in Li^+-treated retinal explants, its expression pattern was investigated by ISH in *CatnbΔex3;LacZ* mice since previous studies reported its expression in the CM region in chick during development (Dong et al., 2002). The expression of *Col18a1* in *Catnb*$^{+/+}$*;LacZ* controls (E14) was primarily localized to the peripheral regions of the optic cup with weaker expression throughout the retina (Fig. 16). However, unlike other Wnt targets that were identified in this study, the expression of *Col18a1* in E14 *CatnbΔex3;LacZ* mutant eyes did not co-localize with *Msx1* expression or β-gal staining for Wnt activity (Fig. 16). Unlike the expression pattern of *Msx1*, which broadens within the expanded CM of the *CatnbΔex3* mice, *Col18a1* expression in the mutant appears to be displaced by the CM. This

Figure 14. Expression of *Med12* and *Lix* in CatnbΔex3 mutant eyes. Serial retinal sections from E14.5 control littermates (a, b), and CatnbΔex3 mutant mice (c, d), were processed by ISH for *Med12* (a, c) and *Lix* (b, d). Expression of *Med12* in mutant eyes (c) was detected throughout the eye similar to wild-type eyes (a) and *Lix* is undetectable in mutant (d) or control eyes (b). Scale bar: 100μm.

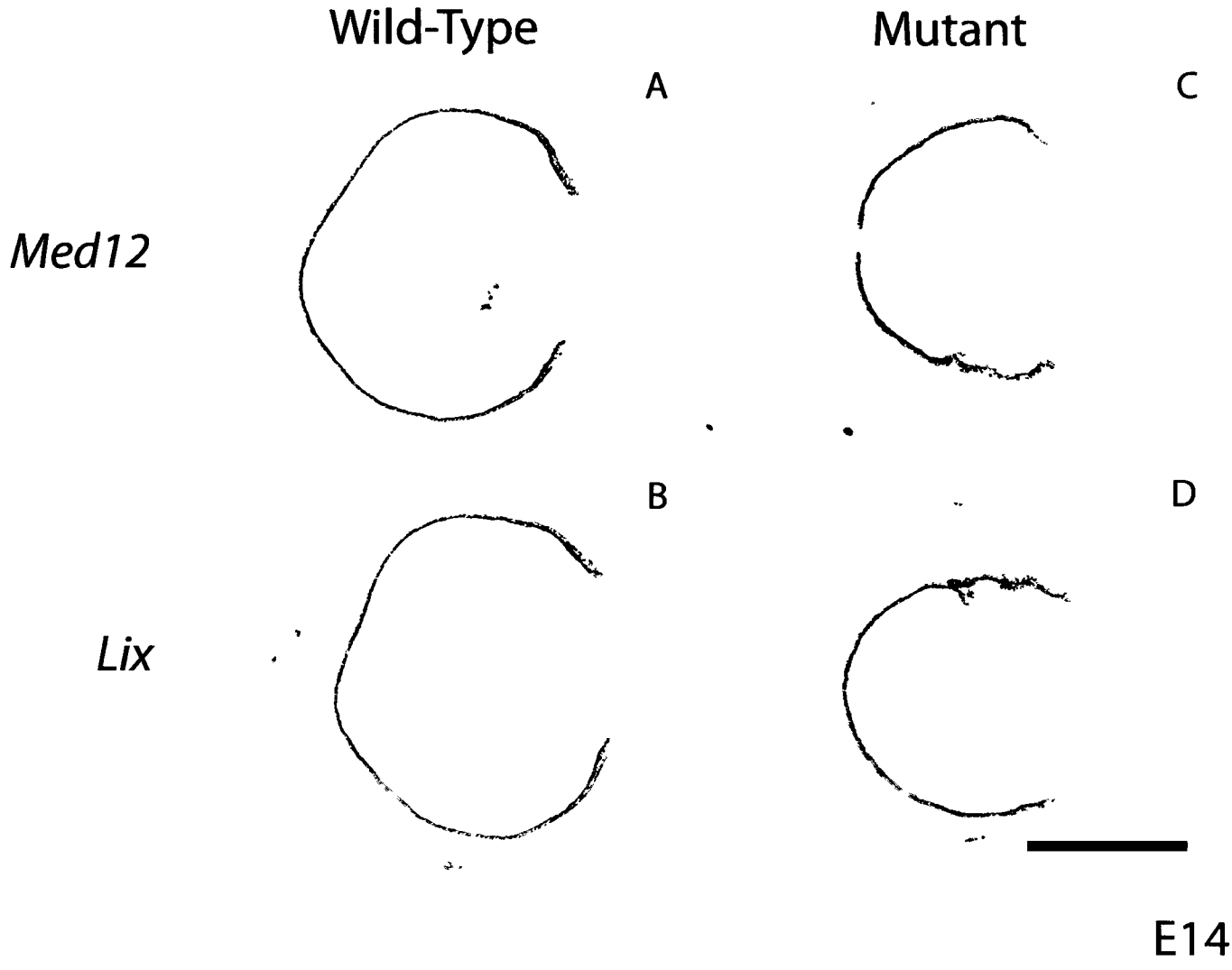
Wild-Type
Mutant
A
C
Med12
B
D
Lix
E14

Table 6. Summary of candidate microarray gene validation.

Candidate Genes from Microarray	Validated by q-PCR in explants	Validated by q-PCR in mutants	Validated by ISH
Wif1	+	+	+
Axin2	+	+	-
Epha2	-	-	-
Efna3	-	-	-
Syt13	+	-	+
Prickle1	+	-	-
Ndrg2	+	-	-
Cdkn1a	+	+	+
Serpine2	+	-	-
Klf10	+	-	-
Cdc25b	+	-	-
Lix1	+	+	-
Tnfrsf19	+	+	+
Med12	-	-	-

Genes that were validated in the specified experiment are marked with a (+) and those that were not with a (-). Genes that did not validate in retinal explants or mutant tissue include *Epha2, Efna3,* and *Med12. Cdkn1a* and *Tnfrsf19* were validated in all experiments.

Figure 15. Q-PCR analysis of *Col* and *Slc* gene expression in Li^+-treated retinal explants. Quantitative RT-PCR (normalized to GAPDH and 18S) was performed for the indicated genes on RNA extracted from retinal explants cultured in Li^+ for 24 h. A total of 3 independent experiments were performed in triplicate (n=3). Numbers in parenthesis indicate the fold change reported from the microarray analysis. Results are expressed as mean fold change in Li^+ compared with NaCl-treated explants ± S.D. *$p<0.05$.

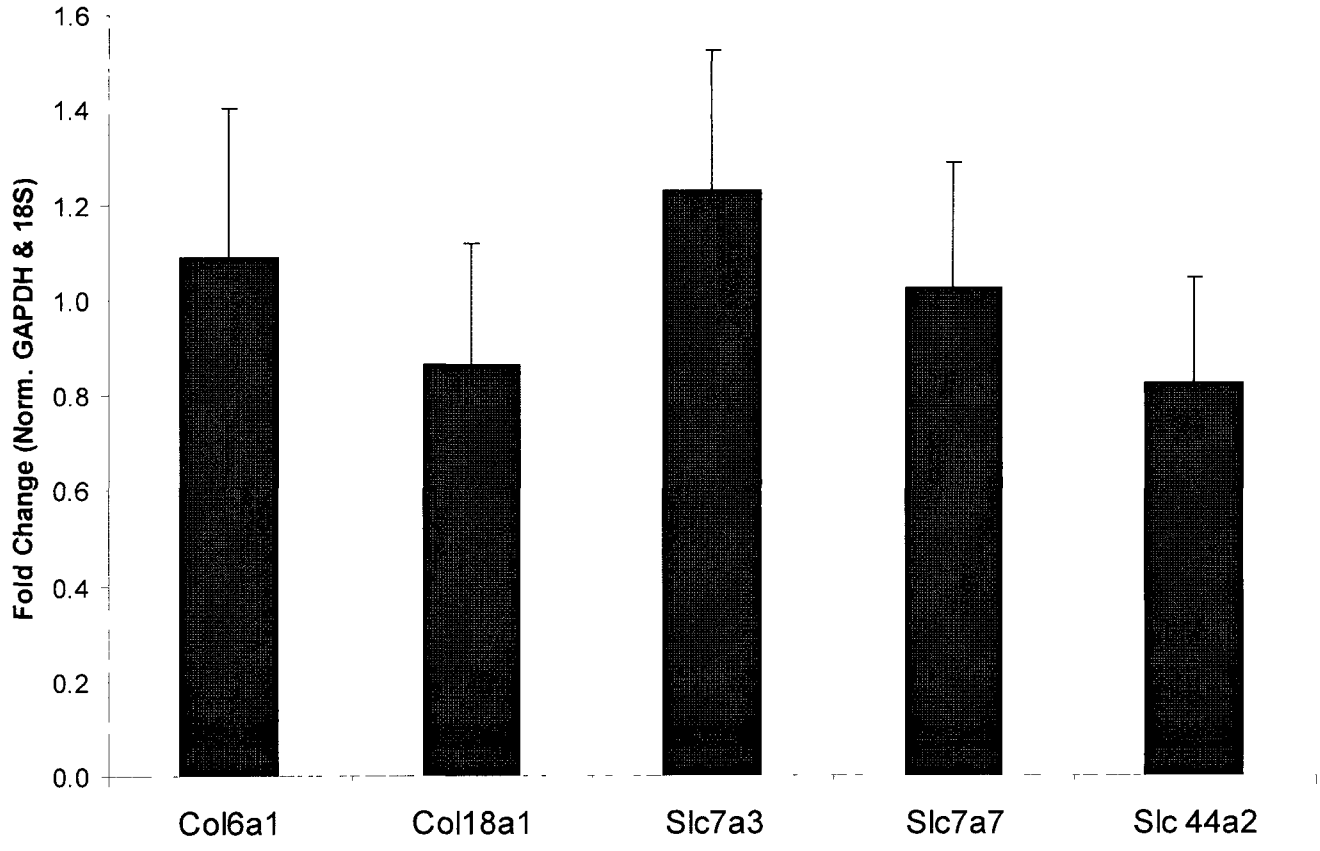
Fold Change (Norm. GAPDH & 18S)
1.6
1.4
1.2
1.0
0.8
0.6
0.4
0.2
0.0
Col6a1
Col18a1
Slc7a3
Slc7a7
Slc 44a2

Figure 16. Expression of *Col18a1* in CatnbΔex3 mutant eyes. Serial retinal sections from E14.5 wild-type littermates (a-d) and CatnbΔex3 mutant mice (e-h) were processed for β-gal staining and ISH for mRNA of *Msx1* (b, e), *Col18a1* (c, g), and *CyclinD1* (d, h). *Col18a1* (f) was detected outside the CM marked by *Msx1* (e) and is detected in low levels within neural retina, as marked by *CyclinD1* (g). Dotted line indicates expanded CM region. Scale bar: 100μm.

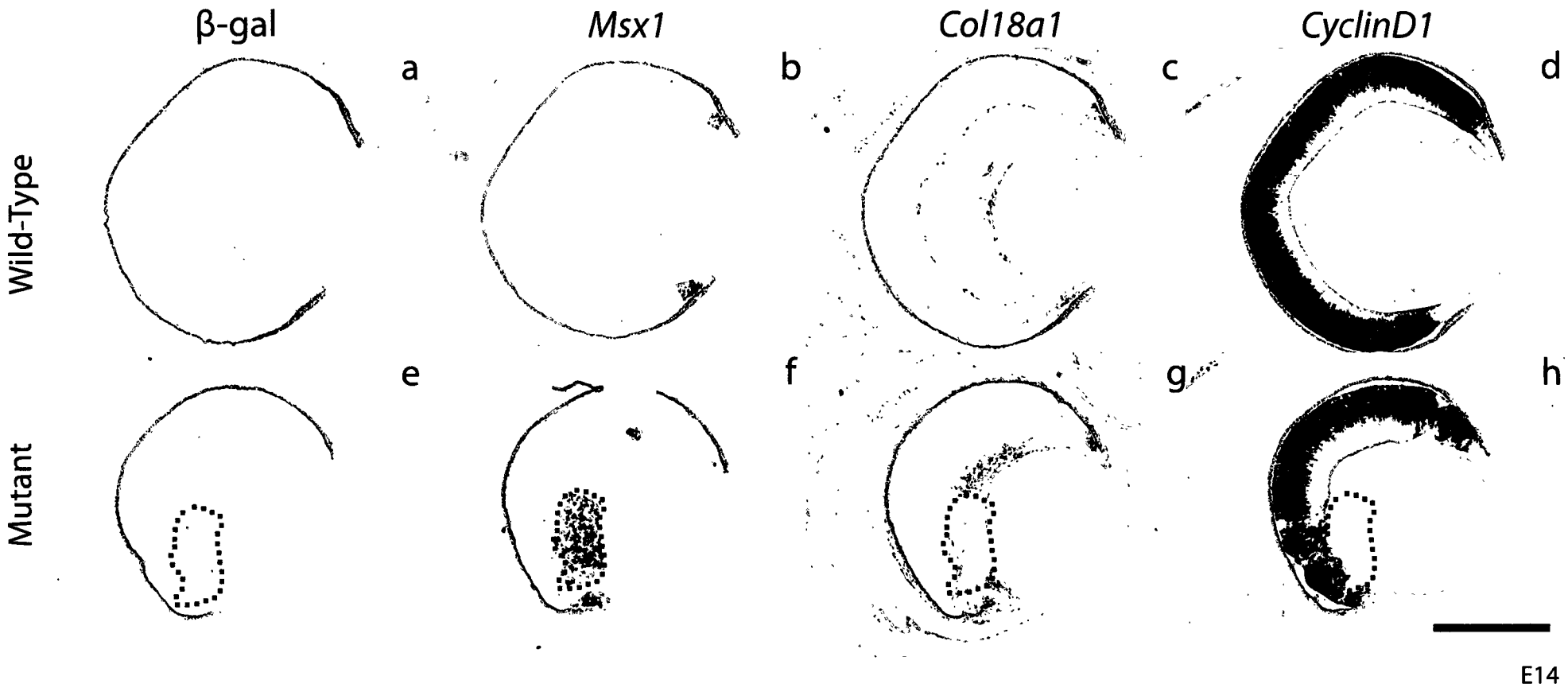
β-gal
Msx1
Col18a1
CyclinD1
Wild-Type
Mutant
a
b
c
d
e
f
g
h
E14

observation suggests that *Col18a1* is not a CM marker in mouse development despite its expression in the developing chick CM.

3.2 Functional Analysis of Msx1 as a Wnt target in CM development

The vertebrate muscle segment homeobox gene, *Msx1,* has been previously characterized as a CM marker (Monaghan et al., 1991) and is upregulated following activation of canonical Wnt signaling in the developing CM (reviewed by Ramos and Robert, 2005). However, the function of this gene downstream of Wnt signaling in the CM has not been characterized. Therefore, the effect of ectopic *Msx1* expression on retinal progenitor proliferation and gene expression was examined. E14 retinal explants were co-electroporated with *Msx1* and GFP or GFP alone (control) and cultured for 3 days. ISH and IHC demonstrated co-localization of *Msx1* expression and GFP activity in serial sections of co-electroporated explants. In contrast, in GFP electroporated control explants, GFP immunofluorescence was detected but *Msx1* expression was absent (Fig. 17). Furthermore, ISH demonstrated that *Msx1* is able to be ectopically expressed in regions of GFP activity in *Msx1*/GFP co-electroporated explants.

Msx1 has been shown to inhibit neurogenesis through inhibition of bHLH genes (Bendall and Abate-Shen, 2000). Therefore, Q-PCR analysis was performed to monitor the expression of bHLH genes in electroporated retinal explants. As outlined above, retinal explants were electroporated with *Msx1*/GFP and GFP alone and cultured for three days. The expression of several bHLH genes were analyzed by pooling 2-3 explants for each

Figure 17. Ectopic expression of *Msx1* in retinal explants. E14 retinal explants from CD1 mice were electroporated with GFP or a combination of GFP and *Msx1* expression vectors and cultured for 3 days. Cross sections from explants were analyzed for GFP immunoflourescence and *Msx1* expression by ISH. GFP activity is in the control and Msx1-electroporated explants, and Msx1 expression was detected only in the GFP + *Msx1* sample and was localized to the region with GFP activity. (n=7). Scale bar: 100μm.

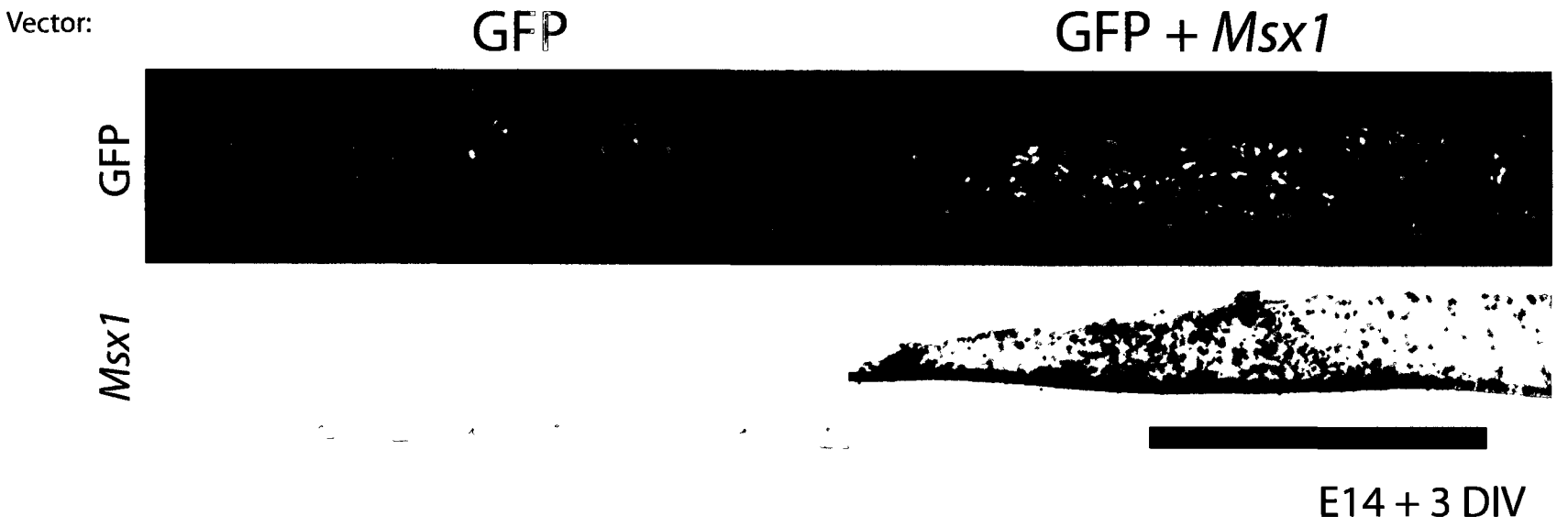
Vector:
GFP
GFP + Msx1
GFP
Msx1
E14 + 3 DIV

sample in 3 independent experiments. CT values from each experiment were normalized to GFP. *Math3* and *Math5* expression were reduced in *Msx1*-transfected retinal explants (Fig. 18). Ectopic expression of *Msx1* did not globally inhibit transcription in transfection explants, as expression of the cell cycle regulator p21 was unchanged (Fig 18). Therefore, we found that ectopic expression of *Msx1* is associated with reduced expression of at least two pro-neuronal bHLH genes in the retina, consistent with the downregulation of neurogenesis in mice with constitutively active Wnt signaling (Cho and Cepko, 2006; Liu et al., 2007).

Previous work done in our laboratory has shown that increased Wnt/β-catenin signaling is associated with a reduction in proliferation (Liu et al., 2007). As Msx1 has been previously shown to inhibit neuronal differentiation and proliferation (Bendall and Abate-Shen, 2000), I investigated whether Msx1affects the rate of proliferation in the retina. To assess cell proliferation, the Ki-67-labelling index was measured in E14 retinas that had been electroporated with *Msx1* and GFP and cultured for three days. The Ki-67 protein is present during all phases of the cell cycle, therefore it is considered an excellent cellular marker for proliferation. To quantify the Ki-67 labeling index in transfected cells, the explants were dissociated into single cells and the proportion of double positive $Ki67^{+}GFP^{+}$ / GFP^{+} cells was determined. The proportion of $Ki\text{-}67^{+}GFP^{+}$ / GFP^{+} cells was not significantly different in explants that were electroporated with *Msx1* compared to controls (Fig. 19), showing that proliferation was not affected by *Msx1* expression. Therefore, ectopic *Msx1* expression does not reduce proliferation in the eye during development.

Figure 18. Q-PCR analysis of bHLH gene expression in *Msx1*-transfected explants. Quantitative RT-PCR (normalized to GAPDH and 18S) was performed for the indicated genes on RNA extracted from E14 retinal explants electroporated with GFP or a combination of GFP and *Msx1* expression vectors and cultured for 3 days. A total of 3 independent experiments were performed in triplicate (n=3). Data is expressed as mean fold change in *Msx1*/GFP-transfected explants compared to GFP-transfected control explants ± S.D. *$p<0.05$.

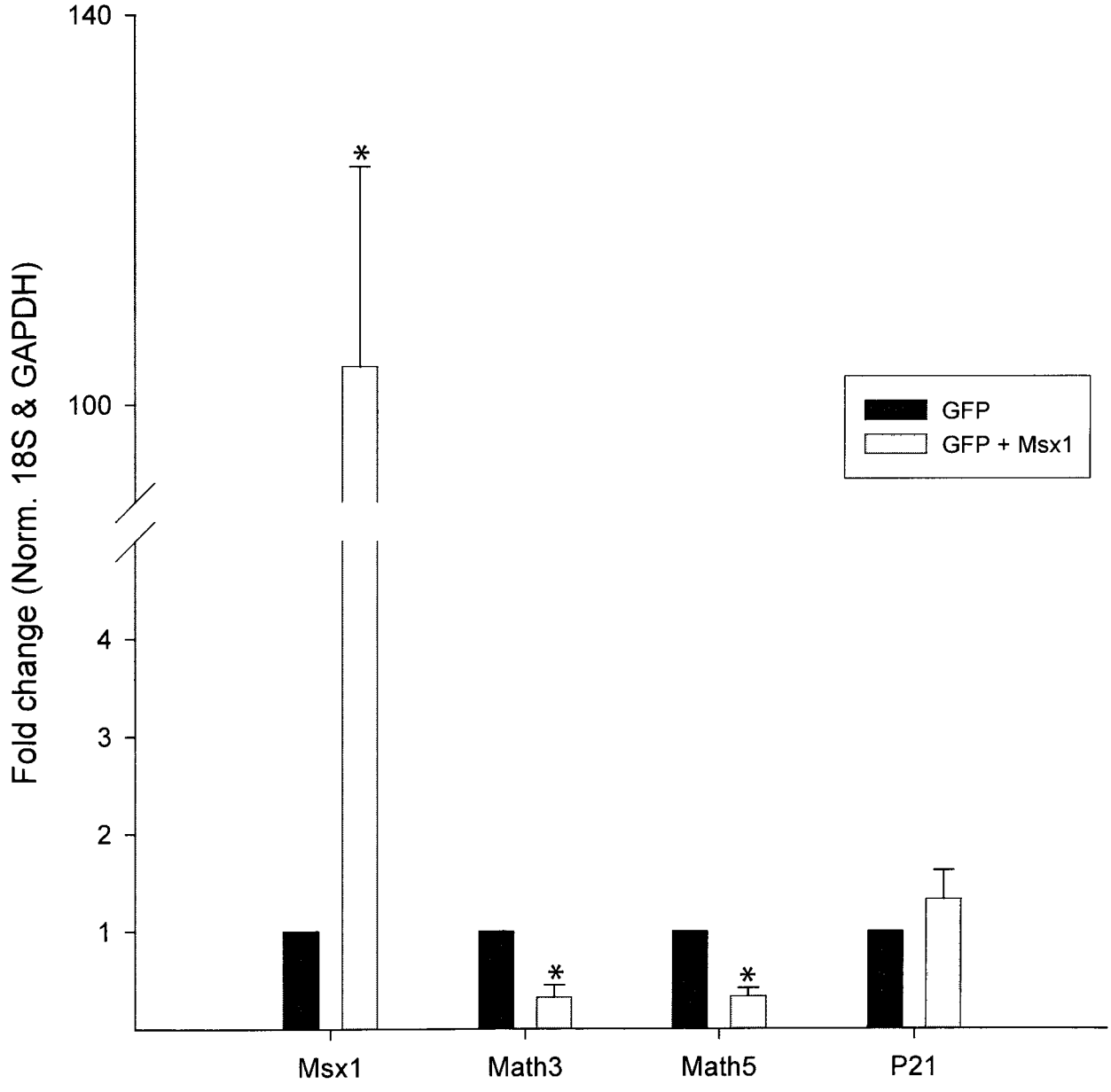
140
100
4
3
2
1
Fold change (Norm. 18S & GAPDH)
*
*
*
GFP
GFP + Msx1
Msx1
Math3
Math5
P21

Figure 19. Ectopic *Msx1* expression has no effect on proliferation in retinal explants. E14 retinal explants were electroporated with GFP or a combination of GFP and *Msx1* expression vectors and cultured for 3 days. Single cell dissociates of the explants were plated on slides, immunostained with anti-GFP and anti-Ki67 antibodies and the Ki67 labelling index of the Gfp^+ cohort was quantified. Data are expressed as % of $Ki67^+GFP^+/GFP^+$ cells ± S.D n=3.

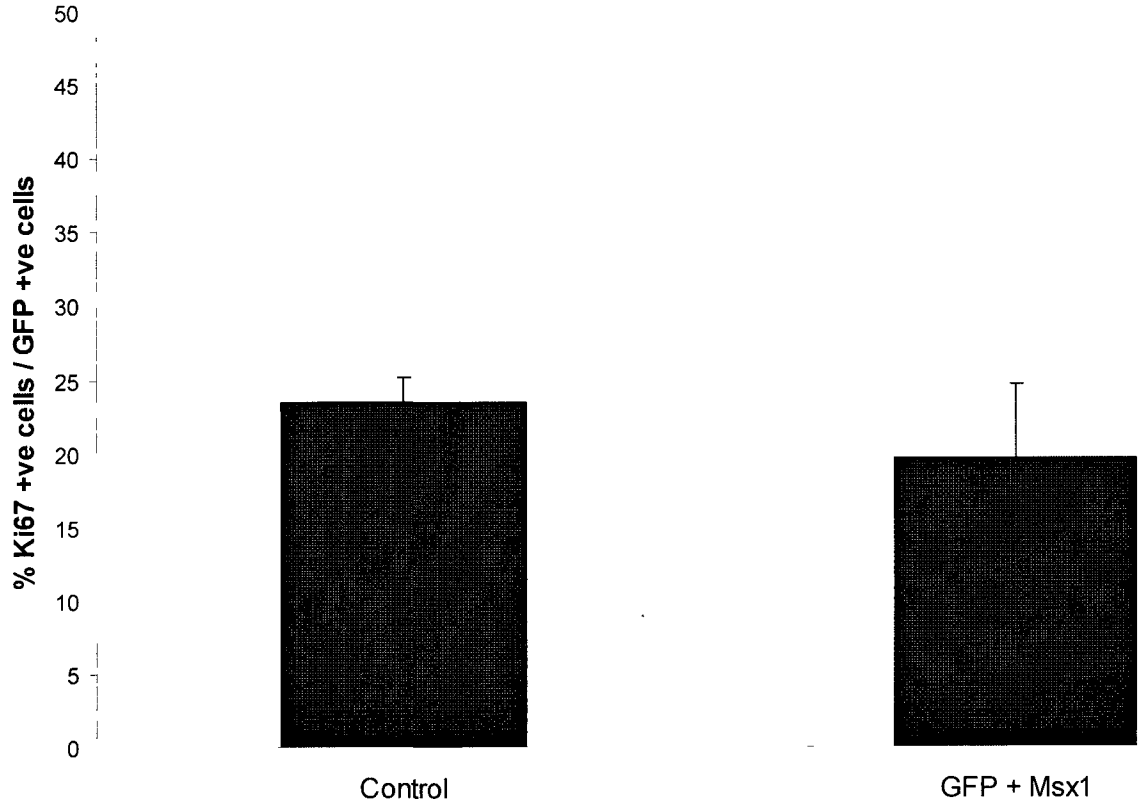
% Ki67 +ve cells / GFP +ve cells
50
45
40
35
30
25
20
15
10
5
0
Control
GFP + Msx1

In previous studies, activation of Wnt/β-catenin signaling inhibited cell cycle activity and neurogenesis (reviewed by Ciani and Salinas, 2005; Reya et al., 2003; Wodarz and Nusse, 1998). *Msx1* is a candidate to mediate some of these effects as it is upregulated by Wnt signaling in the retina both *in vitro* and *in vivo* (Ramos and Robert, 2005). Although ectopic *Msx1* expression in the eye was not found to affect proliferation, it was found to downregulate proneural bHLH gene expression suggesting that it could mediate the inhibition of neurogenesis in the CM, however further studies are required to elucidate the mechanism of *Msx1* activity in eye development.

4.0 Discussion

The first objective of this study was to identify novel target genes of Wnt signaling that are involved in regulating CM development. Microarray analysis and bioinformatic screening facilitated the identification of a number of putative Wnt target genes that were differentially expressed in response to Wnt/β-catenin activation in retinal tissue. Several of these candidate genes were validated as Wnt responsive targets in vitro using RT-QPCR analyses of Li^+-treated retinal explants and in vivo using RT-QPCR and ISH in *CatnbΔex3* mutant retinal material. Therefore, I was able to identify several candidate targets of Wnt signaling that are expressed in the transdifferentiated CM region.

The second objective was to perform a functional analysis of the role of *Msx1* in CM development. Overexpression of *Msx1* in cultured retinal explants resulted in the downregulation of several proneural bHLH genes. Additionally, ectopic *Msx1* expression did not affect proliferation in retinal explants. Therefore, *Msx1* may act to inhibit neurogenesis in the retina by affecting transcription of proneural genes; however, it does not impact proliferation at this stage of retinal development.

4.1 Identification of candidate genes from microarray

Using the microarray analysis as well as bioinformatics, I was able to identify a number of potential candidate target genes of Wnt/β-catenin signaling that may have a role in CM development. A number of functional groups that were identified from the microarray analysis also fit in with the proposed model of CM development, where genes

involved in the regulation of cellular differentiation and proliferation were upregulated while genes involved in neurogenesis were found to be downregulated. Of the genes that were validated from the microarray analysis, *Tnfrsf19* and *Cdkn1a* show the highest potential of acting as Wnt/β-catenin targets in CM development. *Tnfrsf19* encodes a member of the tumour necrosis factor receptor superfamily (TNFRSF) of proteins that are involved in apoptosis, differentiation and proliferation (Banchereau et al., 1994; Gruss and Dower, 1995; Smith et al., 1994). Expression of *Tnfrsf19* has been reported in the embryonic epithelium of numerous mouse tissues including tooth, mammary gland, limb bud, brain and olfactory bulb (Hisaoka et al., 2003; Hisaoka et al., 2004; Kojima et al., 2000; Morikawa et al., 2008; Pispa et al., 2003), and it is strongly expressed postnatally in hair follicles and neurons (Kojima et al., 2000). Loss-of-function studies using *Tnfrsf19*$^{-/-}$ mice have shown the gene to be required for hair follicle development (Pispa et al., 2008) as well as the regulation of axon regeneration in adult mice (Shao et al., 2005) although no eye phenotype has yet to be reported. Additionally, it has been suggested that *Tnfrsf19* may have a role in the temporal regulation of neurogenesis in the mouse hippocampus by maintaining the precursor cell population in this region in an undifferentiated state (Hisaoka et al., 2003). This function of *Tnfrsf19* in the hippocampus raises the possibility that it also has a role in regulating the precursor cell population located in the CM and that this action may be directed by Wnt signaling, as *Tnfrsf19* has been previously identified as a direct target of Wnt signaling in somitogenesis (Buttitta et al., 2003). *Cdkn1a* is a repressor of cell cycle progression and acts to inhibit cyclin dependent kinase activity. Although it is generally known as a member of the p53-dependent damage response pathway (reviewed by Levine, 1997), it has also been found to play a role in development where it is expressed in differentiating melanocytes

(Jiang et al., 1995) as well as acting as a positive cofactor of microphthalmia-associated transcription factor (MITF) expression in melanoma cells (Sestakova et al., epub. 2010). Loss-of-function studies using *Cdkn1a* deficient mice have shown that *Cdkn1a* represses neuronal proliferation in the subgranular zone of the dentate gyrus of the hippocampus, suggesting that it functions to restrain neurogenesis in this region (Pechnick et al., 2008). *Cdkn1a* activity also regulates the proliferative capacity of neural stem cells (NSC) in the mammalian brain with loss of *Cdkn1a* function resulting in a reduced NSC population in the forebrain of adult *Cdkn1a* knockout mice compared to wild-type mice (Kippin et al., 2005). Although *Cdkn1a* expression was not detected in the eyes of wild-type mice in this and previous studies (Bishop et al., 2006; Zhang et al., 1998), it has been shown to control patterning in development of the RPE (Bishop et al., 2006). The ability of *Cdkn1a* to arrest cell cycle progression makes it a possible candidate in Wnt-mediated CM development as constitutive β-catenin signaling resulted in a reduction of proliferation in the peripheral retina (Liu et al., 2007).

The presence of other candidate genes from the microarray in the CM such as the Wnt target *Wif1* (Nusse, 2009) confirms the activity of Wnt/β-catenin signaling in this region of the eye. Additionally, the observed downregulation of *Syt13* suggests that Wnt/β-catenin signaling is able to inhibit expression of neurogenic genes and possibly facilitate a transdifferentiation of NR to CM.

4.2 Validation of Microarray analysis

During validation of the results from the microarray analysis, a number of discrepancies were observed. Several candidate genes that were confirmed to be differentially expressed by RT-QPCR analysis of Li^+ treated retinal explants were not changed in RNA samples from whole eyes of *CatnbΔex3* mutant mice. One possible explanation for this inconsistency is the degree of activation of β-catenin signaling in Li^+-treated explants compared to the β-catenin mutant retina. The majority of the cells in the explants were exposed to Li^+ whereas only the Cre-expressing cells in the peripheral retina of the mutant mice exhibit β-catenin activation. Because the entire eye of the β-catenin mutant mice was harvested and processed for RT-QPCR validation, the RNA from the peripheral mutant region of the retina will be diluted by transcripts from the central retina, thereby limiting the sensitivity of this approach for detecting modest, region-restricted alterations in gene expression. Validation of microarray hits by ISH of *CatnbΔex3* mutant eyes resulted in a number of anomalies. First, the expression of a number of candidate genes that were validated as Li^+ responsive by RT-QPCR was not detected in murine eyes by ISH *in vivo*. A possible explanation for this observation is that the expression level of the mRNA transcripts in question may be at a level that is detectable by QPCR, but below the sensitivity threshold of ISH with the riboprobes that were used for the experiment.

Two of the candidate genes that were verified as Wnt responsive by ISH in mutant eyes, *Tnfrsf19* and *Cdkn1a*, also displayed some anomalies in their expression patterns. Both genes were significantly upregulated in Li^+ treated explants and were robustly expressed in the region with activated β-catenin in the *CatnbΔex3* mutant mice *in vivo*. However, the expression of *Tnfrsf19* and *Cdkn1a* was not detected in the CM of WT mice. There are two explanations for this discrepancy. First, the transcript levels in WT mice may

be too low to detect by ISH, whereas transgenic β-catenin activation increases the expression of these genes above the threshold required for detection by ISH. Second, the expression of these genes could be regulated by combinatorial signaling with β-catenin and other pathways that may be active in the transgenic, but not the wild-type CM. This possibility is consistent with the regulation of the zebrafish T-box transcription factor *tbx6*, where combinatorial Wnt and Bmp signaling, but neither pathway alone (Szeto and Kimelman, 2004) is sufficient to induce the expression of the gene (Szeto and Kimelman, 2004). Thus, in addition to canonical Wnt signaling, *Tnfrsf19* and *Cdkn1a* expression could be co-regulated by another unknown signaling pathway that is not active in the WT retina at the developmental stage in which the ISH validation was conducted, but which could have been induced in the region of transgenic β-catenin expression at the developmental stage that was examined.

4.3 Limitations on the microarray analysis approach

Microarrays are a useful gene survey tool because they can perform rapid comparative gene expression analysis of the experimental condition; however, there are limitations to using this approach. The experimental setup in which microarrays are utilized can have a significant impact on these analyses. Addressing these potential limitations facilitates a rigorous and conservative interpretation of the results and identifies potential issues to be reconciled in future studies.

4.3.1 The use of Li^+ treated explant cultures as a model for the microarray analysis

As Li^+ had been characterized as a pharmacological activator of the canonical Wnt signaling pathway by inhibiting GSK-3β activity (Hedgepeth et al., 1997; Kao and Elinson, 1998; Klein and Melton, 1996), it was a logical approach to use Li^+-treated retinal explants as a method to find novel targets of Wnt signaling in CM development using microarray analysis. However, Li^+ has been found to act on other targets in addition to GSK-3β, including inositol monophosphase, inositol polyphosphate 1-phosphatase, biphosphate nucleotides, fructose 1,6-biphosphastase and phosphoglucomutase (reviewed by Quiroz et al., 2004). Additionally, inhibiting GSK-3β activity may result in β-catenin-independent effects, as other known substrates for GSK-3β include the tumor suppressor protein p53, activator protein 1 (AP-1), nuclear factor-κB (NF-κB), and Gli transcription factors (Beurel and Jope, 2006; Grimes and Jope, 2001; Jia et al., 2002; Manoukian and Woodgett, 2002; Ougolkov and Billadeau, 2006; Price and Kalderon, 2002). Therefore, the gene expression changes in Li^+-treated cultures may, in addition to β-catenin activity, include the effects of altered activity of other Li^+ and GSK3β targets. Although the action of Li^+ on any of these alternate target complexes may have caused a difference in the expression of candidate genes in a Wnt-independent manner, this problem is mitigated as Li^+ treatment and transgenic β-catenin activation share a similar phenotype in retinal tissue, consistent with the possibility that both models are activating a common pathway (Liu et al., 2006; Liu et al., 2007). Another concern for using retinal explants to conduct the microarray analysis is that the cellular composition of the E14 harvested retinal explants is not identical to the β-catenin activated region of the retina of the in vivo transgenic mouse model. Cre-mediated conditional activation of β-catenin is initiated in the peripheral retina as early as E12 (Liu et al., 2007), which is prior to the onset of neurogenesis in this region of the retina. By E14,

however, the stage when retinal explants were Li^+-treated, neurogenesis is underway. Thus, the population of cells exposed to the gain-of-function for β-catenin *in vivo* will differ from those exposed to Li^+ at E14, potentially accounting for discrepancies in the validation of candidate Wnt target genes identified by the microarray. To avoid these issues laser capture microdissection (LCM) can be used to harvest tissue from the CM region of both wild-type and β-catenin activated mice directly for comparative analysis in a microarray. This approach would mitigate any abnormalities that may have been caused by Wnt-independent effects of Li^+ treatment or the retinal explant culture environment. There are some drawbacks to this method, however, as the fixative-free tissue sections required for this process is technically difficult to prepare, and the total yield of RNA is low and may require amplification for a microarray analysis.

4.3.2 Functional gene categories

When selecting candidate genes for validating the microarray analysis, we focused on genes that were involved in proliferation, differentiation, cell cycle regulation and neuronal development. By selecting these functional groups for further analysis, a number of genes that represented other functional groups, including programmed cell death and chromatin modification were not addressed. A number of apoptotic pathway genes were upregulated in Li^+-treated explants, however, these genes were given low priority because our previous studies suggested that increased cell death is related to the culture system (Liu, 2007). The expression of a number of histone encoding genes was downregulated in the microarray analysis of Li^+-treated explants. As histone gene transcription increases as cells progress

from G1 to S phase (Marzluff et al., 2002), the reported downregulation in this case could be attributed to the large upregulation of *Cdkn1a* that was observed and is consistent with the inhibitory effects of Li^+ on proliferation in retinal explants (Liu, 2007). Although these candidate genes were initially not selected when validating the microarray results, since the mechanisms governing CM development are poorly understood, these genes may have an unknown role in this developmental process that has yet to be characterized.

4.4 Future studies based on the microarray analysis

Although the microarray analysis identified a number of genes that are candidate targets of Wnt/β-catenin signaling in CM development, there are a number of studies that are required to confirm these genes as Wnt targets. The differential gene expression of the candidate genes was validated in retinal explants and β-catenin mutant mice by QPCR and ISH, however, the corresponding protein changes need to be confirmed by either IHC or western blot. In addition, it would be useful to determine whether potential Wnt targets are direct targets of β-catenin signaling using ChIP and reporter analyses.

Identifying novel functional targets of signaling cascades is only one part in fully understanding the complete mechanisms that govern the development of this unique region of the eye. Despite the identification of a number of genes whose expression is restricted to the CM region (reviewed by Napier and Kidson, 2007), little is known about how these genes control the morphogenesis of this tissue. One possible avenue of research to address this matter includes combining gene expression studies with those that investigate

morphological events to find any possible relationships between these two developmental events. One other matter that needs to be addressed is the multi-functional role of signaling cascades, including those involving Wnt and Bmp proteins. Since these signaling pathways are involved in a variety of cellular processes, they may have multiple roles throughout the course of CM development. Isolating the temporal effects would be required as each of these processes may have unique developmental characteristics at certain stages of eye development.

Perhaps one additional method to further our understanding on CM development is to examine other regions that have similar developmental processes such as the choroid plexus. The choroid plexus shares the same developmental origins as that of the CB in which a non-neural secretory epithelium structure develops from the neuroepithelium. This structure is involved in secretion of cerebrospinal fluid (CSF) that assists in maintaining the internal environment surrounding the brain (reviewed by Dziegielewska et al., 2001). Similar to the CM, Wnt and Bmp signaling has also been found to be expressed in the developing choroid plexus (Grove et al., 1998; Hebert et al., 2002). Therefore, these shared developmental characteristics suggest that a developmental event observed in one of these structures may provide general insight into developmental processes in both structures.

4.5 Msx1 and the regulation of bHLH gene expression

Ectopic *Msx1* expression in retinal explants resulted in the downregulation of the pro-neural bHLH genes *Math3* and *Math5*, as determined by QPCR analysis of RNA

isolated from whole retinal explants. This result is consistent with experiments in the chick neural tube where *Msx1* overexpression resulted in the significant repression of the bHLH transcription factors *Cath1*, *Mash1*, neurogenin1(*Ngn1*) and neurogenin 2 (*Ngn2*) (Liu et al., 2004). The downregulation of bHLH gene expression in the retina by *Msx1*, together with the restriction of *Msx1* expression in the CM (Monaghan et al., 1991) suggests that it has a role for blocking neurogenesis in this region, although analysis of other bHLH gene expression is required to corroborate this observation. Additionally, analysis of the effect of *Msx1* activity on the expression of paired homeodomain transcription factors in the retina needs to be investigated, as *Msx1* has been shown to repress activity of these genes in other developing systems including the chick neural tube where ectopic *Msx1* expression represses the expression of the homeobox gene *Dbx2* (Timmer et al., 2002).

4.6 Msx1 expression does not affect proliferation in the retina

CM development is associated with a reduced rate of proliferation (Fischer and Reh, 2000; Kubota et al., 2004). Since ectopic β-catenin expression and Li^+ reduce proliferation and increase *Msx1* expression (Liu et al., 2006; Liu et al., 2007), it is possible that Msx1 could also affect the proliferation of CM cells. However, ectopic *Msx1* expression did not affect proliferation in retinal explants. This result is similar to what was previously observed where *Msx1* expression did not have a strong mitogenic effect in embryonic fibroblasts and limb buds (Hu et al., 2001; Song et al., 1992). Although *Msx1* activity does not seem to modulate proliferation in neural retinal cells in explants, there is the possibility that it

influences proliferation in the context of the CM, therefore modulating the expression of *Msx1* exclusively in CM cells is required.

4.7 Future directions for Msx1

Although the results in this study shed light on the role of *Msx1* in CM development, a number of future studies will be required to fully elucidate this role.

4.7.1 Effect of Msx1 on neuronal differentiation within the retina

Msx1 expression has been shown to have an effect on neuronal development as *Msx1* deficient mice exhibit hydrocephalus as well as diencephalon defects, including the absence of the subcommissural organ (SCO) and abnormal development of the posterior commissure (Bach et al., 2003; Fernandez-Llebrez et al., 2004; Ramos et al., 2004a). *Msx1* expression has also been shown to inhibit neuronal differentiation in the neural tube (Liu et al., 2004), and is required for the formation of the dorsal midline in the developing neural tube (Bach et al., 2003). Additionally, as an effector of Bmp signaling in neural precursor cells, *Msx1* is thought to form a dorsal midline boundary within the cortex (Hu et al., 2008). This developmental bias against neuronal differentiation is also seen in the dorsal-ventral patterning of the *Xenopus* gastrula where *Msx1* promotes an epidermal versus neural fate from ectoderm (Suzuki et al., 1997). *Msx1* expression is also detected within the choroid plexus (Ramos et al., 2004b), a region that shares many characteristics with the CM as it is also a non-neural secretory tissue with neuroepithelial origins (Dziegielewska et al., 2001).

These observations suggest that *Msx1* activity may have a role in the development of the CM by inhibiting neuronal differentiation in the peripheral retina. This can be determined by investigating whether ectopic *Msx1* expression disrupts the differentiation of neuronal cell types in the retina such as photoreceptors, RGCs, and amacrine cells as well as whether ectopic neurogenesis occurs in the CM when *Msx1* is knocked down in this region.

4.7.2 Msx1 and Msx2 redundancy

Development of the CM was reported as unperturbed in *Msx1*$^{-/-}$ mice (Satokata and Maas, 1994). Limb development is also normal in *Msx1*$^{-/-}$ mice, despite the high levels of expression of *Msx1* in the limb bud (Hill et al., 1989). The lack of correlation between *Msx1* expression and developmental anomalies can be explained by functional compensation with other Msx genes. *Msx2* expression overlaps with *Msx1* in several tissues, including the eye (Davidson, 1995), which raises the possibility that *Msx2* is able to act in a redundant or compensatory role for *Msx1*. Consistent with a compensatory role for *Msx2*, *Msx1*$^{-/-}$;*Msx2*$^{-/-}$ double mutant mice exhibit abnormalities in a number of tissues (Bei and Maas, 1998; Ishii et al., 2005; Lallemand et al., 2005; Satokata et al., 2000). Disruption of *Msx1* and *Msx2* expression has been shown to result in eye defects, including enlarged optic vesicles and a thinning of the neuroepithelium in the optic vesicle (Foerst-Potts and Sadler, 1997), however this study was conducted using anti-sense oligodeoxynucleotides and needs to be confirmed in *Msx1*$^{-/-}$;*Msx2*$^{-/-}$ mutant mice. Furthermore, *Msx2* may have a role in patterning the optic vesicle into neural and pigmented domains in chick (Holme et al., 2000). Therefore, to fully

investigate the role of *Msx1* in eye development, the functional redundancy between *Msx1* and *Msx2* must be addressed.

4.7.3 Msx1 as a Wnt target in eye development

Determining the mechanisms in which *Msx1* expression is regulated can further ascertain its role in eye and CM development. Studies in mutant mice that express a constitutively active allele of β-catenin suggest that *Msx1* may be a target of Wnt signaling in the CM (Liu et al., 2007), as in other systems where Msx genes are targets of the Wnt pathway (Hussein et al., 2003; Willert et al., 2002). Moreover, a highly conserved TCF binding site is located in the proximal enhancer of the *Msx1* gene (Miller et al., 2007). Therefore it would be beneficial to determine if *Msx1* acts as a direct or indirect target of Wnt signaling in CM development as elucidating the mechanism of β-catenin/Msx1 in the retina could provide insight into mechanisms in other tissues.

5.0 Conclusions

Since ectopic activation of Wnt/β-catenin signaling within the retina promotes the transdifferentiation of NR tissue to the CB in both chick and mice (Cho and Cepko, 2006; Liu et al., 2007), I hypothesized that the activation of Wnt target genes promoted the specification of CM tissue during retinal development. Using a combination of microarray and bioinformatic analyses, I was able to identify a number of candidate Wnt target genes that were expressed within the expanded CB region where β-catenin signaling was ectopically activated. Additionally, I also determined that ectopic expression of the CM marker and Wnt target *Msx1* resulted in the downregulation of several bHLH genes that are involved in neuronal development of the retina.

There are a number of additional experiments that arise from this study. Although I was able to validate a number of candidate genes from the microarray analysis, there are still many genes that have yet to be validated and functionally evaluated. Also, the functional mechanisms of *Msx1* and other candidate Wnt target genes can be investigated further using techniques such as siRNA knockdowns and transgenic mice to fully elucidate their role in CM development.

In conclusion, the data in this study identifies potential mechanisms in which Wnt signaling mediates CM development. Microarray and bioinformatic analysis combined with explant and transgenic models of Wnt activation have identified many candidate genes that can potentially act as effectors of Wnt signaling during this developmental process. This identification of candidate Wnt target genes contributes to the understanding of the role of Wnt signaling in retinal development.

6.0 References

Acampora, D., S. Mazan, V. Avantaggiato, P. Barone, F. Tuorto, Y. Lallemand, P. Brulet, and A. Simeone. 1996. Epilepsy and brain abnormalities in mice lacking the Otx1 gene. *Nat Genet.* 14:218-22.

Ahmad, I., L. Tang, and H. Pham. 2000. Identification of neural progenitors in the adult mammalian eye. *Biochem Biophys Res Commun.* 270:517-21.

Bach, A., Y. Lallemand, M.A. Nicola, C. Ramos, L. Mathis, M. Maufras, and B. Robert. 2003. Msx1 is required for dorsal diencephalon patterning. *Development.* 130:4025-36.

Bafico, A., G. Liu, A. Yaniv, A. Gazit, and S.A. Aaronson. 2001. Novel mechanism of Wnt signalling inhibition mediated by Dickkopf-1 interaction with LRP6/Arrow. *Nat Cell Biol.* 3:683-6.

Banchereau, J., F. Bazan, D. Blanchard, F. Briere, J.P. Galizzi, C. van Kooten, Y.J. Liu, F. Rousset, and S. Saeland. 1994. The CD40 antigen and its ligand. *Annu Rev Immunol.* 12:881-922.

Bao, Z.Z., and C.L. Cepko. 1997. The expression and function of Notch pathway genes in the developing rat eye. *J Neurosci.* 17:1425-34.

Barolo, S. 2006. Transgenic Wnt/TCF pathway reporters: all you need is Lef? *Oncogene.* 25:7505-11.

Beebe, D.C. 1986. Development of the ciliary body: a brief review. *Trans Ophthalmol Soc U K.* 105 (Pt 2):123-30.

Bei, M., and R. Maas. 1998. FGFs and BMP4 induce both Msx1-independent and Msx1-dependent signaling pathways in early tooth development. *Development.* 125:4325-33.

Bendall, A.J., and C. Abate-Shen. 2000. Roles for Msx and Dlx homeoproteins in vertebrate development. *Gene.* 247:17-31.

Beurel, E., and R.S. Jope. 2006. The paradoxical pro- and anti-apoptotic actions of GSK3 in the intrinsic and extrinsic apoptosis signaling pathways. *Prog Neurobiol.* 79:173-89.

Bhanot, P., M. Brink, C.H. Samos, J.C. Hsieh, Y. Wang, J.P. Macke, D. Andrew, J. Nathans, and R. Nusse. 1996. A new member of the frizzled family from Drosophila functions as a Wingless receptor. *Nature.* 382:225-30.

Bishop, A.J., B. Kosaras, M.C. Hollander, A. Fornace, Jr., R.L. Sidman, and R.H. Schiestl. 2006. p21 controls patterning but not homologous recombination in RPE development. *DNA Repair (Amst).* 5:111-20.

Bodine, P.V., W. Zhao, Y.P. Kharode, F.J. Bex, A.J. Lambert, M.B. Goad, T. Gaur, G.S. Stein, J.B. Lian, and B.S. Komm. 2004. The Wnt antagonist secreted frizzled-related protein-1 is a negative regulator of trabecular bone formation in adult mice. *Mol Endocrinol.* 18:1222-37.

Bovolenta, P., P. Esteve, J.M. Ruiz, E. Cisneros, and J. Lopez-Rios. 2008. Beyond Wnt inhibition: new functions of secreted Frizzled-related proteins in development and disease. *J Cell Sci.* 121:737-46.

Bradley, R.S., and A.M. Brown. 1995. A soluble form of Wnt-1 protein with mitogenic activity on mammary epithelial cells. *Mol Cell Biol.* 15:4616-22.

Brannon, M., M. Gomperts, L. Sumoy, R.T. Moon, and D. Kimelman. 1997. A beta-catenin/XTcf-3 complex binds to the siamois promoter to regulate dorsal axis specification in Xenopus. *Genes Dev.* 11:2359-70.

Brembeck, F.H., M. Rosario, and W. Birchmeier. 2006. Balancing cell adhesion and Wnt signaling, the key role of beta-catenin. *Curr Opin Genet Dev.* 16:51-9.

Burrus, L.W., and A.P. McMahon. 1995. Biochemical analysis of murine Wnt proteins reveals both shared and distinct properties. *Exp Cell Res.* 220:363-73.

Bustin, S.A. 2002. Quantification of mRNA using real-time reverse transcription PCR (RT-PCR): trends and problems. *J Mol Endocrinol.* 29:23-39.

Buttitta, L., T.S. Tanaka, A.E. Chen, M.S. Ko, and C.M. Fan. 2003. Microarray analysis of somitogenesis reveals novel targets of different WNT signaling pathways in the somitic mesoderm. *Dev Biol.* 258:91-104.

Cavallo, R.A., R.T. Cox, M.M. Moline, J. Roose, G.A. Polevoy, H. Clevers, M. Peifer, and A. Bejsovec. 1998. Drosophila Tcf and Groucho interact to repress Wingless signalling activity. *Nature.* 395:604-8.

Cepko, C.L., C.P. Austin, X. Yang, M. Alexiades, and D. Ezzeddine. 1996. Cell fate determination in the vertebrate retina. *Proc Natl Acad Sci U S A.* 93:589-95.

Cho, S.H., and C.L. Cepko. 2006. Wnt2b/beta-catenin-mediated canonical Wnt signaling determines the peripheral fates of the chick eye. *Development.* 133:3167-77.

Ciani, L., and P.C. Salinas. 2005. WNTs in the vertebrate nervous system: from patterning to neuronal connectivity. *Nat Rev Neurosci.* 6:351-62.

Civan, M.M., and A.D. Macknight. 2004. The ins and outs of aqueous humour secretion. *Exp Eye Res.* 78:625-31.

Cwinn, M., B. McNeill, A. Ha, and V.A. Wallace. 2010. Histogenesis, Cell Fate, and Signaling Factors. *In* Encyclopedia of the Eye. Vol. 2. D.A. Dartt, editor. Oxford: Academic Press. 244-250.

Dakubo, G.D., Y.P. Wang, C. Mazerolle, K. Campsall, A.P. McMahon, and V.A. Wallace. 2003. Retinal ganglion cell-derived sonic hedgehog signaling is required for optic disc and stalk neuroepithelial cell development. *Development.* 130:2967-80.

Davidson, D. 1995. The function and evolution of Msx genes: pointers and paradoxes. *Trends Genet.* 11:405-11.

de Iongh, R.U., H.E. Abud, and G.R. Hime. 2006. WNT/Frizzled signaling in eye development and disease. *Front Biosci.* 11:2442-64.

Dong, S., J. Landfair, M. Balasubramani, M.E. Bier, G. Cole, and W. Halfter. 2002. Expression of basal lamina protein mRNAs in the early embryonic chick eye. *J Comp Neurol.* 447:261-73.

Dufort, D., L. Schwartz, K. Harpal, and J. Rossant. 1998. The transcription factor HNF3beta is required in visceral endoderm for normal primitive streak morphogenesis. *Development.* 125:3015-25.

Dyer, M.A., and C.L. Cepko. 2001. Regulating proliferation during retinal development. *Nat Rev Neurosci.* 2:333-42.

Dziegielewska, K.M., J. Ek, M.D. Habgood, and N.R. Saunders. 2001. Development of the choroid plexus. *Microsc Res Tech.* 52:5-20.

Ekker, M., M.A. Akimenko, M.L. Allende, R. Smith, G. Drouin, R.M. Langille, E.S. Weinberg, and M. Westerfield. 1997. Relationships among msx gene structure and function in zebrafish and other vertebrates. *Mol Biol Evol.* 14:1008-22.

Fernandez-Llebrez, P., J.M. Grondona, J. Perez, M.F. Lopez-Aranda, G. Estivill-Torrus, P.F. Llebrez-Zayas, E. Soriano, C. Ramos, Y. Lallemand, A. Bach, and B. Robert. 2004. Msx1-deficient mice fail to form prosomere 1 derivatives, subcommissural organ, and posterior commissure and develop hydrocephalus. *J Neuropathol Exp Neurol.* 63:574-86.

Fischer, A.J., A. Hendrickson, and T.A. Reh. 2001. Immunocytochemical characterization of cysts in the peripheral retina and pars plana of the adult primate. *Invest Ophthalmol Vis Sci.* 42:3256-63.

Fischer, A.J., and T.A. Reh. 2000. Identification of a proliferating marginal zone of retinal progenitors in postnatal chickens. *Dev Biol.* 220:197-210.

Foerst-Potts, L., and T.W. Sadler. 1997. Disruption of Msx-1 and Msx-2 reveals roles for these genes in craniofacial, eye, and axial development. *Dev Dyn.* 209:70-84.

Gould, D.B., R.S. Smith, and S.W. John. 2004. Anterior segment development relevant to glaucoma. *Int J Dev Biol.* 48:1015-29.

Grimes, C.A., and R.S. Jope. 2001. The multifaceted roles of glycogen synthase kinase 3beta in cellular signaling. *Prog Neurobiol.* 65:391-426.

Grove, E.A., S. Tole, J. Limon, L. Yip, and C.W. Ragsdale. 1998. The hem of the embryonic cerebral cortex is defined by the expression of multiple Wnt genes and is compromised in Gli3-deficient mice. *Development.* 125:2315-25.

Gruss, H.J., and S.K. Dower. 1995. Tumor necrosis factor ligand superfamily: involvement in the pathology of malignant lymphomas. *Blood.* 85:3378-404.

Gustavson, M.D., H.C. Crawford, B. Fingleton, and L.M. Matrisian. 2004. Tcf binding sequence and position determines beta-catenin and Lef-1 responsiveness of MMP-7 promoters. *Mol Carcinog.* 41:125-39.

Harada, N., Y. Tamai, T. Ishikawa, B. Sauer, K. Takaku, M. Oshima, and M.M. Taketo. 1999. Intestinal polyposis in mice with a dominant stable mutation of the beta-catenin gene. *EMBO J.* 18:5931-42.

Harris, W.A., and M. Perron. 1998. Molecular recapitulation: the growth of the vertebrate retina. *Int J Dev Biol.* 42:299-304.

Hausmann, G., C. Banziger, and K. Basler. 2007. Helping Wingless take flight: how WNT proteins are secreted. *Nat Rev Mol Cell Biol.* 8:331-6.

Hebert, J.M., Y. Mishina, and S.K. McConnell. 2002. BMP signaling is required locally to pattern the dorsal telencephalic midline. *Neuron.* 35:1029-41.

Hedgepeth, C.M., L.J. Conrad, J. Zhang, H.C. Huang, V.M. Lee, and P.S. Klein. 1997. Activation of the Wnt signaling pathway: a molecular mechanism for lithium action. *Dev Biol.* 185:82-91.

Hill, R.E., P.F. Jones, A.R. Rees, C.M. Sime, M.J. Justice, N.G. Copeland, N.A. Jenkins, E. Graham, and D.R. Davidson. 1989. A new family of mouse homeo box-containing genes: molecular structure, chromosomal location, and developmental expression of Hox-7.1. *Genes Dev.* 3:26-37.

Hisaoka, T., Y. Morikawa, T. Kitamura, and E. Senba. 2003. Expression of a member of tumor necrosis factor receptor superfamily, TROY, in the developing mouse brain. *Brain Res Dev Brain Res.* 143:105-9.

Hisaoka, T., Y. Morikawa, T. Kitamura, and E. Senba. 2004. Expression of a member of tumor necrosis factor receptor superfamily, TROY, in the developing olfactory system. *Glia.* 45:313-24.

Holme, R.H., S.J. Thomson, and D.R. Davidson. 2000. Ectopic expression of Msx2 in chick retinal pigmented epithelium cultures suggests a role in patterning the optic vesicle. *Mech Dev.* 91:175-87.

Hu, G., H. Lee, S.M. Price, M.M. Shen, and C. Abate-Shen. 2001. Msx homeobox genes inhibit differentiation through upregulation of cyclin D1. *Development.* 128:2373-84.

Hu, J.S., L.T. Doan, D.S. Currle, M. Paff, J.Y. Rheem, R. Schreyer, B. Robert, and E.S. Monuki. 2008. Border formation in a Bmp gradient reduced to single dissociated cells. *Proc Natl Acad Sci U S A.* 105:3398-403.

Hussein, S.M., E.K. Duff, and C. Sirard. 2003. Smad4 and beta-catenin co-activators functionally interact with lymphoid-enhancing factor to regulate graded expression of Msx2. *J Biol Chem.* 278:48805-14.

Ishii, M., J. Han, H.Y. Yen, H.M. Sucov, Y. Chai, and R.E. Maxson, Jr. 2005. Combined deficiencies of Msx1 and Msx2 cause impaired patterning and survival of the cranial neural crest. *Development.* 132:4937-50.

Itasaki, N., C.M. Jones, S. Mercurio, A. Rowe, P.M. Domingos, J.C. Smith, and R. Krumlauf. 2003. Wise, a context-dependent activator and inhibitor of Wnt signalling. *Development.* 130:4295-305.

Jean, D., K. Ewan, and P. Gruss. 1998. Molecular regulators involved in vertebrate eye development. *Mech Dev.* 76:3-18.

Jensen, A.M., and V.A. Wallace. 1997. Expression of Sonic hedgehog and its putative role as a precursor cell mitogen in the developing mouse retina. *Development.* 124:363-71.

Jho, E.H., T. Zhang, C. Domon, C.K. Joo, J.N. Freund, and F. Costantini. 2002. Wnt/beta-catenin/Tcf signaling induces the transcription of Axin2, a negative regulator of the signaling pathway. *Mol Cell Biol.* 22:1172-83.

Jia, J., K. Amanai, G. Wang, J. Tang, B. Wang, and J. Jiang. 2002. Shaggy/GSK3 antagonizes Hedgehog signalling by regulating Cubitus interruptus. *Nature.* 416:548-52.

Jiang, H., J. Lin, Z.Z. Su, M. Herlyn, R.S. Kerbel, B.E. Weissman, D.R. Welch, and P.B. Fisher. 1995. The melanoma differentiation-associated gene mda-6, which encodes the cyclin-dependent kinase inhibitor p21, is differentially expressed during growth, differentiation and progression in human melanoma cells. *Oncogene.* 10:1855-64.

Kao, K.R., and R.P. Elinson. 1998. The legacy of lithium effects on development. *Biol Cell.* 90:585-9.

Karolchik, D., R. Baertsch, M. Diekhans, T.S. Furey, A. Hinrichs, Y.T. Lu, K.M. Roskin, M. Schwartz, C.W. Sugnet, D.J. Thomas, R.J. Weber, D. Haussler, and W.J. Kent. 2003. The UCSC Genome Browser Database. *Nucleic Acids Res.* 31:51-4.

Kent, W.J., R. Baertsch, A. Hinrichs, W. Miller, and D. Haussler. 2003. Evolution's cauldron: duplication, deletion, and rearrangement in the mouse and human genomes. *Proc Natl Acad Sci U S A.* 100:11484-9.

Kippin, T.E., D.J. Martens, and D. van der Kooy. 2005. p21 loss compromises the relative quiescence of forebrain stem cell proliferation leading to exhaustion of their proliferation capacity. *Genes Dev.* 19:756-67.

Klein, P.S., and D.A. Melton. 1996. A molecular mechanism for the effect of lithium on development. *Proc Natl Acad Sci U S A.* 93:8455-9.

Klingensmith, J., and R. Nusse. 1994. Signaling by wingless in Drosophila. *Dev Biol.* 166:396-414.

Kojima, T., Y. Morikawa, N.G. Copeland, D.J. Gilbert, N.A. Jenkins, E. Senba, and T. Kitamura. 2000. TROY, a newly identified member of the tumor necrosis factor receptor superfamily, exhibits a homology with Edar and is expressed in embryonic skin and hair follicles. *J Biol Chem.* 275:20742-7.

Korinek, V., N. Barker, K. Willert, M. Molenaar, J. Roose, G. Wagenaar, M. Markman, W. Lamers, O. Destree, and H. Clevers. 1998. Two members of the Tcf family implicated in Wnt/beta-catenin signaling during embryogenesis in the mouse. *Mol Cell Biol.* 18:1248-56.

Kubo, F., M. Takeichi, and S. Nakagawa. 2003. Wnt2b controls retinal cell differentiation at the ciliary marginal zone. *Development.* 130:587-98.

Kubo, F., M. Takeichi, and S. Nakagawa. 2005. Wnt2b inhibits differentiation of retinal progenitor cells in the absence of Notch activity by downregulating the expression of proneural genes. *Development.* 132:2759-70.

Kubota, R., J.N. Hokoc, A. Moshiri, C. McGuire, and T.A. Reh. 2002. A comparative study of neurogenesis in the retinal ciliary marginal zone of homeothermic vertebrates. *Brain Res Dev Brain Res.* 134:31-41.

Kubota, R., C. McGuire, B. Dierks, and T.A. Reh. 2004. Identification of ciliary epithelial-specific genes using subtractive libraries and cDNA arrays in the avian eye. *Dev Dyn.* 229:529-40.

Lallemand, Y., M.A. Nicola, C. Ramos, A. Bach, C.S. Clement, and B. Robert. 2005. Analysis of Msx1; Msx2 double mutants reveals multiple roles for Msx genes in limb development. *Development.* 132:3003-14.

Leaf, I., J. Tennessen, M. Mukhopadhyay, H. Westphal, and W. Shawlot. 2006. Sfrp5 is not essential for axis formation in the mouse. *Genesis.* 44:573-8.

Lee, H.S., M.H. Park, S.J. Yang, K.C. Park, N.S. Kim, Y.S. Kim, D.I. Kim, H.S. Yoo, E.J. Choi, and Y.I. Yeom. 2007. Novel candidate targets of Wnt/beta-catenin signaling in hepatoma cells. *Life Sci.* 80:690-8.

Levine, A.J. 1997. p53, the cellular gatekeeper for growth and division. *Cell.* 88:323-31.

Li, Y., and G. Bu. 2005. LRP5/6 in Wnt signaling and tumorigenesis. *Future Oncol.* 1:673-81.

Liu, H. 2007. The Role of Wnt Signaling Pathway in Mammalian Retinal Development. *In* Department of Biochemistry, Microbiology and Immunology. Vol. Ph.D. University of Ottawa, Ottawa. 195.

Liu, H., O. Mohamed, D. Dufort, and V.A. Wallace. 2003. Characterization of Wnt signaling components and activation of the Wnt canonical pathway in the murine retina. *Dev Dyn.* 227:323-34.

Liu, H., S. Thurig, O. Mohamed, D. Dufort, and V.A. Wallace. 2006. Mapping canonical Wnt signaling in the developing and adult retina. *Invest Ophthalmol Vis Sci.* 47:5088-97.

Liu, H., S. Xu, Y. Wang, C. Mazerolle, S. Thurig, B.L. Coles, J.C. Ren, M.M. Taketo, D. van der Kooy, and V.A. Wallace. 2007. Ciliary margin transdifferentiation from neural retina is controlled by canonical Wnt signaling. *Dev Biol.* 308:54-67.

Liu, Y., A.W. Helms, and J.E. Johnson. 2004. Distinct activities of Msx1 and Msx3 in dorsal neural tube development. *Development.* 131:1017-28.

Livesey, F.J., and C.L. Cepko. 2001. Vertebrate neural cell-fate determination: lessons from the retina. *Nat Rev Neurosci.* 2:109-18.

Logan, C.Y., and R. Nusse. 2004. The Wnt signaling pathway in development and disease. *Annu Rev Cell Dev Biol.* 20:781-810.

Lustig, B., and J. Behrens. 2003. The Wnt signaling pathway and its role in tumor development. *J Cancer Res Clin Oncol.* 129:199-221.

Manoukian, A.S., and J.R. Woodgett. 2002. Role of glycogen synthase kinase-3 in cancer: regulation by Wnts and other signaling pathways. *Adv Cancer Res.* 84:203-29.

Mao, B., W. Wu, G. Davidson, J. Marhold, M. Li, B.M. Mechler, H. Delius, D. Hoppe, P. Stannek, C. Walter, A. Glinka, and C. Niehrs. 2002. Kremen proteins are Dickkopf receptors that regulate Wnt/beta-catenin signalling. *Nature.* 417:664-7.

Marquardt, T., R. Ashery-Padan, N. Andrejewski, R. Scardigli, F. Guillemot, and P. Gruss. 2001. Pax6 is required for the multipotent state of retinal progenitor cells. *Cell.* 105:43-55.

Martinez-Morales, J.R., M. Signore, D. Acampora, A. Simeone, and P. Bovolenta. 2001. Otx genes are required for tissue specification in the developing eye. *Development.* 128:2019-30.

Marzluff, W.F., P. Gongidi, K.R. Woods, J. Jin, and L.J. Maltais. 2002. The human and mouse replication-dependent histone genes. *Genomics.* 80:487-98.

Matsuda, T., and C.L. Cepko. 2004. Electroporation and RNA interference in the rodent retina in vivo and in vitro. *Proc Natl Acad Sci U S A.* 101:16-22.

McNeill, B., D. Wall, S. Beug, and V.A. Wallace. 2007. Probing the Hedgehog Pathway in Retinal Development. *In* Signal Transduction in the Retina. S.J. Fliesler, Kisselev, O.G., editor. CRC Press. 408.

Miller, J.R. 2002. The Wnts. *Genome Biol.* 3:REVIEWS3001.

Miller, K.A., J. Barrow, J.M. Collinson, S. Davidson, M. Lear, R.E. Hill, and A. Mackenzie. 2007. A highly conserved Wnt-dependent TCF4 binding site within the proximal enhancer of the anti-myogenic Msx1 gene supports expression within Pax3-expressing limb bud muscle precursor cells. *Dev Biol.* 311:665-78.

Mohamed, O.A., H.J. Clarke, and D. Dufort. 2004. Beta-catenin signaling marks the prospective site of primitive streak formation in the mouse embryo. *Dev Dyn.* 231:416-24.

Monaghan, A.P., D.R. Davidson, C. Sime, E. Graham, R. Baldock, S.S. Bhattacharya, and R.E. Hill. 1991. The Msh-like homeobox genes define domains in the developing vertebrate eye. *Development.* 112:1053-61.

Morikawa, Y., T. Hisaoka, T. Kitamura, and E. Senba. 2008. TROY, a novel member of the tumor necrosis factor receptor superfamily in the central nervous system. *Ann N Y Acad Sci.* 1126:A1-10.

Napier, H.R., and S.H. Kidson. 2007. Molecular events in early development of the ciliary body: a question of folding. *Exp Eye Res.* 84:615-25.

Nassr, M.A., C.L. Morris, P.A. Netland, and Z.A. Karcioglu. 2009. Intraocular pressure change in orbital disease. *Surv Ophthalmol.* 54:519-44.

Nelson, W.J., and R. Nusse. 2004. Convergence of Wnt, beta-catenin, and cadherin pathways. *Science.* 303:1483-7.

Nusse, R. 2009. The Wnt Homepage.

Nusse, R., and H.E. Varmus. 1982. Many tumors induced by the mouse mammary tumor virus contain a provirus integrated in the same region of the host genome. *Cell.* 31:99-109.

Ougolkov, A.V., and D.D. Billadeau. 2006. Targeting GSK-3: a promising approach for cancer therapy? *Future Oncol.* 2:91-100.

Pechnick, R.N., S. Zonis, K. Wawrowsky, J. Pourmorady, and V. Chesnokova. 2008. p21Cip1 restricts neuronal proliferation in the subgranular zone of the dentate gyrus of the hippocampus. *Proc Natl Acad Sci U S A.* 105:1358-63.

Pei, Y.F., and J.A. Rhodin. 1970. The prenatal development of the mouse eye. *Anat Rec.* 168:105-25.

Perron, M., and W.A. Harris. 2000. Retinal stem cells in vertebrates. *Bioessays.* 22:685-8.

Pispa, J., M.L. Mikkola, T. Mustonen, and I. Thesleff. 2003. Ectodysplasin, Edar and TNFRSF19 are expressed in complementary and overlapping patterns during mouse embryogenesis. *Gene Expr Patterns.* 3:675-9.

Pispa, J., M. Pummila, P.A. Barker, I. Thesleff, and M.L. Mikkola. 2008. Edar and Troy signalling pathways act redundantly to regulate initiation of hair follicle development. *Hum Mol Genet.* 17:3380-91.

Pressman, C.L., H. Chen, and R.L. Johnson. 2000. LMX1B, a LIM homeodomain class transcription factor, is necessary for normal development of multiple tissues in the anterior segment of the murine eye. *Genesis.* 26:15-25.

Price, M.A., and D. Kalderon. 2002. Proteolysis of the Hedgehog signaling effector Cubitus interruptus requires phosphorylation by Glycogen Synthase Kinase 3 and Casein Kinase 1. *Cell.* 108:823-35.

Quiroz, J.A., T.D. Gould, and H.K. Manji. 2004. Molecular effects of lithium. *Mol Interv.* 4:259-72.

Radonic, A., S. Thulke, I.M. Mackay, O. Landt, W. Siegert, and A. Nitsche. 2004. Guideline to reference gene selection for quantitative real-time PCR. *Biochem Biophys Res Commun.* 313:856-62.

Ramos, C., P. Fernandez-Llebrez, A. Bach, B. Robert, and E. Soriano. 2004a. Msx1 disruption leads to diencephalon defects and hydrocephalus. *Dev Dyn.* 230:446-60.

Ramos, C., A. Martinez, B. Robert, and E. Soriano. 2004b. Msx1 expression in the adult mouse brain: characterization of populations of beta-galactosidase-positive cells in the hippocampus and fimbria. *Neuroscience.* 127:893-900.

Ramos, C., and B. Robert. 2005. msh/Msx gene family in neural development. *Trends Genet.* 21:624-32.

Rehm, H.L., D.S. Zhang, M.C. Brown, B. Burgess, C. Halpin, W. Berger, C.C. Morton, D.P. Corey, and Z.Y. Chen. 2002. Vascular defects and sensorineural deafness in a mouse model of Norrie disease. *J Neurosci.* 22:4286-92.

Reya, T., A.W. Duncan, L. Ailles, J. Domen, D.C. Scherer, K. Willert, L. Hintz, R. Nusse, and I.L. Weissman. 2003. A role for Wnt signalling in self-renewal of haematopoietic stem cells. *Nature.* 423:409-14.

Rijsewijk, F., M. Schuermann, E. Wagenaar, P. Parren, D. Weigel, and R. Nusse. 1987. The Drosophila homolog of the mouse mammary oncogene int-1 is identical to the segment polarity gene wingless. *Cell.* 50:649-57.

Riveiro-Alvarez, R., M.J. Trujillo-Tiebas, A. Gimenez-Pardo, M. Garcia-Hoyos, D. Cantalapiedra, I. Lorda-Sanchez, M. Rodriguez de Alba, C. Ramos, and C. Ayuso. 2005. Genotype-phenotype variations in five Spanish families with Norrie disease or X-linked FEVR. *Mol Vis.* 11:705-12.

Roose, J., and H. Clevers. 1999. TCF transcription factors: molecular switches in carcinogenesis. *Biochim Biophys Acta.* 1424:M23-37.

Satoh, W., T. Gotoh, Y. Tsunematsu, S. Aizawa, and A. Shimono. 2006. Sfrp1 and Sfrp2 regulate anteroposterior axis elongation and somite segmentation during mouse embryogenesis. *Development.* 133:989-99.

Satokata, I., L. Ma, H. Ohshima, M. Bei, I. Woo, K. Nishizawa, T. Maeda, Y. Takano, M. Uchiyama, S. Heaney, H. Peters, Z. Tang, R. Maxson, and R. Maas. 2000. Msx2 deficiency in mice causes pleiotropic defects in bone growth and ectodermal organ formation. *Nat Genet.* 24:391-5.

Satokata, I., and R. Maas. 1994. Msx1 deficient mice exhibit cleft palate and abnormalities of craniofacial and tooth development. *Nat Genet.* 6:348-56.

Schwartz, S., W.J. Kent, A. Smit, Z. Zhang, R. Baertsch, R.C. Hardison, D. Haussler, and W. Miller. 2003. Human-mouse alignments with BLASTZ. *Genome Res.* 13:103-7.

Sestakova, B., L. Ondrusova, and J. Vachtenheim. Cell cycle inhibitor p21/ WAF1/ CIP1 as a cofactor of MITF expression in melanoma cells. *Pigment Cell Melanoma Res.*

Shao, Z., J.L. Browning, X. Lee, M.L. Scott, S. Shulga-Morskaya, N. Allaire, G. Thill, M. Levesque, D. Sah, J.M. McCoy, B. Murray, V. Jung, R.B. Pepinsky, and S. Mi. 2005. TAJ/TROY, an orphan TNF receptor family member, binds Nogo-66 receptor 1 and regulates axonal regeneration. *Neuron.* 45:353-9.

Shibamoto, S., K. Higano, R. Takada, F. Ito, M. Takeichi, and S. Takada. 1998. Cytoskeletal reorganization by soluble Wnt-3a protein signalling. *Genes Cells.* 3:659-70.

Shimeld, S.M., I.J. McKay, and P.T. Sharpe. 1996. The murine homeobox gene Msx-3 shows highly restricted expression in the developing neural tube. *Mech Dev.* 55:201-10.

Siepel, A., G. Bejerano, J.S. Pedersen, A.S. Hinrichs, M. Hou, K. Rosenbloom, H. Clawson, J. Spieth, L.W. Hillier, S. Richards, G.M. Weinstock, R.K. Wilson, R.A. Gibbs, W.J.

Kent, W. Miller, and D. Haussler. 2005. Evolutionarily conserved elements in vertebrate, insect, worm, and yeast genomes. *Genome Res.* 15:1034-50.

Smalley, M.J., and T.C. Dale. 1999. Wnt signalling in mammalian development and cancer. *Cancer Metastasis Rev.* 18:215-30.

Smith, C.A., T. Farrah, and R.G. Goodwin. 1994. The TNF receptor superfamily of cellular and viral proteins: activation, costimulation, and death. *Cell.* 76:959-62.

Smith, R.S., John S.W.M., Nishina, P.M., Sundberg, J.P. 2002. Systematic Evaluation of the Mouse Eye: Anatomy, Pathology, and Biomethods. CRC Press.

Song, K., Y. Wang, and D. Sassoon. 1992. Expression of Hox-7.1 in myoblasts inhibits terminal differentiation and induces cell transformation. *Nature.* 360:477-81.

Suzuki, A., N. Ueno, and A. Hemmati-Brivanlou. 1997. Xenopus msx1 mediates epidermal induction and neural inhibition by BMP4. *Development.* 124:3037-44.

Szeto, D.P., and D. Kimelman. 2004. Combinatorial gene regulation by Bmp and Wnt in zebrafish posterior mesoderm formation. *Development.* 131:3751-60.

Takada, R., Y. Satomi, T. Kurata, N. Ueno, S. Norioka, H. Kondoh, T. Takao, and S. Takada. 2006. Monounsaturated fatty acid modification of Wnt protein: its role in Wnt secretion. *Dev Cell.* 11:791-801.

Tamai, K., M. Semenov, Y. Kato, R. Spokony, C. Liu, Y. Katsuyama, F. Hess, J.P. Saint-Jeannet, and X. He. 2000. LDL-receptor-related proteins in Wnt signal transduction. *Nature.* 407:530-5.

Thumann, G. 2001. Development and cellular functions of the iris pigment epithelium. *Surv Ophthalmol.* 45:345-54.

Thut, C.J., R.B. Rountree, M. Hwa, and D.M. Kingsley. 2001. A large-scale in situ screen provides molecular evidence for the induction of eye anterior segment structures by the developing lens. *Dev Biol.* 231:63-76.

Timmer, J.R., C. Wang, and L. Niswander. 2002. BMP signaling patterns the dorsal and intermediate neural tube via regulation of homeobox and helix-loop-helix transcription factors. *Development.* 129:2459-72.

Travis, A., A. Amsterdam, C. Belanger, and R. Grosschedl. 1991. LEF-1, a gene encoding a lymphoid-specific protein with an HMG domain, regulates T-cell receptor alpha enhancer function [corrected]. *Genes Dev.* 5:880-94.

Tropepe, V., B.L. Coles, B.J. Chiasson, D.J. Horsford, A.J. Elia, R.R. McInnes, and D. van der Kooy. 2000. Retinal stem cells in the adult mammalian eye. *Science.* 287:2032-6.

van Beest, M., D. Dooijes, M. van De Wetering, S. Kjaerulff, A. Bonvin, O. Nielsen, and H. Clevers. 2000. Sequence-specific high mobility group box factors recognize 10-12-base pair minor groove motifs. *J Biol Chem.* 275:27266-73.

van de Wetering, M., M. Oosterwegel, D. Dooijes, and H. Clevers. 1991. Identification and cloning of TCF-1, a T lymphocyte-specific transcription factor containing a sequence-specific HMG box. *EMBO J.* 10:123-32.

Van Raay, T.J., K.B. Moore, I. Iordanova, M. Steele, M. Jamrich, W.A. Harris, and M.L. Vetter. 2005. Frizzled 5 signaling governs the neural potential of progenitors in the developing Xenopus retina. *Neuron.* 46:23-36.

Wallace, V.A., and M.C. Raff. 1999. A role for Sonic hedgehog in axon-to-astrocyte signalling in the rodent optic nerve. *Development.* 126:2901-9.

Wang, Y., G.D. Dakubo, S. Thurig, C.J. Mazerolle, and V.A. Wallace. 2005. Retinal ganglion cell-derived sonic hedgehog locally controls proliferation and the timing of RGC development in the embryonic mouse retina. *Development.* 132:5103-13.

Willert, J., M. Epping, J.R. Pollack, P.O. Brown, and R. Nusse. 2002. A transcriptional response to Wnt protein in human embryonic carcinoma cells. *BMC Dev Biol.* 2:8.

Willert, K., J.D. Brown, E. Danenberg, A.W. Duncan, I.L. Weissman, T. Reya, J.R. Yates, 3rd, and R. Nusse. 2003. Wnt proteins are lipid-modified and can act as stem cell growth factors. *Nature.* 423:448-52.

Willert, K., and R. Nusse. 1998. Beta-catenin: a key mediator of Wnt signaling. *Curr Opin Genet Dev.* 8:95-102.

Wodarz, A., and R. Nusse. 1998. Mechanisms of Wnt signaling in development. *Annu Rev Cell Dev Biol.* 14:59-88.

Xu, Q., Y. Wang, A. Dabdoub, P.M. Smallwood, J. Williams, C. Woods, M.W. Kelley, L. Jiang, W. Tasman, K. Zhang, and J. Nathans. 2004. Vascular development in the retina and inner ear: control by Norrin and Frizzled-4, a high-affinity ligand-receptor pair. *Cell.* 116:883-95.

Yamaguchi, M., N. Tonou-Fujimori, A. Komori, R. Maeda, Y. Nojima, H. Li, H. Okamoto, and I. Masai. 2005. Histone deacetylase 1 regulates retinal neurogenesis in zebrafish by suppressing Wnt and Notch signaling pathways. *Development.* 132:3027-43.

Young, R.W. 1985. Cell proliferation during postnatal development of the retina in the mouse. *Brain Res.* 353:229-39.

Zhang, P., C. Wong, R.A. DePinho, J.W. Harper, and S.J. Elledge. 1998. Cooperation between the Cdk inhibitors p27(KIP1) and p57(KIP2) in the control of tissue growth and development. *Genes Dev.* 12:3162-7.

Zhao, S., Q. Chen, F.C. Hung, and P.A. Overbeek. 2002. BMP signaling is required for development of the ciliary body. *Development.* 129:4435-42.

Zorn, A.M. 2001. Wnt signalling: antagonistic Dickkopfs. *Curr Biol.* 11:R592-5.

7.0 Contributions of Collaborators

The microarray analysis, including cDNA synthesis from total RNA, labeling and microarray hybridization as well as microarray scanning and analysis was performed by Dr. Alan Mears. The bioinformatic analysis, including TCF binding site identification and filtering for degree of conservation of TCF binding sites was performed by Dr. Carolina Perez-Iratxeta.

I performed all the retinal explant cultures, immunohistochemistry, Q-PCR and ISH experiments as well as maintained the transgenic mice crosses.

8.0 Appendices

Appendix A - QPCR Primer Sets

Gene	Sequence (5' → 3')
Otx1	F - CGGGAATGGAACGAAAAC
	R- GCTCGTCTCCGAACCCGA
Pax6	F – ACCAGAGAAGACAGGCCA
	R – GTCTGTTCGGCCCAACAT
Pitx2	F – GAAAGACTCGGCCAGCA
	R – CGCCCACATCCTCATTC
Crx	F – CAATGCCTTGGCTCTGAGT
	R – ACATCCGGGTACTGGGTCT
Msx1	F – CACCGCAACCGCCAT
	R – TGCCCAAGTGCTGCAC
Msx2	F – GCCGCCCAAGGAATC
	R – CCGACTTGACCGAGGC
Cdkn1a	F – AGAGTGCAAGACAGCGACAA
	R – GTCCAATCCTGGTGATGTCC
Cad	F – GGCCTCCATGTTCGTACGA
	R – GACTCGCCCTTTTGGAC
Fyn	F – TACCCAGGCATGAACAACC
	R – CAGCAGTGGATCATGAGC
Lpp	F – TGGAATCTTTATGCGAACTCTT
	R – TAATGGCCAACTGCAACTG
Med12	F – TATACCGGCAGCAGCAAC
	R – GGAAGAACTAGGGGTCATCTG
Wif1	F – TAAGAGGTATGGAGCCAGCC
	R – ATCCCTTCTATCCTCAGCCTT
Efna3	F – GTGAAGATCAACGTGTTGGAA
	R – GAGGCCAAGAGCTGCAT
Axin2	F – AGACCGGTCACAGGAGTG
	R – CAGGCAGACTCCAATGGGTA
Cdc25b	F – ATCCTCAAGAGGCTAGAGCG
	R – ACGGGCCTTAGGTTCTTCA
Epha2	F – TGATCCCCGAGTGTCCA
	R – CAGATAGGAATCCCCACTGTGT
Tnfrsf19	F – GAGAAGTACCAATTCCCTCAA
	R – AGATGCTGCGCTTTCGT
Klf10	F – TTGAGACAGTCCCAGCATTTG
	R – GGCAGCATCGGAGAAAGAT
Chm	F – TATTCTTGATGGAGACAGCTCAC
	R – TACTTTCCTTGTGAGTTTCTGA
Irx2	F – GCAACTACACAAACTACGGGAA
	R – TGTAGTGGTACTCCAGTGAA

Gene	Sequence (5' → 3')
Lix1	F – GCCCTGGACTGGATTATGAA
	R – CGTGAGGCTTAGCTGGTCAG
Ndrg2	F – ACAAGTTAACTGGCCTTACGTCTT
	R – TGCGTGTTGGATGATACCTCT
Prickle1	F – TTGAAGAGAGGGGATCCAG
	R – ATGGGCATACTGGCTATAGAGGTT
Serpine2	F – CTTCATGTCTCTCACATCTTGC
	R – TACTATAAACCAGGGAGGTGATGA
Syt13	F – TTAAGTTCCCGGACATCTATGGT
	R – GACTCCTCTGTGGTCTCCAA
Col6a1	F – TGCAGGCATTGAGATCTTTG
	R – CAGGGCCTGGTAGTTTGGTA
Col18a1	F – CCCAGACATGAAGGAGGAG
	R – GAACCTCAGTCCCAGCAGA
Slc16a6	F – CTGCAGCCGATCAAGAAT
	R – AGAAACAGCTACTGCCCAG
Slc7a3	F – CCTGAGCACCCTCGACTTA
	R – CCAACACAGAGGACAGAGC

Primer sequences for *Otx1, Pax6, Pitx2, Crx, Msx1* and *Msx2* were used to validate gene expression in Li^+-treated retinal explants. Primer sequences for *p21, Cad, Fyn, Lpp, Wif1, Med12, Efna3, Axin2, Cdc25b, Epha3, Tnfrsf19, Klf10, Chm, Irx2, Lix1, Ndrg2, Prickle1, Serpine2, Syt13, Col6a1, col18a1, Slc16a6, Slc7a3* were used to validate gene expression of these genes as reported from the microarray analysis.

Appendix B - Primer Sets for cDNA amplification for ISH riboprobes

Gene	Sequence (5' → 3')
Cdkn1a	F – CGGTGGAACTTTGACTTCGT
	R – CAGGGCAGAGGAAGTACTGG
Tnfrsf19	F – GAGACCCACCTCCGTCCTAC
	R – GGAGTCCTTGGAGCATCCTG
Serpine2	F – TGTGGAATTCTCGGTTTCA
	R – TGTGGGATTGTGTCGGAT
Syt13	F – AGTTGAGGATGTCTGTGTCAT
	R – ACCTTGACAGACACATCCTT
Klf10	F – CATCCGTCACACAGCTGAT
	R – TCTGGACGAGTCAATCTGA
Epha2	F – ATGGTGAGTTCAGTGTACTTCAGT
	R – ATGAAGTGTTCCGTGTACTGTT
Fyn	F – AAGTGTCACGTGACTCGTTG
	R – CTCTTCCGGATCCTTTTTCC
Med12	F – AGACCCCCAACACTGAGATG
	R – ATGCTGCCTTGCGAGATACT
Cdc25b	F – AGTGAGGCTGCTGGAACA
	R – AAAGACACGGGCCTTAGGT
Lix1	F – ACTTGAATGTTGTGTCAATGTTA
	R – ATTCCTGGTGATTCACGC
Prickle1	F – CTGCTCAGGAGATCCAAGT
	R – TTGTCCTCTGAGTAAACTGTGG
Ndrg2	F – CCAGGGACAGACTCACTCT
	R – TTTTGTAGCTGTTCCAGTAGAG
Irx2	F – CGAATCAGGCTCAGAGTGTAA
	R – TGTAGTGGGACTCCAGTGAAT
Wif1	F – CAAGTTGGTTCCCGTGTCT
	R – TTAAGTGAAGGCGTGTGTCG
Axin2	F – GGAAAACACAGCTTACATGAGT
	R – TTTCCAGCTCCAGTTTCAG
Lpp	F – GCCCGTTGTATTTCCACAAT
	R – AACTGCAAAGCGAGGTGTCT
Col6a1	F – ATTAAGAAGGGGCTGGAGGA
	R – TCTCCAGGATCACCCTCATC
Col18a	F – CTCTGCTGGGACTGAGGTTC
	R – TTCCAAAATCTCCAGATGCC
Slc16a6	F – CTTTCGCACCAGCTATCACA
	R – CTCGGTAGCGAAAGTGAAGG
Slc7a3	F – CCTGAGCACCCTCGACTTAG
	R – GTCAAAACCAACGAAGGCAT

Gene	Sequence (5' → 3')
Slc7a7	F – CTTTTCTGCTCCTCCGTGTC
	R – AACAATGCCTGCAATGATGA
Slc44a2	F – TCTTGTTGCTCTGCATTGCC
	R - GATCCGATGGGTGAAGAAGA

Appendix C - Buffer Solutions

100x Denhart's solution:

2% BSA, 2% Ficoll, 2% polyvinyl pyrolidone

10x Salt:

Tris-HCL pH 7.5 (14.04 g), NaCl (114 g), Tris base (1.34 g), Na_2HPO_4 (7.1 g), NaH_2PO_4 $2H_20$ (7.8 g), 0.5 M EDTA (100 ml), water to 1 L.

ISH Hybridization Buffer:

1x Denhart's, 1x salt, 50% deionized formamide, 10% dextran sulfate, rRNA (1 mg/ml), water

Wetting Buffer:

50% formamide, 1x salt, water

Wash Buffer:

1x SCC, 50% formamide, 0.1% Tween-20, water. Pre-warm to 65 °C before use

5x MABT, pH 7.5:

0.5 M maleic acid, pH adjusted to 7.5 using NaOH, 0.75 M NaCl, 0.5% Tween-20, water

ISH Blocking reagent:

10% Blocking reagent (Roche) in 1x MABT

ISH Blocking solution:

20% sheep serum, 2% blocking reagent, 1x MABT, water

ISH Prestain buffer:

100 mM NaCl, 50 mM MgCl2, 100 mM Tris, pH 9-9.5, 0.1% Tween20, water.

ISH Staining buffer:

100 ml NaCl, 100 mM Tris, pH 9-9.5, water, 10% polyvinyl alcohol heat to 85-90 °C to dissolve), cooled to RT and 50 mM MgCl2 and Tween-20 (70 µl) added. Prior to incubation NBT (4.5 µl/ml Roche) and BCIP (3.5 µl/ml Roche) added to a final volume of 70 ml.

β-gal staining 0.1M phosphate buffer, Ph 7.3

0.1 M NaH_2PO_4, 0.1 M Na_2HPO_4

β-gal staining Wash Buffer

2mM $MgCl_2$, 0.01% Na deoxycholate, 0.02% Nonidet P-40, 0.1M phosphate buffer, pH 7.3

β-gal LacZ staining buffer (50ml)

47.5 ml Wash buffer, 2.5 ml x-gal (2 % stock in DMSO), 0.1g Ferrocyanide, 0.075g Ferricyanide

Appendix D. Genes upregulated in microarray analysis of Li^+-treated retinal explants

Accession #	Symbol	Fold Change	avA	diffex total
NM_021451	Pmaip1	57.47	11.49	4.00
NM_007669	Cdkn1a	22.78	11.78	4.00
NM_175540	Eda2r	21.56	10.17	4.00
NM_007669	Cdkn1a	20.97	13.56	4.00
NM_145471	E130306I01Rik	19.85	9.94	4.00
NM_183274	0610041G09Rik	17.89	10.97	4.00
NM_013750	Phlda3	16.42	11.58	4.00
NM_009831	Ccng1	13.43	10.90	4.00
NM_009831	Ccng1	11.60	10.49	4.00
NM_009831	Ccng1	10.03	9.59	4.00
	C230069I12Rik	9.83	9.47	4.00
NM_021515	Ak1	9.39	12.55	4.00
NM_007725	Cnn2	8.95	9.22	4.00
NM_009218	Sstr3	8.23	10.87	4.00
NM_009831	Ccng1	7.98	13.19	4.00
NM_011838	Lynx1	7.75	9.78	4.00
NM_009517	Wig1	7.36	10.82	4.00
NM_054087	Slc19a2	7.18	10.95	4.00
NM_001002011	Lmna	5.81	9.89	4.00
NM_146269	Olfr247	5.67	10.88	4.00
	4632434I11Rik	5.62	9.11	4.00
NM_183107	4930474M22Rik	5.21	9.13	4.00
NM_010452	Hoxa3	5.00	12.33	4.00
NM_173447	Ephb1	4.82	10.76	4.00
NM_007906	Eef1a2	4.76	12.13	4.00
NM_026481	2700055K07Rik	4.74	12.39	4.00
NM_080288	Elmo1	4.63	11.05	4.00
NM_001002011	Lmna	4.53	9.69	4.00
NM_022654	Lrdd	4.23	9.41	4.00
NM_011861	Pacsin1	4.15	9.96	4.00
	4933415B22Rik	4.12	9.96	4.00
NM_008975	Ptp4a3	4.11	9.47	4.00
NM_023162	Znrd1	4.03	9.34	4.00
NM_026633	9530058B02Rik	3.95	9.00	4.00
NM_008760	Ogn	3.92	9.06	4.00
NM_019976	5430413I02Rik	3.86	12.08	4.00
NM_008532	Tacstd1	3.59	9.73	4.00

Accession #	Symbol	Fold Change	avA	diffex total
NM_013882	Gtse1	3.53	10.83	4.00
NM_013882	Gtse1	3.48	9.55	4.00
NM_153679	Cpt1c	3.47	10.05	4.00
NM_021897	Trp53inp1	3.45	10.44	4.00
NM_011858	Odz4	3.35	9.42	4.00
NM_026531	2700083B06Rik	3.33	9.70	4.00
NM_133838	Ehd4	3.33	10.41	4.00
NM_009148	Sec8l1	3.32	9.72	4.00
NM_145399	Scgn	3.21	12.28	4.00
NM_177688	E130307C13	3.19	9.46	4.00
NM_001004140	Ckap2	3.18	10.57	4.00
NM_011497	Stk6	3.14	10.90	4.00
NM_017368	Cugbp1	3.01	9.30	4.00
NM_144907	Sesn2	2.99	9.54	4.00
NM_009502	Vcl	2.98	9.90	4.00
NM_026473	2310057H16Rik	2.95	12.50	4.00
NM_016690	Hnrpdl	2.86	9.94	4.00
	A930033M14Rik	2.86	10.58	4.00
NM_007585	Anxa2	2.80	12.78	4.00
NM_199447	AA408556	2.73	9.65	4.00
NM_025365	1110002E23Rik	2.70	10.99	4.00
NM_007837	Ddit3	2.69	10.81	4.00
NM_144823	Acsl6	2.66	11.64	4.00
NM_011861	Pacsin1	2.60	9.11	4.00
NM_175563	B930067F20Rik	2.58	9.20	4.00
NM_021555	Brp16	2.55	10.11	4.00
NM_025681	Lix1	2.54	9.56	4.00
XM_485065	1700041B20Rik	2.52	10.23	4.00
NM_033610	Sncb	2.50	9.22	4.00
	1500001E21Rik	2.45	9.98	4.00
NM_010764	Man2b1	2.42	9.57	4.00
NM_028766	1200015A22Rik	2.39	11.26	4.00
NM_183405	Cox6b2	2.33	12.91	4.00
NM_023525	Cad	2.24	10.09	4.00
NM_138745	Mthfd1	2.18	10.25	4.00
NM_026785	Ube2c	2.13	13.05	4.00
NM_026531	2700083B06Rik	27.24	8.05	4.00
NM_009255	Serpine2	25.13	8.24	4.00

Accession #	Symbol	Fold Change	avA	diffex total
	4933433G08Rik	24.84	8.84	4.00
NM_007725	Cnn2	18.32	8.48	4.00
NM_175540	Eda2r	15.39	8.13	4.00
NM_019932	Cxcl4	11.12	8.90	4.00
NM_152804	Plk2	7.12	8.90	4.00
NM_012048	Polk	7.01	8.16	4.00
NM_008760	Ogn	5.57	8.53	4.00
XM_149840	D330027H18Rik	5.35	8.88	4.00
	Rnu68	4.83	8.91	4.00
NM_009684	Apaf1	3.76	8.07	4.00
NM_010070	Dok1	3.48	8.43	4.00
NM_175108	2310047C17Rik	3.42	8.47	4.00
BC044883	1810027I20Rik	2.98	8.51	4.00
XM_128377	4921511H13Rik	2.93	8.72	4.00
NM_023544	1700027M01Rik	2.91	8.40	4.00
	2610002F03Rik	2.91	8.33	4.00
NM_011125	Pltp	2.81	8.55	4.00
NM_198308	4930402E16Rik	2.69	8.46	4.00
	2810012D02Rik	2.68	8.44	4.00
NM_015747	Slc20a1	2.23	8.94	4.00
NM_011915	Wif1	29.22	7.68	4.00
NM_020275	Tnfrsf10b	28.22	7.38	4.00
NM_177233	C130034I18Rik	25.73	7.81	4.00
NM_183190	Ms4a5	22.47	7.26	4.00
NM_013869	Tnfrsf19	20.86	7.56	4.00
NM_008871	Serpine1	19.81	7.16	4.00
XM_488744	Pvt1	17.36	7.15	4.00
NM_008508	Lor	15.43	7.39	4.00
NM_011838	Lynx1	15.43	7.67	4.00
	4931415C17Rik	14.31	7.38	4.00
NM_009146	Sdfr2	13.76	7.41	4.00
NM_177828	4933429F08Rik	11.83	7.14	4.00
NM_026531	2700083B06Rik	9.92	7.93	4.00
NM_008863	Pkib	9.17	7.88	4.00
NM_178907	Mapkapk3	8.05	7.60	4.00
NM_133746	2810048G17Rik	7.34	7.62	4.00
NM_009608	Actc1	7.14	7.07	4.00
NM_023456	Npy	6.99	7.11	4.00

Accession #	Symbol	Fold Change	avA	diffex total
XM_284175	1110055E19Rik	5.86	7.05	4.00
NM_021429	Hs1bp3	4.40	7.62	4.00
NM_031158	Ank1	4.32	7.14	4.00
AK047273		4.07	7.09	4.00
NM_011066	Per2	3.82	7.56	4.00
NM_181397	2310015N21Rik	3.62	7.61	4.00
NM_010145	Ephx1	3.42	7.34	4.00
XM_354672	Mipol1	3.37	7.26	4.00
NM_013749	Tnfrsf12a	3.25	7.79	4.00
NM_028112	Seh1l	3.21	7.40	4.00
NM_026507	2310031L18Rik	3.12	7.87	4.00
NM_054041	Antxr1	2.84	7.84	4.00
	D330023I04Rik	2.74	7.79	4.00
NM_029546	Pwp2h	2.73	7.81	4.00
NM_026633	9530058B02Rik	3.35	9.18	3.85
	2900057K09Rik	2.90	10.38	3.85
NM_025681	Lix1	2.70	9.22	3.85
NM_010180	Fbln1	2.64	10.07	3.85
NM_177325	AW550801	2.41	10.67	3.85
NM_178679	Zfp365	2.36	9.74	3.85
NM_023065	Ifi30	2.29	10.17	3.85
NM_013692	Tieg1	2.26	11.94	3.85
NM_026467	Rps27l	2.23	14.55	3.85
NM_177214	Ascc3l1	2.21	12.15	3.85
NM_172301	Ccnb1	2.21	12.38	3.85
NM_007527	Bax	2.20	13.64	3.85
XM_131052	Cgn	2.19	10.17	3.85
NM_018822	Sgsh	2.19	9.73	3.85
NM_172301	Ccnb1	2.15	10.99	3.85
XM_354699	AW555464	2.14	10.85	3.85
NM_028057	Nqo3a2	3.48	8.94	3.85
	2210411K19Rik	3.43	8.51	3.85
NM_009331	Tcf7	3.22	8.78	3.85
NM_007825	Cyp7b1	3.17	8.55	3.85
NM_016808	Usp2	2.88	8.43	3.85
	1700030C10Rik	2.81	8.82	3.85
NM_026728	D4Ertd765e	2.79	8.34	3.85

Accession #	Symbol	Fold Change	avA	diffex total
NM_009138	Ccl25	2.71	8.71	3.85
NM_010353	Gsg2	2.24	8.86	3.85
NM_010664	Krt1-18	14.28	7.12	3.85
NM_023057	B230120H23Rik	6.36	7.25	3.85
	Thada	3.25	7.62	3.85
NM_152807	3110023B02Rik	3.10	7.91	3.85
XM_355248	Pappa2	2.93	7.71	3.85
NM_008512	Lrp1	2.67	7.47	3.85
NM_009621	Adamts1	2.57	7.40	3.85
NM_030179	1700024K14Rik	2.54	7.14	3.85
NM_016722	Galns	2.42	7.16	3.85
	6530415H11Rik	2.19	7.45	3.85
NM_178794	U2af1-rs2	2.30	10.02	3.70
NM_010635	Klf1	2.30	11.04	3.70
NM_139237	Nol6	2.18	9.98	3.70
	2410006H16Rik	2.17	11.10	3.70
NM_010792	Mettl1	2.06	10.65	3.70
NM_139236	Nol6	2.03	9.88	3.70
	Rnu22	2.00	11.22	3.70
NM_025881	Luc7l	2.34	8.07	3.70
	2900076A07Rik	2.15	8.99	3.70
NM_025447	1500031M22Rik	3.36	7.30	3.70
NM_009413	Tpd52l1	3.10	7.77	3.70
NM_028874	Snx19	2.34	7.60	3.70
NM_029945	4122402O22Rik	2.10	7.91	3.70
NM_153544	BC030867	3.03	9.06	3.58
NM_008745	Ntrk2	2.93	11.06	3.58
NM_027541	Prpf3	2.87	9.15	3.58
NM_019390	Lmna	2.73	11.73	3.58
NM_016776	Mybbp1a	2.55	9.66	3.58
NM_172284	2810457M08Rik	2.54	9.93	3.58
NM_008087	Gas2	2.34	9.19	3.58
NM_175168	Ptk7	2.30	10.24	3.58
NM_024198	Gpx7	2.27	10.31	3.58
	6230400I06Rik	2.23	9.66	3.58
NM_019587	Plxnb3	2.22	10.00	3.58
NM_025681	Lix1	2.21	9.71	3.58
NM_007515	Slc7a3	2.17	9.89	3.58

Accession #	Symbol	Fold Change	avA	diffex total
NM_019417	Pdlim4	2.16	9.46	3.58
NM_147778	Commd3	2.16	12.67	3.58
NM_172668	Lrp4	2.12	9.14	3.58
NM_019547	Rnpc1	2.10	11.31	3.58
	2810008D09Rik	2.09	9.49	3.58
NM_172015	Iars	2.07	9.18	3.58
NM_008060	Ganab	2.07	10.64	3.58
NM_023731	D19Ertd678e	2.06	10.70	3.58
NM_178642	AU040576	2.06	10.29	3.58
AK013903		2.04	10.52	3.58
NM_013742	Cars	2.03	11.09	3.58
XM_355637	Sbno1	2.03	9.07	3.58
NM_133952	AW538196	2.02	9.10	3.58
NM_027541	Prpf3	2.01	12.30	3.58
NM_008598	Mgmt	3.06	8.43	3.58
NM_030246	Wdr21	2.72	8.50	3.58
NM_011015	Orc1l	2.71	8.29	3.58
NM_027541	Prpf3	2.64	8.92	3.58
XM_126772	Usp36	2.63	8.06	3.58
NM_133686	Qprt	2.49	8.21	3.58
	9530056D24Rik	2.42	8.05	3.58
NM_017392	Celsr2	2.24	8.19	3.58
NM_019570	Rev1l	2.21	8.86	3.58
NM_145920	Evc2	1.96	8.94	3.58
NM_013506	Eif4a2	13.64	7.64	3.58
NM_010139	Epha2	8.37	7.30	3.58
XM_132796	Fancd2	8.11	7.28	3.58
NM_080637	Nme5	5.73	7.25	3.58
NM_031258	Chrdl1	4.55	7.60	3.58
NM_009963	Cry2	3.91	7.33	3.58
NM_175398	6530418L21Rik	3.89	7.12	3.58
NM_028712	Rap2b	3.85	7.87	3.58
NM_178665	Lpp	3.73	7.72	3.58
NM_025465	1810029B16Rik	3.59	7.14	3.58
NM_011957	Creb3l1	3.32	7.79	3.58
NM_010180	Fbln1	3.21	7.93	3.58
NM_028121	Adpgk	3.06	7.88	3.58
NM_008773	P2ry2	2.92	7.46	3.58

Accession #	Symbol	Fold Change	avA	diffex total
NM_025926	Dnajb4	2.70	7.61	3.58
XM_192925	Itch	2.59	7.65	3.58
NM_013555	Hoxd9	2.40	7.51	3.58
NM_009089	Polr2a	2.31	7.19	3.58
NM_025876	Cdk5rap1	2.09	7.41	3.58
NM_144835	B130016L12Rik	2.04	9.97	3.55
NM_009933	Col6a1	1.98	11.29	3.55
NM_176897	C530043A13Rik	2.70	9.97	3.43
NM_134033	BC018601	2.32	11.10	3.43
NM_017376	Tef	2.11	10.58	3.43
NM_009929	Col18a1	2.07	11.06	3.43
NM_019512	Tcerg1	2.04	9.58	3.43
NM_172015	Iars	2.04	10.45	3.43
	Rnu65	2.02	10.21	3.43
	1700096P03Rik	2.01	9.73	3.43
NM_016776	Mybbp1a	1.97	13.10	3.43
XM_131118	Ttf2	1.97	9.62	3.43
NM_019547	Rnpc1	1.96	11.76	3.43
NM_026277	1700021I09Rik	1.96	11.64	3.43
NM_010180	Fbln1	1.95	11.33	3.43
NM_133655	Cd81	1.90	14.27	3.43
NM_013568	Kcna6	3.59	8.01	3.43
NM_010801	Mlf1	2.82	8.81	3.43
NM_011125	Pltp	2.54	8.22	3.43
NM_026331	Mscp	2.47	8.49	3.43
NM_009423	Traf4	2.27	8.61	3.43
NM_008770	Cldn11	2.27	8.84	3.43
NM_028115	2610009I02Rik	2.19	8.23	3.43
NM_017376	Tef	2.14	8.63	3.43
NM_011361	Sgk	2.07	8.58	3.43
	D930030F02Rik	3.31	7.35	3.43
NM_009017	Raet1b	3.10	7.57	3.43
	4930413O22Rik	2.55	7.15	3.43
NM_177462	9330177P20Rik	2.42	7.36	3.43
NM_010893	Neu1	2.35	7.69	3.43
	Ccnb1-rs1	1.95	12.52	3.28
NM_028120	2610507L03Rik	1.95	10.62	3.28

Accession #	Symbol	Fold Change	avA	diffex total
NM_019642	Rpn2	1.91	10.36	3.28
NM_026453	2600016B03Rik	1.89	10.93	3.28
NM_054070	Afg3l1	1.88	9.04	3.28
NM_009770	Btg3	1.86	10.68	3.28
	AI506816	1.82	9.59	3.28
NM_139236	Nol6	2.20	8.61	3.28
NM_199007	Sgol2	2.04	8.43	3.28
NM_144857	BC011248	1.98	8.99	3.28
NM_153808	Smc5l1	1.97	8.17	3.28
		2.01	7.14	3.28
NM_177836	AW046396	1.94	7.99	3.28
NM_026507	2310031L18Rik	2.37	9.10	3.16
NM_178939	Pdrg1	2.30	11.48	3.16
	1500012F01Rik	2.19	13.99	3.16
NM_144835	B130016L12Rik	2.13	10.21	3.16
NM_016776	Mybbp1a	2.11	9.55	3.16
NM_029546	Pwp2h	2.09	10.99	3.16
NM_026166	1200009F10Rik	2.04	9.22	3.16
NM_021521	Tnrc11	1.99	9.60	3.16
NM_025907	1600013P15Rik	1.98	9.16	3.16
NM_007594	Calu	1.97	10.07	3.16
NM_172757	C030036P15Rik	1.95	9.16	3.16
NM_213728	AI507495	1.91	9.35	3.16
NM_026502	1110004E09Rik	1.91	11.11	3.16
NM_207264	BC052040	1.89	10.17	3.16
NM_153805	Pkn3	1.89	10.14	3.16
	1700054E11Rik	1.88	9.17	3.16
NM_023117	Cdc25b	1.86	11.13	3.16
XM_133997	2310057J16Rik	1.85	9.22	3.16
NM_134139	5730436H21Rik	1.83	10.37	3.16
NM_009016	Raet1a	5.23	8.36	3.16
NM_030143	Ddit4l	3.05	8.44	3.16
NM_029556	Clybl	2.63	8.07	3.16
NM_008968	Ptgis	2.46	8.04	3.16
NM_010835	Msx1	2.34	8.18	3.16
NM_175353	Sec15l1	2.23	8.12	3.16
NM_144520	Sec14l2	2.07	8.83	3.16
XM_488563	2310036D04Rik	2.00	8.21	3.16

Accession #	Symbol	Fold Change	avA	diffex total
NM_173437	Nav1	1.97	8.96	3.16
NM_177861	5330408M12Rik	1.88	8.37	3.16
	5730409K12Rik	1.83	8.39	3.16
NM_153092	Nupl2	6.71	7.13	3.16
NM_172558	Gemin5	6.01	7.96	3.16
NM_152808	1110028E10Rik	2.47	7.08	3.16
NM_025465	1810029B16Rik	2.28	7.17	3.16
NM_019809	1110001A05Rik	1.94	7.21	3.16
NM_011405	Slc7a7	1.87	7.96	3.16
XM_488851	9130209A04Rik	1.82	7.88	3.16
NM_175104	2810012G03Rik	1.84	7.79	3.13
XM_283286	Troap	2.04	9.91	3.01
NM_007485	Rhod	1.98	9.61	3.01
NM_145610	Ppan	1.91	11.31	3.01
XM_358330	Pprc1	1.87	9.26	3.01
NM_030693	Atf5	1.85	13.61	3.01
NM_009994	Cyp1b1	1.84	10.38	3.01
NM_172308	Fthfsdc1	1.82	9.80	3.01
NM_013562	Ifrd1	1.82	11.62	3.01
NM_007601	Capn3	1.81	12.66	3.01
XM_134644	2410001E19Rik	1.81	9.16	3.01
NM_011234	Rad51	1.79	10.26	3.01
XM_358343	Sulf2	1.79	12.55	3.01
NM_134011	Tbrg4	1.78	10.05	3.01
NM_146067	C530044N13Rik	1.77	10.90	3.01
NM_025422	1110055L24Rik	1.98	8.32	3.01
NM_175096	D5Ertd593e	1.88	8.50	3.01
NM_020517	Lenep	1.84	8.71	3.01
XM_125586	Qrsl1	1.82	8.31	3.01
NM_172700	Zmpste24	1.81	8.16	3.01
NM_001003919	Ddx11	2.24	7.60	3.01
	4930558N01Rik	2.13	7.30	3.01
NM_026932	Ebna1bp2	2.10	7.62	3.01
NM_010820	Mpdz	1.84	7.90	3.01
NM_029834	Ppp1r12c	1.74	7.45	3.01
NM_008100	Gcg	3.08	9.99	3.00
NM_138659	Prpf8	2.52	9.02	3.00
NM_134033	BC018601	2.25	12.22	3.00

Accession #	Symbol	Fold Change	avA	diffex total
NM_008529	Ly6e	2.22	12.68	3.00
NM_025412	Pycrl	2.22	9.10	3.00
NM_010792	Mettl1	2.20	9.69	3.00
NM_145557	9430015G10Rik	2.19	9.10	3.00
NM_138659	Prpf8	2.12	12.11	3.00
NM_023066	Asph	2.10	9.28	3.00
NM_009658	Akr1b3	2.10	10.28	3.00
NM_028762	Rbm19	2.09	9.50	3.00
NM_025522	Dhrs7	2.08	9.00	3.00
NM_027052	Slc38a4	2.07	9.01	3.00
NM_011821	Gpc6	2.04	9.23	3.00
NM_013603	Mt3	1.98	9.91	3.00
NM_023372	Rpl38	1.95	10.56	3.00
NM_010286	Dsip1	1.88	9.82	3.00
XM_131572	Eif2b3	1.88	9.65	3.00
NM_026637	A030007L17Rik	1.83	9.35	3.00
NM_177287	C030025P15Rik	4.60	8.10	3.00
XM_150103	D130029J02Rik	3.79	8.16	3.00
NM_025549	Arrdc4	3.72	8.98	3.00
XM_140553	BC046418	3.47	8.79	3.00
NM_172398	2310005E10Rik	3.47	8.10	3.00
NM_015732	Axin2	2.82	8.00	3.00
NM_010397	H2-T22	2.66	8.32	3.00
NM_139236	Nol6	2.62	8.66	3.00
NM_027541	Prpf3	2.53	8.53	3.00
NM_028121	Adpgk	2.51	8.65	3.00
XM_144142	1810045K06Rik	2.48	8.01	3.00
NM_145362	Alg1	2.46	8.30	3.00
NM_145406	Slc10a3	2.45	8.01	3.00
NM_008808	Pdgfa	2.40	8.86	3.00
	AU020206	2.36	8.25	3.00
	5730488B01Rik	2.34	8.94	3.00
NM_008408	Itm1	2.22	8.79	3.00
XM_181420	Cgref1	2.18	8.99	3.00
	6330509M23Rik	2.17	8.70	3.00
NM_198607	4930572J05Rik	2.16	8.68	3.00
NM_177331	5830483C08Rik	2.15	8.47	3.00
NM_152807	3110023B02Rik	2.15	8.87	3.00

Accession #	Symbol	Fold Change	avA	diffex total
NM_011632	Traf3	2.15	8.80	3.00
NM_009138	Ccl25	2.15	8.62	3.00
NM_007398	Ada	2.15	8.66	3.00
NM_030560	BC003993	2.11	8.89	3.00
AK053156		2.08	8.70	3.00
NM_021525	Rcl1	2.07	8.24	3.00
	1700042D18Rik	2.01	8.99	3.00
NM_015728	Slc33a1	1.95	8.23	3.00
NM_029519	5830461H18Rik	1.91	8.63	3.00
NM_015828	Gne	1.87	8.80	3.00
NM_029291	1700011I11Rik	1.84	8.04	3.00
NM_011023	Otx1	1.82	8.17	3.00
BC031849	Sdha	1.74	8.88	3.00
	1110004P15Rik	8.65	7.55	3.00
NM_020275	Tnfrsf10b	8.16	7.61	3.00
NM_029291	1700011I11Rik	7.77	7.35	3.00
NM_010516	Cyr61	7.61	7.00	3.00
AK049469		7.58	7.37	3.00
NM_008054	Fyn	4.26	7.27	3.00
NM_009089	Polr2a	4.08	7.25	3.00
NM_134038	Slc16a6	3.88	7.78	3.00
NM_013742	Cars	3.59	7.83	3.00
NM_009376	Tg737Rpw	3.48	7.72	3.00
NM_009312	Tac2	3.46	7.14	3.00
NM_011677	Ung	3.38	7.11	3.00
NM_173450	4921503C21Rik	3.36	7.22	3.00
NM_172501	8030451K01Rik	3.23	7.10	3.00
AF357417		3.23	7.22	3.00
NM_148953	Asb16	3.20	7.29	3.00
NM_021555	Brp16	3.20	7.45	3.00
NM_026344	Dph2l2	3.10	7.51	3.00
NM_011065	Per1	3.05	7.54	3.00
NM_201372	D630044F24Rik	3.00	7.74	3.00
NM_175746	Edaradd	2.86	7.42	3.00
NM_019444	Ramp2	2.82	7.37	3.00
NM_027756	Mfap3l	2.79	7.20	3.00
NM_026728	D4Ertd765e	2.72	7.94	3.00
NM_028002	2310069P03Rik	2.71	7.37	3.00

Accession #	Symbol	Fold Change	avA	diffex total
NM_172699	C330039G02Rik	2.62	7.30	3.00
NM_028300	2700059L22Rik	2.61	7.37	3.00
NM_029545	6530401N04Rik	2.60	7.19	3.00
NM_029128	Qtrtd1	2.50	7.25	3.00
NM_172926	Snx14	2.50	7.04	3.00
NM_026507	2310031L18Rik	2.48	7.58	3.00
NM_133808	Hdlbp	2.42	7.50	3.00
NM_177858	4933431E20	2.41	7.15	3.00
NM_022032	Perp	2.36	7.84	3.00
NM_008881	Plxna1	2.34	7.92	3.00
NM_023042	Recql	2.33	7.51	3.00
NM_172259	BC037527	2.21	7.84	3.00
NM_172743	Plekha7	2.18	7.28	3.00
NM_024169	Fkbp11	2.14	7.96	3.00
NM_178772	B230106I24Rik	2.13	7.55	3.00
NM_026140	3230401I01Rik	2.11	7.89	3.00
NM_026855	1110067L22Rik	2.07	7.09	3.00
NM_023066	Asph	2.07	7.65	3.00
NM_025769	5430404L10Rik	2.04	7.87	3.00
NM_030562	Lrfn1	2.03	7.73	3.00
NM_007407	Adcyap1r1	1.96	7.91	3.00
NM_172518	Fbxo42	1.92	7.44	3.00
NM_008179	Gspt2	1.91	7.19	3.00
	Sco1	1.86	7.63	3.00
XM_204001	Efna3	1.72	7.75	3.00

Genes are sorted first by diffex total, then by fold change

Fold Change – calculated fold change
avA – signal intensity in Log_2. Signal intensity over background levels. A cut-off value of 7 was used to determine if transcript was detectable (present vs absent)
Diffex total. – Sum of diffex values from 4 arrays based on actual threshold of fold-changes in Log_2. A cut-off value of 3 was used. Diffex value were assigned to each array based on observed fold change for each probe/transcript/gene as follows:

- Greater than 2-fold change = 1
- Less than 2-fold but greater than 1.8-fold = 0.85
- Less than 1.85-fold but greater than 1.5-fold = 0.58

Therefore a gene that is upregulated by 2-fold or higher in all four arrays would get a score of 4.

Appendix E. Genes downregulated in microarray analysis of Li^+-treated retinal explants

Accession #	Symbol	Fold Change	avA	diffex total
XM_358428	Dio3as	-78.34	9.67	-4.00
NM_009215	Sst	-11.12	11.27	-4.00
NM_013653	Ccl5	-10.40	9.26	-4.00
	2700090O03Rik	-8.52	9.31	-4.00
NM_178207	Hist1h3i	-6.95	9.34	-4.00
NM_175267	E130112H22Rik	-6.66	9.40	-4.00
NM_009127	Scd1	-6.61	9.08	-4.00
NM_026897	Haghl	-5.85	10.21	-4.00
NM_016662	Mxd3	-5.77	9.42	-4.00
NM_031166	Idb4	-5.68	9.91	-4.00
NM_011795	C1ql1	-5.41	9.14	-4.00
NM_033037	Cdo1	-5.17	9.45	-4.00
NM_172119	Dio3	-5.08	9.97	-4.00
NM_007671	Cdkn2c	-4.58	9.14	-4.00
NM_178193	Hist1h4b	-4.55	10.24	-4.00
NM_011129	Sept4	-4.21	9.63	-4.00
NM_178203	Hist1h3b	-4.04	10.71	-4.00
NM_177023	E130114P18Rik	-3.99	10.52	-4.00
NM_027397	Isl2	-3.94	9.25	-4.00
XM_485370	1700008B15Rik	-3.89	10.64	-4.00
NM_021272	Fabp7	-3.88	11.48	-4.00
NM_011837	Ly6h	-3.86	9.59	-4.00
NM_019585	Espn	-3.77	10.49	-4.00
NM_025378	Ifitm3	-3.71	9.46	-4.00
NM_010496	Idb2	-3.62	11.76	-4.00
NM_026616	1500026D16Rik	-3.62	11.39	-4.00
NM_009214	Sms	-3.59	9.29	-4.00
XM_131355	Pnrc1	-3.56	12.03	-4.00
NM_007501	Neurod4	-3.55	9.21	-4.00
NM_175177	Bdh	-3.52	9.35	-4.00
NM_026731	Ppp1r14a	-3.47	11.40	-4.00
NM_021459	Isl1	-3.40	11.71	-4.00
NM_007536	Bcl2a1d	-3.30	9.03	-4.00
	Ng23	-3.30	12.33	-4.00
NM_011428	Snap25	-3.25	9.83	-4.00
NM_023121	Gngt2	-3.21	11.96	-4.00
NM_018809	Ptf1a	-3.17	10.29	-4.00

Accession #	Symbol	Fold Change	avA	diffex total
NM_011837	Ly6h	-3.14	9.59	-4.00
NM_153198	Hbp1	-3.13	10.75	-4.00
NM_178399	3110035E14Rik	-3.13	9.47	-4.00
NM_134469	Fdps	-3.11	12.39	-4.00
NM_009936	Col9a3	-3.09	9.09	-4.00
NM_026530	E130307M08Rik	-3.08	13.00	-4.00
NM_013905	Heyl	-3.05	9.05	-4.00
	6430520M22Rik	-3.01	10.45	-4.00
NM_013543	H2-Ke6	-3.00	11.98	-4.00
NM_029798	2810417J12Rik	-2.98	10.32	-4.00
NM_007741	Col9a2	-2.96	10.72	-4.00
NM_133221	Slc24a6	-2.96	9.59	-4.00
NM_134022	6330403K07Rik	-2.95	11.41	-4.00
NM_153173	Hist1h4h	-2.93	10.26	-4.00
NM_153526	Insig1	-2.89	9.02	-4.00
XM_355444	1700021C14Rik	-2.88	9.62	-4.00
NM_008083	Gap43	-2.85	13.35	-4.00
NM_145942	Hmgcs1	-2.84	15.23	-4.00
NM_008741	Nsg2	-2.82	11.05	-4.00
NM_011328	Sct	-2.81	10.08	-4.00
NM_008409	Itm2a	-2.81	11.63	-4.00
NM_009221	Snca	-2.81	11.01	-4.00
NM_011311	S100a4	-2.79	11.01	-4.00
NM_008665	Myt1	-2.79	9.93	-4.00
NM_027419	2810408A11Rik	-2.78	9.01	-4.00
NM_178202	Hist1h2bp	-2.75	12.24	-4.00
NM_008553	Ascl1	-2.74	10.91	-4.00
NM_175663	Hist1h2ba	-2.73	10.76	-4.00
NM_016743	Nell2	-2.72	9.02	-4.00
NM_023249	Ypel1	-2.70	9.92	-4.00
NM_008321	Idb3	-2.70	12.98	-4.00
NM_007635	Ccng2	-2.68	11.03	-4.00
NM_025674	Tcf19	-2.66	9.88	-4.00
NM_007752	Cp	-2.64	9.73	-4.00
NM_026530	E130307M08Rik	-2.61	12.63	-4.00
NM_175664	Hist1h2bb	-2.59	10.81	-4.00
NM_013687	Tcp11	-2.58	9.29	-4.00
NM_030251	Abtb1	-2.58	9.31	-4.00

Accession #	Symbol	Fold Change	avA	diffex total
NM_025436	Sc4mol	-2.54	11.69	-4.00
NM_001001980	3732412D22Rik	-2.54	10.25	-4.00
NM_025285	Stmn2	-2.50	12.37	-4.00
NM_015786	Hist1h1c	-2.50	10.11	-4.00
NM_008800	Pde1b	-2.50	10.83	-4.00
NM_012061	Cadps	-2.45	9.20	-4.00
NM_198627	Gm691	-2.44	11.32	-4.00
NM_022424	Fndc4	-2.40	9.62	-4.00
NM_010884	Ndrg1	-2.39	11.10	-4.00
NM_019479	Hes6	-2.38	14.43	-4.00
NM_008506	Lmyc1	-2.38	11.27	-4.00
NM_030696	Slc16a3	-2.35	10.44	-4.00
NM_009223	Snn	-2.32	11.71	-4.00
NM_178197	Hist1h2bh	-2.19	11.81	-4.00
NM_144510	Ing4	-2.10	12.12	-4.00
NM_013706	Cd52	-86.13	8.22	-4.00
NM_175138	Dnaic1	-9.57	8.44	-4.00
NM_183152	6330514A18Rik	-8.90	8.20	-4.00
	C130091E20	-7.83	8.34	-4.00
NM_010185	Fcer1g	-5.85	8.14	-4.00
NM_177023	E130114P18Rik	-5.75	8.35	-4.00
NM_026418	Rgs10	-5.30	8.41	-4.00
NM_011662	Tyrobp	-5.04	8.09	-4.00
NM_013652	Ccl4	-4.74	8.74	-4.00
NM_021281	Ctss	-4.58	8.05	-4.00
NM_009830	Ccne2	-4.46	8.31	-4.00
NM_007494	Ass1	-4.42	8.04	-4.00
NM_019975	1600020H07Rik	-4.33	8.51	-4.00
NM_011153	Gsbs	-4.25	8.32	-4.00
NM_027733	5133400G04Rik	-4.21	8.55	-4.00
	A930005K07Rik	-3.66	8.28	-4.00
	1700102H20Rik	-3.51	8.04	-4.00
	2610100L16Rik	-3.44	8.62	-4.00
NM_008394	Isgf3g	-3.37	8.02	-4.00
NM_009308	Syt4	-3.30	8.85	-4.00
NM_007586	Calb2	-3.25	8.76	-4.00
NM_025324	Zfp524	-3.12	8.28	-4.00
	BB179718	-3.04	8.09	-4.00

Accession #	Symbol	Fold Change	avA	diffex total
NM_023438	Gm644	-2.94	8.38	-4.00
NM_146008	E430026E19Rik	-2.92	8.54	-4.00
NM_018747	Akap7	-2.68	8.64	-4.00
NM_178208	Hist1h4c	-2.49	8.54	-4.00
NM_020557	Tyki	-2.45	8.43	-4.00
NM_010574	Irx2	-2.41	8.03	-4.00
	Drld	-77.74	7.71	-4.00
AK078038		-28.81	7.12	-4.00
BC057690		-22.57	7.61	-4.00
NM_013550	Hist1h3a	-19.93	7.88	-4.00
NM_007705	Cirbp	-18.51	7.88	-4.00
NM_030707	Msr2	-17.13	7.32	-4.00
	3300002P09Rik	-14.34	7.21	-4.00
NM_010698	Ldb2	-13.88	7.18	-4.00
XM_129176	Mpeg1	-12.57	7.30	-4.00
NM_021099	Kit	-11.33	7.69	-4.00
NM_030725	Syt13	-11.02	7.36	-4.00
NM_007752	Cp	-10.06	7.00	-4.00
NM_011337	Ccl3	-8.51	7.98	-4.00
NM_145387	BC023151	-8.43	7.36	-4.00
AK031718		-7.90	7.16	-4.00
NM_010686	Laptm5	-7.44	7.40	-4.00
NM_175653	Hist1h3c	-7.36	7.65	-4.00
NM_007535	Bcl2a1c	-7.20	7.31	-4.00
XM_128308	Prickle1	-6.10	7.86	-4.00
NM_027733	5133400G04Rik	-5.91	7.45	-4.00
NM_010834	Gdf8	-5.64	7.37	-4.00
NM_024441	Hspb2	-4.93	7.65	-4.00
BC061227		-4.67	7.48	-4.00
NM_019960	Hspb3	-4.46	7.05	-4.00
NM_001001999	Gp1bb	-4.37	7.08	-4.00
NM_011909	Usp18	-4.06	7.19	-4.00
	C030014I23Rik	-4.01	7.77	-4.00
NM_009853	Cd68	-4.00	7.93	-4.00
NM_025912	2010011I20Rik	-3.85	7.44	-4.00
NM_177139	E130115E03Rik	-3.75	7.66	-4.00
NM_017372	Lyzs	-3.64	7.12	-4.00
NM_011447	Sox8	-3.48	7.06	-4.00

Accession #	Symbol	Fold Change	avA	diffex total
NM_080853	Slc17a6	-3.43	7.69	-4.00
NM_009062	Rgs4	-3.36	7.56	-4.00
AK087461		-3.32	7.78	-4.00
BC055725		-3.31	7.59	-4.00
NM_026629	2410066E13Rik	-3.16	7.99	-4.00
XM_128980	C330018D20Rik	-3.04	7.67	-4.00
XM_149496	1110065P20Rik	-3.02	7.90	-4.00
	4930524J08Rik	-2.97	7.07	-4.00
NM_019811	Acas2	-2.81	7.94	-4.00
	2300006M17Rik	-2.79	7.46	-4.00
	A730034C02	-2.78	7.91	-4.00
NM_008737	Nrp	-2.70	7.69	-4.00
NM_175181	2600010E01Rik	-2.61	7.19	-4.00
NM_031404	Actl6	-2.39	7.67	-4.00
NM_144932	BC021611	-2.24	7.23	-4.00
XM_129087	Tm7sf2	-3.34	9.40	-3.85
NM_010488	Elavl4	-3.24	10.29	-3.85
NM_019479	Hes6	-2.67	13.03	-3.85
NM_175656	Hist1h4i	-2.66	10.39	-3.85
NM_178198	Hist1h2bj	-2.51	11.44	-3.85
NM_145129	Chrna3	-2.49	11.14	-3.85
NM_013844	Zfp68	-2.32	10.01	-3.85
NM_024215	3110024A21Rik	-2.32	11.29	-3.85
NM_134122	Nrm	-2.26	12.14	-3.85
XM_130829	6130401L20Rik	-2.25	9.52	-3.85
NM_025455	1810010N17Rik	-2.25	10.76	-3.85
NM_010825	Mrg1	-2.22	9.69	-3.85
NM_207267	4930488E11Rik	-2.16	9.53	-3.85
NM_010497	Idh1	-2.16	13.05	-3.85
NM_177618	BC030477	-2.12	9.53	-3.85
NM_011428	Snap25	-2.10	10.69	-3.85
NM_010497	Idh1	-2.03	12.33	-3.85
NM_009168	Shd	-3.02	8.76	-3.85
NM_011677	Ung	-2.86	8.72	-3.85
NM_177192	D030011O10Rik	-2.85	8.79	-3.85
NM_178045	Rassf4	-2.59	8.85	-3.85
NM_172372	Wdrx1	-2.58	8.27	-3.85
NM_144942	Csad	-2.50	8.91	-3.85

Accession #	Symbol	Fold Change	avA	diffex total
NM_007534	Bcl2a1b	-2.45	8.01	-3.85
NM_183297	Nxph4	-2.27	8.86	-3.85
NM_030244	Ier5l	-2.11	8.72	-3.85
NM_019467	Aif1	-9.20	7.09	-3.85
NM_176971	Rab9b	-6.87	7.23	-3.85
XM_486157	4931428F04Rik	-4.24	7.01	-3.85
NM_053105	Klhl1	-3.39	7.54	-3.85
NM_030253	BC003281	-3.38	7.45	-3.85
NM_178227	Scn3b	-2.98	7.13	-3.85
NM_133677	2310061J03Rik	-2.61	7.83	-3.85
NM_010818	Cd200	-2.56	7.18	-3.85
NM_028188	Rusc1	-2.38	7.81	-3.85
NM_172788	4831416G18Rik	-2.29	7.60	-3.85
NM_176948	9330133O14Rik	-2.21	7.30	-3.85
NM_178111	Trp53inp2	-2.57	9.67	-3.70
NM_178211	Hist1h4k	-2.32	9.52	-3.70
NM_009387	Tk1	-2.27	10.73	-3.70
NM_010315	Gng2	-2.21	11.57	-3.70
NM_013496	Crabp1	-2.18	10.94	-3.70
NM_009214	Sms	-2.15	12.09	-3.70
XM_128511	0610011F06Rik	-2.15	10.44	-3.70
NM_175116	P2y5	-2.13	9.50	-3.70
NM_008502	Llglh	-2.03	12.61	-3.70
NM_029564	Tax1bp3	-1.99	13.15	-3.70
NM_023699	Nfatc4	-2.18	8.83	-3.70
	C630043F03Rik	-2.04	8.55	-3.70
NM_198093	Elmo1	-2.60	7.13	-3.70
NM_028733	Pacsin3	-2.51	7.32	-3.70
NM_173030	Galnt13	-2.48	7.57	-3.70
NM_207530	Osbpl1a	-2.23	7.96	-3.70
NM_009250	Serpini1	-2.20	7.43	-3.70
	9130203F04Rik	-2.90	9.63	-3.58
NM_011430	Sncg	-2.71	13.39	-3.58
NM_175655	Hist1h4f	-2.65	10.84	-3.58
	1110029I05Rik	-2.54	10.11	-3.58
NM_030210	Aacs	-2.53	10.09	-3.58
XM_127534	3110001E11Rik	-2.49	9.95	-3.58
NM_018854	0610009H04Rik	-2.45	10.50	-3.58

Accession #	Symbol	Fold Change	avA	diffex total
NM_175665	Hist1h2bk	-2.45	10.83	-3.58
NM_008681	Ndrl	-2.42	10.94	-3.58
NM_178195	Hist1h2bf	-2.36	12.06	-3.58
XM_131537	6430559E15Rik	-2.29	9.22	-3.58
NM_145125	Wdr9	-2.28	9.24	-3.58
NM_201359	D15Ertd405e	-2.27	10.23	-3.58
NM_013888	Dnajc12	-2.26	9.73	-3.58
NM_178200	Hist1h2bm	-2.23	12.45	-3.58
NM_010773	Mbd2	-2.22	9.49	-3.58
NM_013928	Schip1	-2.21	9.85	-3.58
NM_033325	Loxl2	-2.19	9.20	-3.58
	9430041J06Rik	-2.16	14.27	-3.58
XM_129894	Acsl3	-2.10	12.16	-3.58
NM_148938	Slc1a3	-2.04	11.83	-3.58
NM_134023	Tbc1d10	-2.03	9.21	-3.58
NM_026148	Lims1	-1.99	13.06	-3.58
NM_133858	4930504E06Rik	-1.99	9.81	-3.58
NM_025347	Ypel3	-1.97	11.32	-3.58
NM_145492	Zfp521	-4.62	8.27	-3.58
NM_026954	Tusc1	-3.98	8.63	-3.58
NM_175138	Dnaic1	-3.94	8.89	-3.58
NM_175519	Kctd8	-3.10	8.90	-3.58
XM_488712	A930011O12Rik	-2.91	8.87	-3.58
NM_009830	Ccne2	-2.86	8.01	-3.58
NM_172485	D130067I03Rik	-2.83	8.33	-3.58
NM_029338	1700027N10Rik	-2.78	8.49	-3.58
NM_007873	Doc2b	-2.43	8.14	-3.58
NM_010574	Irx2	-2.32	8.28	-3.58
NM_146208	BC034753	-2.21	8.72	-3.58
NM_178762	A930025D01Rik	-2.15	8.03	-3.58
NM_009538	Plagl1	-1.99	8.02	-3.58
NM_026278	2310006J04Rik	-12.44	7.70	-3.58
NM_010474	Hs3st1	-6.81	7.03	-3.58
NM_015783	G1p2	-3.84	7.05	-3.58
NM_153155	C1ql3	-3.65	7.59	-3.58
NM_026439	2610001E17Rik	-3.56	7.04	-3.58
NM_009150	Selenbp1	-3.50	7.15	-3.58
NM_175157	2610204G22Rik	-3.38	7.02	-3.58

Accession #	Symbol	Fold Change	avA	diffex total
NM_009625	Adcyap1	-3.26	7.87	-3.58
XM_486751	3110007F17Rik	-3.16	7.55	-3.58
	2310015A10Rik	-3.04	7.91	-3.58
NM_138945	Pou4f3	-3.02	7.49	-3.58
NM_026887	Ap1s2	-2.90	7.97	-3.58
NM_170599	Igsf11	-2.88	7.95	-3.58
NM_177716	AI836003	-2.73	7.32	-3.58
NM_010014	Dab1	-2.60	7.57	-3.58
NM_026887	Ap1s2	-2.57	7.92	-3.58
	Fbxl10	-2.46	7.65	-3.58
NM_173868	St18	-2.45	7.82	-3.58
NM_026268	Dusp6	-2.39	7.74	-3.58
NM_022428	Irx6	-2.35	7.89	-3.58
NM_013779	Magel2	-2.32	7.50	-3.58
NM_001004357	Cntnap2	-2.28	7.27	-3.58
NM_018818	Chm	-2.13	7.78	-3.58
	2900075A18Rik	-2.12	9.92	-3.55
NM_145584	Spon1	-2.06	10.58	-3.55
NM_080555	Ppap2b	-2.40	10.16	-3.43
NM_145940	D11Ertd498e	-2.30	9.29	-3.43
NM_134030	4632423N09Rik	-2.24	10.01	-3.43
NM_013530	Gnb3	-2.19	9.62	-3.43
NM_178199	Hist1h2bl	-2.17	12.76	-3.43
	F630025I20Rik	-2.14	9.49	-3.43
NM_178201	Hist1h2bn	-2.14	12.60	-3.43
NM_009306	Syt1	-2.13	9.41	-3.43
NM_019738	Nupr1	-2.11	14.16	-3.43
NM_030082	Hist3h2ba	-2.11	12.48	-3.43
NM_173770	B230399E16Rik	-2.11	10.03	-3.43
	1110046J11Rik	-2.09	9.55	-3.43
NM_172434	Tnrc4	-2.06	12.84	-3.43
NM_178192	Hist1h4a	-2.05	10.85	-3.43
XM_489103	A230057G18Rik	-2.05	10.83	-3.43
NM_175654	Hist1h4d	-2.04	11.34	-3.43
NM_009761	Bnip3l	-2.03	11.21	-3.43
NM_026167	Klhl13	-2.00	9.14	-3.43
NM_177603	Frat2	-2.00	12.60	-3.43
NM_025623	Nipsnap3a	-1.98	9.78	-3.43

Accession #	Symbol	Fold Change	avA	diffex total
NM_010634	Fabp5	-1.96	10.13	-3.43
NM_178628	Spg3a	-1.96	9.49	-3.43
NM_008828	Pgk1	-1.96	13.15	-3.43
NM_133236	Glcci1	-1.93	9.79	-3.43
AK014166		-2.78	8.56	-3.43
XM_134869	3300001A09Rik	-2.09	8.47	-3.43
NM_011663	U2af1-rs1	-2.07	8.10	-3.43
NM_172523	Slc18a2	-2.04	8.20	-3.43
NM_007647	Entpd5	-1.98	8.26	-3.43
NM_009703	Araf1	-1.98	8.04	-3.43
NM_007574	C1qg	-3.43	7.76	-3.43
NM_011158	Prkar2b	-2.62	7.75	-3.43
NM_029173	4930519N16Rik	-2.21	7.55	-3.43
NM_019790	Tmeff2	-2.19	7.47	-3.43
NM_010751	Mad	-2.02	7.50	-3.43
NM_011353	Serf1	-2.02	13.03	-3.28
NM_031202	Tyrp1	-1.93	9.34	-3.28
NM_007866	Dll3	-1.92	11.81	-3.28
NM_138580	Rdbp	-1.89	10.85	-3.28
NM_009133	Stmn3	-1.88	14.13	-3.28
NM_008885	Pmp22	-1.88	9.89	-3.28
NM_138601	D10Jhu81e	-1.88	11.92	-3.28
NM_009955	Dpysl2	-1.87	13.06	-3.28
NM_172893	Zc3hdc1	-2.49	8.48	-3.28
NM_175521	6430598A04Rik	-2.00	8.60	-3.28
NM_019980	Litaf	-1.90	8.96	-3.28
NM_011625	Ppp1r13b	-2.14	7.81	-3.28
NM_173739	Galntl4	-1.86	7.21	-3.28
NM_011728	Xpa	-2.28	9.43	-3.16
NM_133223	Rac3	-2.23	10.18	-3.16
NM_172588	A130038L21Rik	-2.23	9.67	-3.16
NM_011074	Pftk1	-2.14	9.07	-3.16
NM_026880	Pink1	-2.14	9.65	-3.16
BC050855	AI255170	-2.14	9.03	-3.16
NM_007548	Prdm1	-2.11	9.54	-3.16
NM_021438	Fibp	-2.11	10.57	-3.16
NM_025455	1810010N17Rik	-2.10	10.50	-3.16
NM_009387	Tk1	-2.08	10.64	-3.16

Accession #	Symbol	Fold Change	avA	diffex total
NM_008538	Marcks	-2.03	14.88	-3.16
NM_138656	Mvd	-1.98	10.27	-3.16
	2900009C16Rik	-1.96	9.59	-3.16
NM_007792	Csrp2	-1.96	14.30	-3.16
NM_133986	Tcta	-1.96	9.52	-3.16
NM_007684	Cetn3	-1.91	12.48	-3.16
XM_358772	1810015A11Rik	-1.86	9.14	-3.16
NM_024211	Slc25a11	-1.85	10.55	-3.16
NM_145360	Idi1	-1.83	12.94	-3.16
NM_010025	Dcx	-2.38	8.89	-3.16
NM_008632	Mtap2	-2.26	8.16	-3.16
NM_134147	D930010J01Rik	-2.24	8.52	-3.16
NM_013761	Srr	-2.17	8.80	-3.16
NM_012040	Pnck	-2.13	8.07	-3.16
NM_022995	Tmepai	-2.08	8.94	-3.16
NM_028763	Nptxr	-2.08	8.08	-3.16
NM_011286	Rph3a	-2.04	8.54	-3.16
NM_009721	Atp1b1	-1.99	8.85	-3.16
XM_284425	2810422J05Rik	-1.99	8.36	-3.16
NM_172560	9830165K03Rik	-1.95	8.87	-3.16
NM_017464	Nedd9	-1.84	8.92	-3.16
NM_015763	Lpin1	-5.20	7.31	-3.16
NM_175460	Nmnat2	-2.93	7.67	-3.16
NM_183177	BC052046	-2.56	7.44	-3.16
	2900008C10Rik	-2.43	7.55	-3.16
NM_009326	Tcea2	-2.41	7.51	-3.16
BC004758		-2.37	7.89	-3.16
NM_028711	Slc25a27	-2.28	7.79	-3.16
NM_172738	5730403M16Rik	-2.09	7.87	-3.16
NM_026116	Bbs2	-2.03	7.75	-3.16
NM_178076	Mcf2l	-1.87	9.33	-3.13
NM_207238	Fbxo27	-2.22	9.25	-3.01
	BC050254	-2.14	9.01	-3.01
NM_153088	Ctdsp1	-2.10	9.65	-3.01
	5830411O07Rik	-2.09	9.33	-3.01
NM_016709	Auh	-1.91	10.67	-3.01
NM_011353	Serf1	-1.91	13.31	-3.01
NM_172275	Fln29	-1.91	9.48	-3.01

Accession #	Symbol	Fold Change	avA	diffex total
NM_153526	Insig1	-1.90	9.24	-3.01
NM_015807	Nt5c	-1.89	11.90	-3.01
BC059844		-1.88	9.10	-3.01
NM_053091	Cox4i2	-1.88	12.08	-3.01
NM_019733	Rbpms	-1.86	10.55	-3.01
XM_126043	H2afv	-1.86	13.90	-3.01
NM_146122	6030446I19Rik	-1.83	9.91	-3.01
NM_021487	Kcne1l	-1.82	9.86	-3.01
NM_025618	Sri	-1.81	11.59	-3.01
NM_008409	Itm2a	-1.80	12.82	-3.01
NM_146177	Suv420h2	-1.79	11.28	-3.01
NM_133345	Ing4	-1.76	11.06	-3.01
NM_172935	5730457F11Rik	-1.96	8.56	-3.01
NM_053246	Dok4	-1.96	8.34	-3.01
NM_145940	D11Ertd498e	-1.87	8.07	-3.01
NM_023595	Dutp	-2.13	7.34	-3.01
NM_133235	Khdrbs2	-1.96	7.64	-3.01
NM_008697	Nin	-1.80	7.52	-3.01
NM_176933	Dusp4	-1.79	7.50	-3.01
NM_028041	Ddx54	-1.75	7.94	-3.01
NM_053007	Cntf	-1.71	7.93	-3.01
NM_175657	Hist1h4m	-2.94	10.57	-3.00
NM_007586	Calb2	-2.90	9.45	-3.00
NM_018747	Akap7	-2.71	9.31	-3.00
NM_007770	Crx	-2.43	11.82	-3.00
NM_010941	Nsdhl	-2.28	9.59	-3.00
NM_145705	Tinf2	-2.28	9.11	-3.00
NM_007494	Ass1	-2.26	10.32	-3.00
NM_010296	Gli	-2.25	9.88	-3.00
NM_007378	Abca4	-2.24	9.41	-3.00
NM_026887	Ap1s2	-2.24	9.37	-3.00
NM_019561	Ensa	-2.23	9.49	-3.00
NM_144879	B130052G07Rik	-2.18	10.31	-3.00
NM_153526	Insig1	-2.17	11.98	-3.00
NM_133697	1110003E01Rik	-2.13	11.23	-3.00
NM_029564	Tax1bp3	-2.10	13.26	-3.00
NM_025623	Nipsnap3b	-2.08	9.58	-3.00
NM_009384	Tiam1	-2.08	9.35	-3.00

Accession #	Symbol	Fold Change	avA	diffex total
NM_009294	Stx4a	-2.07	9.09	-3.00
NM_027166	Ypel5	-2.03	10.22	-3.00
NM_019754	Tagln3	-2.01	13.20	-3.00
NM_008721	Npdc1	-1.99	10.85	-3.00
NM_008776	Pafah1b3	-1.96	13.15	-3.00
NM_010941	Nsdhl	-1.95	10.87	-3.00
NM_026928	1810014F10Rik	-1.93	9.95	-3.00
NM_025623	Nipsnap3a	-1.86	10.74	-3.00
NM_009599	Ache	-4.46	8.14	-3.00
	6330404F12Rik	-4.23	8.13	-3.00
NM_175658	Hist1h2aa	-4.07	8.32	-3.00
NM_010593	Jup	-3.09	8.01	-3.00
	E130119J07Rik	-2.74	8.36	-3.00
NM_053271	Rims2	-2.62	8.33	-3.00
NM_146182	Klc3	-2.58	8.22	-3.00
NM_174876	Impg2	-2.57	8.05	-3.00
NM_008963	Ptgds	-2.44	8.16	-3.00
	2810409C01Rik	-2.33	8.07	-3.00
NM_027196	Pold4	-2.27	8.72	-3.00
	1110036D12Rik	-2.18	8.90	-3.00
NM_026714	0610037D15Rik	-2.18	8.94	-3.00
NM_007960	Etv1	-2.18	8.19	-3.00
NM_174848	BC043118	-2.14	8.78	-3.00
NM_025303	Stau2	-2.12	8.97	-3.00
NM_019961	Pex3	-2.07	8.36	-3.00
NM_008822	Pex7	-2.07	8.46	-3.00
NM_007472	Aqp1	-2.05	8.08	-3.00
	9130023H24Rik	-2.00	8.07	-3.00
NM_016974	Dbp	-1.96	8.12	-3.00
	Col6a3	-1.89	8.20	-3.00
NM_009343	Phf1	-1.89	8.77	-3.00
NM_173767	3830422K02Rik	-9.27	7.27	-3.00
NM_172893	Zc3hdc1	-8.95	7.54	-3.00
	2500002B13Rik	-8.76	7.24	-3.00
NM_182807	AI851790	-6.18	7.16	-3.00
NM_133694	Fbxl15	-3.69	7.93	-3.00
NM_177546	Pcyt1b	-3.54	7.64	-3.00
NM_010316	Gng3	-3.41	7.09	-3.00

Accession #	Symbol	Fold Change	avA	diffex total
NM_028036	2410015B03Rik	-3.12	7.73	-3.00
NM_173406	AI591476	-3.10	7.67	-3.00
NM_013864	Ndrg2	-2.84	7.72	-3.00
NM_008736	Nrl	-2.83	7.96	-3.00
NM_007537	Bcl2l2	-2.81	7.34	-3.00
NM_173403	E130304D01	-2.63	7.24	-3.00
NM_011151	Ppm1b	-2.62	7.76	-3.00
NM_008278	Hpgd	-2.52	7.84	-3.00
NM_010045	Dfy	-2.45	7.62	-3.00
NM_172960	Adck5	-2.40	7.81	-3.00
NM_019949	Ube2l6	-2.38	7.49	-3.00
NM_198011	E430018J23Rik	-2.34	7.39	-3.00
NM_138682	Lrrc4	-2.32	7.29	-3.00
NM_176849	9430010O03Rik	-2.32	7.97	-3.00
NM_033146	1500005A01Rik	-2.27	7.59	-3.00
NM_019957	Dnase2b	-2.24	7.03	-3.00
	6330570A01Rik	-2.23	7.15	-3.00
NM_177645	C430010P07Rik	-2.09	7.68	-3.00
NM_145969	A630054L15Rik	-2.08	7.27	-3.00
	A230098E07Rik	-2.08	7.23	-3.00
NM_175404	3010003L21Rik	-2.04	7.69	-3.00
NM_009558	Zfp51	-2.01	7.49	-3.00
NM_011789	Apc2	-1.87	7.94	-3.00

Genes are sorted first by diffex total, then by fold change

Fold Change – calculated fold change
avA – signal intensity in Log_2. Signal intensity over background levels. A cut-off value of 7 was used to determine if transcript was detectable (present vs absent)
Diffex total. – Sum of diffex values from 4 arrays based on actual threshold of fold-changes in Log_2. A cut-off value of 3 was used. Diffex value were assigned to each array based on observed fold change for each probe/transcript/gene as follows:

- Greater than 2-fold change = -1
- Less than 2-fold but greater than 1.8-fold = -0.85
- Less than 1.85-fold but greater than 1.5-fold = -0.58

Therefore a gene that is downregulated by 2-fold or higher in all four arrays would get a score of -4.

Appendix F. Upregulated Genes with conserved TCF site

Gene Symbol	Gene Name	# TCF binding sites	Fold Change
Commd3	COMM domain containing 3	13	2.16
Rap2b	RAP2B, member of RAS oncogene family	12	3.85
Lix1	limb expression 1	12	2.54
Tef	thyrotroph embryonic factor isoform 1	12	2.11
Tmem67	transmembrane protein 67	12	1.88
Tnfrsf19	tumor necrosis factor receptor superfamily,	10	20.86
Slc25a37	solute carrier family 25, member 37	10	2.47
1110004E09Rik	hypothetical protein LOC68001	10	1.91
Eda2r	ectodysplasin A2 isoform receptor	9	21.56
Eif4a2	eukaryotic translation initiation factor 4A2	9	13.64
Isg20l1	interferon stimulated exonuclease gene 20-like	9	9.92
Elmo1	engulfment and cell motility 1 isoform 1	9	4.63
Lpp	LIM domain containing preferred translocation	9	3.73
H2-T22	histocompatibility 2, T region locus 22	9	2.66
Snx19	sorting nexin 19	9	2.34
Adamts1	a disintegrin-like and metalloprotease	9	2.17
Pdlim4	PDZ and LIM domain 4	9	2.16
Heatr3	HEAT repeat containing 3	9	1.95
Cd81	CD 81 antigen	9	1.90
BC052040	hypothetical protein LOC399568	9	1.89
2810012G03Rik	hypothetical protein LOC66306	9	1.84
Otx1	orthodenticle 1	9	1.82
Zmpste24	zinc metalloproteinase, STE24 homolog	9	1.81

Gene Symbol	Gene Name	# TCF binding sites	Fold Change
Pmaip1	phorbol-12-myristate-13-acetate-induced protein	8	57.47
Fyn	protein-tyrosine kinase fyn	8	4.26
Gtse1	G two S phase expressed protein 1	8	3.53
8030451K01Rik	hypothetical protein LOC212114	8	3.23
Gcg	glucagon	8	3.08
Mfap3l	microfibrillar-associated protein 3-like	8	2.79
Orc1l	origin recognition complex, subunit 1 isoform A	8	2.71
Traf4	Tnf receptor associated factor 4	8	2.27
Ube2c	ubiquitin-conjugating enzyme E2C	8	2.13
Ears2	glutamyl-tRNA synthetase 2	8	2.11
Med12	mediator of RNA polymerase II transcription,	8	1.99
BC011248	hypothetical protein LOC224823	8	1.98
Sdha	succinate dehydrogenase Fp subunit	8	1.74
Wif1	Wnt inhibitory factor 1	7	29.22
C130034I18Rik	TAFA4 protein	7	25.73
Pkib	cAMP-dependent protein kinase inhibitor beta	7	9.17
Npy	neuropeptide Y	7	6.99
Nupl2	nucleoporin like 2	7	6.71
Olfr247	olfactory receptor 247	7	5.67
Hoxa3	homeobox A3	7	5.00
Ptp4a3	protein tyrosine phosphatase 4a3	7	4.11
Cry2	cryptochrome 2 (photolyase-like)	7	3.91
Ift88	Tg737 protein	7	3.48
Scgn	secretagogin, EF-hand calcium binding protein	7	3.21
Seh1l	sec13-like protein isoform b	7	3.21

Gene Symbol	Gene Name	# TCF binding sites	Fold Change
Cyp7b1	cytochrome P450, family 7, subfamily b,	7	3.17
Aurka	serine/threonine protein kinase 6	7	3.14
Antxr1	anthrax toxin receptor 1	7	2.84
Galns	galactosamine (N-acetyl)-6-sulfate sulfatase	7	2.42
Zfp365	zinc finger protein 365	7	2.36
Mettl1	methyltransferase-like 1	7	2.20
4930572J05Rik	mesenchymal stem cell protein DSCD75 homolog	7	2.16
Dhrs7	retinal short-chain dehydrogenase/reductase 4	7	2.08
Gpc6	glypican 6 isoform 2	7	2.04
Sco1	SCO cytochrome oxidase deficient homolog 1	7	1.86
Rad51	RAD51 homolog	7	1.79
Serpine1	serine (or cysteine) proteinase inhibitor, clade	6	19.81
Phlda3	pleckstrin homology-like domain, family A,	6	16.42
Lor	loricrin	6	15.43
Frrs1	ferric-chelate reductase 1	6	13.76
Cxcl4	chemokine (C-X-C motif) ligand 4	6	11.12
Tubb6	tubulin, beta 6	6	2.95
Rsc1a1	regulatory solute carrier protein, family 1,	6	2.91
Hnrpdl	heterogeneous nuclear ribonucleoprotein D-like	6	2.86
Axin2	axin2	6	2.82
Mlf1	myeloid leukemia factor 1 isoform a	6	2.82
Clybl	citrate lyase beta like	6	2.63
Pih1d2	PIH1 domain containing 2	6	2.61
Prr11	proline rich 11	6	2.58
Clip4	CAP-GLY domain containing linker protein family,	6	2.54

Gene Symbol	Gene Name	# TCF binding sites	Fold Change
Ddx19b	DDX19 homolog	6	2.54
Zwilch	Zwilch	6	2.37
Perp	PERP, TP53 apoptosis effector	6	2.36
Msx1	homeo box, msh-like 1	6	2.34
Celsr2	cadherin EGF LAG seven-pass G-type receptor 2	6	2.24
Rps27l	ribosomal protein S27-like	6	2.23
9430015G10Rik	hypothetical protein LOC230996	6	2.19
5830483C08Rik	hypothetical protein LOC209334	6	2.15
Traf3	Tnf receptor-associated factor 3 isoform a	6	2.15
Lrp4	low density lipoprotein receptor-related protein	6	2.12
Col18a1	procollagen, type XVIII, alpha 1 isoform 2	6	2.07
Eif2b3	eukaryotic translation initiation factor 2B,	6	1.88
Tsc22d3	glucocorticoid-induced leucine zipper isoform 2	6	1.88
Slc7a7	solute carrier family 7 (cationic amino acid	6	1.87
Atf5	ativating transcription factor 5	6	1.85
Cyp1b1	cytochrome P450, family 1, subfamily b,	6	1.84
4933429F08Rik	hypothetical protein LOC328967	5	11.83
Mapkapk3	mitogen-activated protein kinase-activated	5	8.05
Plk2	polo-like kinase 2	5	7.12
B230120H23Rik	leucine zipper- and sterile alpha	5	6.36
Hs1bp3	HCLS1 binding protein 3	5	4.40
Apaf1	apoptotic protease activating factor 1	5	3.76
Tacstd1	tumor-associated calcium signal transducer 1	5	3.59
Tnfrsf12a	tumor necrosis factor receptor superfamily,	5	3.25
Tpd52l1	tumor protein D52-like 1	5	3.10

Gene Symbol	Gene Name	# TCF binding sites	Fold Change
BC030867	hypothetical protein LOC217216	5	3.03
Vcl	vinculin	5	2.98
Usp2	ubiquitin-specific protease 2 isoform Usp2-69	5	2.88
Dus4l	dihydrouridine synthase 4-like	5	2.71
Foxj3	forkhead box J3	5	2.62
6530401N04Rik	hypothetical protein LOC328092	5	2.60
Itch	itchy, E3 ubiquitin protein ligase	5	2.59
Snx14	sorting nexin 14	5	2.50
Man2b1	mannosidase 2, alpha B1	5	2.42
Hoxd9	homeo box D9	5	2.40
Recql	RecQ protein-like	5	2.33
Exoc6	exocyst complex component 6	5	2.23
Nol6	nucleolar protein family 6	5	2.20
Mthfd1	methylenetetrahydrofolate dehydrogenase 1	5	2.18
Slc7a3	solute carrier family 7 (cationic amino acid	5	2.17
BC003993	hypothetical protein LOC80744	5	2.11
Asph	aspartyl beta-hydroxylase isoform 2	5	2.10
Iars	isoleucyl-tRNA synthetase	5	2.07
Mettl6	methyltransferase like 6	5	1.98
Rhod	ras homolog D	5	1.98
Calu	calumenin isoform 1	5	1.97
Rap2a	RAP2A, member of RAS oncogene family	5	1.91
Lenep	lens epithelial protein	5	1.84
A030007L17Rik	hypothetical protein LOC68252	5	1.83
Mthfd1l	methylenetetrahydrofolate dehydrogenase (NADP+	5	1.82

Gene Symbol	Gene Name	# TCF binding sites	Fold Change
Capn3	calpain 3 isoform a	5	1.81
C530044N13Rik	hypothetical protein LOC223978	5	1.77
Krt18	keratin 18	4	14.28
Epha2	Eph receptor A2	4	8.37
Tnfrsf10b	tumor necrosis factor receptor superfamily,	4	8.16
Cyr61	cysteine rich protein 61	4	7.61
Nme5	expressed in non-metastatic cells 5	4	5.73
Raet1a	retinoic acid early transcript 1, alpha	4	5.23
Znrd1	nuclear RNA polymerase I small specific subunit	4	4.03
Ogn	osteoglycin	4	3.92
Psrc1	proline/serine-rich coiled-coil 1	4	3.86
Per2	period homolog 2	4	3.82
Rftn1	raft-linking protein	4	3.62
Kcna6	potassium voltage-gated channel, shaker-related,	4	3.59
Dok1	docking protein 1	4	3.48
Trp53inp1	transformation related protein 53 inducible	4	3.45
Rpusd2	RNA pseudouridylate synthase domain containing	4	3.36
Exoc4	SEC8	4	3.32
Tcf7	transcription factor 7, T-cell specific	4	3.22
Dph2	diptheria toxin resistance protein required for	4	3.10
Adpgk	ATP-dependent glucokinase	4	3.06
Cugbp1	CUG triplet repeat, RNA-binding protein 1	4	3.01
Ntrk2	neurotrophic tyrosine kinase, receptor, type 2	4	2.93
P2ry2	purinergic receptor P2Y, G-protein coupled 2	4	2.92
Pwp2	PWP2 periodic tryptophan protein homolog	4	2.73

Gene Symbol	Gene Name	# TCF binding sites	Fold Change
Prickle4	prickle homolog 4	4	2.70
Lrp1	low density lipoprotein receptor-related protein	4	2.67
Prpf8	pre-mRNA processing factor 8	4	2.52
Alg1	beta-1,4-mannosyltransferase	4	2.46
Hdlbp	high density lipoprotein binding protein	4	2.42
Gpx7	glutathione peroxidase 7	4	2.27
Cad	carbamoyl-phosphate synthetase 2, aspartate	4	2.24
Ddx11	DEAD/H (Asp-Glu-Ala-Asp/His) box polypeptide 11	4	2.24
Pycrl	pyrroline-5-carboxylate reductase-like	4	2.22
Rev1	REV1-like	4	2.21
Slc38a4	solute carrier family 38, member 4	4	2.07
Ccdc86	coiled-coil domain containing 86	4	2.06
Gspt2	G1 to phase transition 2	4	1.91
Krt72	keratin 72	4	1.91
Pkn3	protein kinase N3	4	1.89
Rbm13	RNA binding motif protein 13	4	1.89
Afg3l1	AFG3(ATPase family gene 3)-like 1	4	1.88
Gne	glucosamine	4	1.87
Pprc1	peroxisome proliferative activated receptor,	4	1.87
Cdc25b	cell division cycle 25 homolog B	4	1.86
Ifrd1	interferon-related developmental regulator 1	4	1.82
Qrsl1	glutaminyl-tRNA synthase	4	1.82
Ppp1r12c	protein phosphatase 1, regulatory subunit 12C	4	1.74
Efna3	ephrin A3	4	1.72
Cdkn1a	cyclin-dependent kinase inhibitor 1A (P21)	3	22.78

Gene Symbol	Gene Name	# TCF binding sites	Fold Change
Lrrc14	leucine rich repeat containing 14	3	19.85
Ccng1	cyclin G1	3	13.43
2810048G17Rik	hypothetical protein LOC72691	3	7.34
Slc19a2	solute carrier family 19 (thiamine transporter),	3	7.18
Actc1	actin, alpha, cardiac	3	7.14
Polk	polymerase (DNA directed), kappa	3	7.01
Ephb1	Eph receptor B1	3	4.82
Eef1a2	eukaryotic translation elongation factor 1 alpha	3	4.76
Chrdl1	chordin-like 1	3	4.55
Ank1	ankyrin 1, erythroid isoform 2	3	4.32
2310005E10Rik	aldo-keto reductase family 1, member B10	3	3.47
Ung	uracil DNA glycosylase isoform b	3	3.38
Ehd4	EH-domain containing 4	3	3.33
Fbln1	fibulin 1	3	3.21
Ckap2	cytoskeleton associated protein 2	3	3.18
Mgmt	O-6-methylguanine-DNA methyltransferase	3	3.06
Per1	period homolog 1	3	3.05
Ccdc84	coiled-coil domain containing 84	3	3.00
Prpf3	PRP3 pre-mRNA processing factor 3 homolog	3	2.87
Ramp2	receptor activity modifying protein 2	3	2.82
Anxa2	annexin A2	3	2.80
Rrp12	ribosomal RNA processing 12 homolog	3	2.73
Wdr21	WD repeat domain 21	3	2.72
Dnajb4	DnaJ (Hsp40) homolog, subfamily B, member 4	3	2.70
4930402E16Rik	pyruvate dehydrogenase phosphatase regulatory	3	2.69

Gene Symbol	Gene Name	# TCF binding sites	Fold Change
Qtrtd1	queuine tRNA-ribosyltransferase domain	3	2.50
Sncb	synuclein, beta	3	2.50
Slc44a2	solute carrier family 44, member 2	3	2.47
Ptgis	prostaglandin I2 (prostacyclin) synthase	3	2.46
Trub1	TSR1, 20S rRNA accumulation	3	2.41
Pdgfa	platelet derived growth factor, alpha	3	2.40
Tmem43	transmembrane protein 43	3	2.39
Neu1	neuraminidase 1	3	2.35
Gas2	growth arrest specific 2	3	2.34
Luc7l	Luc7 homolog (S. cerevisiae)-like isoform 2	3	2.34
Cox6b2	cytochrome c oxidase subunit VIb polypeptide 2	3	2.33
Ccdc117	coiled-coil domain containing 117	3	2.32
Polr2a	polymerase (RNA) II (DNA directed) polypeptide	3	2.31
Ptk7	PTK7 protein tyrosine kinase 7	3	2.30
Ifi30	interferon gamma inducible protein 30	3	2.29
Cldn11	claudin 11	3	2.27
Gsg2	germ cell-specific gene 2	3	2.24
Ly6e	lymphocyte antigen 6 complex, locus E	3	2.22
Ada	adenosine deaminase	3	2.15
Ccl25	chemokine (C-C motif) ligand 25	3	2.15
Aadacl1	arylacetamide deacetylase-like 1	3	2.13
Akr1b3	aldo-keto reductase family 1, member B3 (aldose	3	2.10
Rbm38	seb4	3	2.10
Smpd4	sphingomyelin phosphodiesterase 4	3	2.10
Cdk5rap1	CDK5 regulatory subunit associated protein 1	3	2.09

Gene Symbol	Gene Name	# TCF binding sites	Fold Change
Sgk	serum/glucocorticoid regulated kinase	3	2.07
Lrfn1	leucine rich repeat and fibronectin type III	3	2.03
Col6a1	collagen, type VI, alpha 1	3	1.98
Mt3	metallothionein 3	3	1.98
Nav1	neuron navigator 1	3	1.97
Evc2	Ellis van Creveld syndrome 2 homolog	3	1.96
Ccdc123	coiled-coil domain containing 123	3	1.95
Slc33a1	solute carrier family 33 (acetyl-CoA	3	1.95
Pdlim5	PDZ and LIM domain 5 isoform ENH2	3	1.94
Rpn2	ribophorin II	3	1.91
Btg3	B-cell translocation gene 3	3	1.86
Ascc2	activating signal cointegrator 1 complex subunit	3	1.84
Mpdz	multiple PDZ domain protein	3	1.84
Ak1	adenylate kinase 1	2	9.39
Cnn2	calponin 2	2	8.95
Sstr3	somatostatin receptor 3	2	8.23
Lynx1	Ly6/neurotoxin 1	2	7.75
Lmna	lamin A isoform A	2	5.81
Tppp3	tubulin polymerization-promoting protein family	2	4.74
6530418L21Rik	hypothetical protein LOC109050	2	3.89
Arrdc4	arrestin domain containing 4 isoform 1	2	3.72
Tac2	tachykinin 2	2	3.46
Ephx1	epoxide hydrolase 1, microsomal	2	3.42
Dimt1	dimethyladenosine transferase	2	3.36
Creb3l1	cAMP responsive element binding protein 3-like	2	3.32

Gene Symbol	Gene Name	# TCF binding sites	Fold Change
Asb16	ankyrin repeat and SOCS box-containing 16	2	3.20
H2afj	H2A histone family, member J	2	3.19
Raet1b	retinoic acid early transcript beta	2	3.10
Ddit4l	DNA-damage-inducible transcript 4-like	2	3.05
Sesn2	sestrin 2	2	2.99
Edaradd	EDAR (ectodysplasin-A receptor)-associated death	2	2.86
Pltp	phospholipid transfer protein	2	2.81
Acsl6	acyl-CoA synthetase long-chain family member 6	2	2.66
Slc10a3	protein P3	2	2.45
Zmym6	zinc finger, MYM-type 6	2	2.42
Pdrg1	p53 and DNA damage regulated 1	2	2.30
Zrsr2	U2 small nuclear ribonucleoprotein auxiliary	2	2.30
1810029B16Rik	hypothetical protein LOC66282	2	2.28
Slc20a1	solute carrier family 20, member 1	2	2.23
Plxnb3	plexin B3	2	2.22
Stt3a	intergral membrane protein 1	2	2.22
Ccnb1	cyclin B1	2	2.21
Plekha7	pleckstrin homology domain containing, family A	2	2.18
Ebna1bp2	EBNA1 binding protein 2	2	2.10
Rbm19	RNA binding motif protein 19	2	2.09
Arv1	ARV1 homolog	2	2.07
Ganab	alpha glucosidase 2 alpha neutral subunit	2	2.07
Sec14l2	SEC14-like 2	2	2.07
Tmem16a	transmembrane protein 16A	2	2.06
Efcab1	EF hand calcium binding domain 1	2	2.04

Gene Symbol	Gene Name	# TCF binding sites	Fold Change
Sbno1	sno, strawberry notch homolog 1	2	2.03
Unc45a	smooth muscle cell associated protein-1	2	2.02
Cd302	CD302 antigen	2	1.98
Smc5	structural maintenance of chromosomes 5	2	1.97
Rpl38	ribosomal protein L38	2	1.95
Ppan	peter pan homolog	2	1.91
Wdr74	WD repeat domain 74	2	1.83
Tbrg4	transforming growth factor beta regulated gene	2	1.78
Serpine2	serine (or cysteine) proteinase inhibitor, clade	1	25.13
Ms4a5	membrane-spanning 4-domains, subfamily A	1	22.47
Fancd2	Fanconi anemia, complementation group D2	1	8.11
Zmat3	wild-type p53-induced gene 1	1	7.36
Gemin5	gem (nuclear organelle) associated protein 5	1	6.01
Pacsin1	protein kinase C and casein kinase substrate in	1	4.15
D130029J02Rik	hypothetical protein LOC234695	1	3.79
Cyb5r1	cytochrome b5 reductase 1	1	3.48
Cpt1c	carnitine palmitoyltransferase 1c	1	3.47
Brp16	brain protein 16	1	3.20
Echdc2	enoyl Coenzyme A hydratase domain containing 2	1	2.72
Mybbp1a	MYB binding protein (P160) 1a	1	2.55
Qprt	quinolinate phosphoribosyltransferase	1	2.49
Plxna1	plexin A1	1	2.34
Klf1	Kruppel-like factor 1 (erythroid)	1	2.30
Klf10	Kruppel-like factor 10	1	2.26
Ascc3l1	U5 snRNP-specific protein, 200 kDa	1	2.21

Myl6b	myosin, light polypeptide 6B	1	2.21
Bax	Bcl2-associated X protein	1	2.20
Sgsh	N-sulfoglucosamine sulfohydrolase (sulfamidase)	1	2.19
Rcl1	RNA terminal phosphate cyclase-like 1	1	2.07
Heatr1	BAP28 protein	1	2.04
Adcyap1r1	adenylate cyclase activating polypeptide 1	1	1.96
Fbxo42	F-box protein 42	1	1.92
Stbd1	starch binding domain 1	1	1.88

Genes are sorted first by # TCF binding sites then by fold change

Appendix G. Downregulated genes with conserved TCF site

Gene Symbol	Gene Name	# TCF binding sites	Fold Change
Hist1h4b	histone cluster 1, H4b	14	-4.55
Hist1h3b	histone cluster 1, H3b	14	-4.03
Nsdhl	NAD(P) dependent steroid dehydrogenase-like	14	-2.28
Hist1h2bb	histone cluster 1, H2bb	13	-2.59
Bcl2a1c	B-cell leukemia/lymphoma 2 related protein A1c	12	-7.20
Hs3st1	heparan sulfate (glucosamine)	12	-6.81
Cd68	CD68 antigen	12	-4.00
Snca	synuclein, alpha	12	-2.81
Stmn2	stathmin-like 2	12	-2.50
Hist1h2bm	histone cluster 1, H2bm	12	-2.23
Hist1h3c	histone cluster 1, H3c	11	-7.36
Lypd6	LY6/PLAUR domain containing 6	11	-3.75
Bcl2a1d	B-cell leukemia/lymphoma 2 related protein A1d	11	-3.30
Snap25	synaptosomal-associated protein 25	11	-3.25
Tcp11l2	t-complex 11 (mouse) like 2	11	-2.92
Bcl2a1b	B-cell leukemia/lymphoma 2 related protein A1b	11	-2.45
Hist1h2bf	histone cluster 1, H2bf	11	-2.36
Slc25a27	solute carrier family 25, member 27	11	-2.28
Pftk1	PFTAIRE protein kinase 1	11	-2.14
Isl1	ISL1 transcription factor, LIM/homeodomain	10	-3.40
Hbp1	high mobility group box transcription factor 1	10	-3.13
Itm2a	integral membrane protein 2A	10	-2.81
Myt1	myelin transcription factor 1	10	-2.79

Gene Symbol	Gene Name	# TCF binding sites	Fold Change
Hist1h4c	histone cluster 1, H4c	10	-2.49
Fbxl10	F-box and leucine-rich repeat protein 10 isoform	10	-2.46
Hist1h2bh	histone cluster 1, H2bh	10	-2.19
Idi1	isopentenyl-diphosphate delta isomerase isoform	10	-1.83
Prickle1	prickle like 1	9	-6.10
Elavl4	ELAV-like 4 isoform a	9	-3.24
Ccng2	cyclin G2	9	-2.68
Elmo1	engulfment and cell motility 1 isoform 1	9	-2.60
Hist1h1c	histone cluster 1, H1c	9	-2.50
Mbd2	methyl-CpG binding domain protein 2	9	-2.22
Hist1h2bl	histone cluster 1, H2bl	9	-2.17
B230399E16Rik	hypothetical protein LOC240479	9	-2.11
Prdm1	PR domain containing 1, with ZNF domain	9	-2.11
Nipsnap3a	nipsnap homolog 3A	9	-2.08
Hist1h4d	histone cluster 1, H4d	9	-2.04
Ypel5	yippee protein homolog	9	-2.03
Entpd5	ectonucleoside triphosphate diphosphohydrolase 5	9	-1.98
Dusp4	dual specificity phosphatase 4	9	-1.79
Rab9b	RAB9B, member RAS oncogene family	8	-6.87
Cdo1	cysteine dioxygenase 1, cytosolic	8	-5.17
Zfp521	zinc finger protein 521 isoform 1	8	-4.62
Adcyap1	adenylate cyclase activating polypeptide 1	8	-3.26
Hist1h4i	histone cluster 1, H4i	8	-2.66
Cp	ceruloplasmin isoform b	8	-2.64
Prkar2b	protein kinase, cAMP dependent regulatory, type	8	-2.62

Gene Symbol	Gene Name	# TCF binding sites	Fold Change
Ppap2b	phosphatidic acid phosphatase type 2B	8	-2.40
Ccdc28b	coiled coil domain containing 28B	8	-2.25
Serinc5	serine incorporator 5	8	-2.23
Meis2	homeobox protein Meis2	8	-2.22
Gng2	guanine nucleotide binding protein (G protein),	8	-2.21
P2ry5	purinergic receptor P2Y, G-protein coupled, 5	8	-2.13
Syt1	synaptotagmin I	8	-2.13
5730403M16Rik	hypothetical protein LOC232853	8	-2.09
Spon1	spondin 1, (f-spondin) extracellular matrix	8	-2.06
Bbs2	Bardet-Biedl syndrome 2 homolog	8	-2.03
Mxd1	MAX dimerization protein 1	8	-2.02
Khdrbs2	KH domain-containing, RNA-binding, signal	8	-1.96
Spg3a	atlastin	8	-1.96
Sri	sorcin isoform 2	8	-1.81
Gsbs	G substrate	7	-4.25
Klhl1	kelch-like 1	7	-3.39
Zfp524	zinc finger protein 524	7	-3.12
Kctd8	potassium channel tetramerisation domain	7	-3.10
1700027N10Rik	hypothetical protein LOC75564	7	-2.78
Sncg	synuclein, gamma	7	-2.71
Hist1h2bj	histone cluster 1, H2bj	7	-2.51
Csad	cysteine sulfinic acid decarboxylase	7	-2.50
Tcea2	transcription elongation factor A protein 2	7	-2.41
Wipi1	WD repeat domain, phosphoinositide interacting	7	-2.30
Ap1s2	adaptor-related protein complex 1 sigma 2	7	-2.24

Gene Symbol	Gene Name	# TCF binding sites	Fold Change
Tmeff2	transmembrane protein with EGF-like and two	7	-2.19
Nfatc4	cytoplasmic nuclear factor of activated T-cells	7	-2.18
Pex3	peroxisomal biogenesis factor 3	7	-2.07
Bnip3l	BCL2/adenovirus E1B interacting protein 3-like	7	-2.03
Marcks	myristoylated alanine rich protein kinase C	7	-2.03
Frat2	frequently rearranged in advanced T-cell	7	-2.00
4930504E06Rik	hypothetical protein LOC75007	7	-1.99
Fabp5	fatty acid binding protein 5, epidermal	7	-1.96
Mpeg1	macrophage expressed gene 1	6	-12.57
Syt13	synaptotagmin XIII	6	-11.02
Ccl5	chemokine (C-C motif) ligand 5	6	-10.40
Insc	inscuteable	6	-9.27
Mstn	myostatin	6	-5.64
Rgs10	regulator of G-protein signalling 10	6	-5.30
Ache	acetylcholinesterase	6	-4.46
Ly6h	lymphocyte antigen 6 complex, locus H	6	-3.86
Ifitm3	interferon induced transmembrane protein 3	6	-3.71
Rgs4	regulator of G-protein signaling 4	6	-3.36
Ptf1a	pancreas specific transcription factor, 1a	6	-3.17
Hist1h4h	histone cluster 1, H4h	6	-2.93
Thsd7b	thrombospondin, type I, domain containing 7B	6	-2.83
Nsg2	neuron specific gene family member 2	6	-2.82
Hist1h2ba	histone cluster 1, H2ba	6	-2.73
Hist1h4f	histone cluster 1, H4f	6	-2.65
Slc10a4	solute carrier family 10 (sodium/bile acid	6	-2.63

Gene Symbol	Gene Name	# TCF binding sites	Fold Change
Ppm1b	protein phosphatase 1B, magnesium dependent,	6	-2.62
Galnt13	UDP-N-acetyl-alpha-D-galactosamine:polypeptide	6	-2.48
Mycl1	lung carcinoma myc related oncogene 1	6	-2.38
Zfp593	zinc finger protein 593	6	-2.32
Mtap2	microtubule-associated protein 2 isoform 2	6	-2.26
Crabp1	cellular retinoic acid binding protein I	6	-2.18
Etv1	ets variant gene 1	6	-2.18
Hist3h2ba	histone cluster 3, H2ba	6	-2.11
A630054L15Rik	hypothetical protein LOC211922	6	-2.08
Pex7	peroxisome biogenesis factor 7	6	-2.07
Rbpms	RNA binding protein gene with multiple splicing	6	-1.86
Slc25a11	solute carrier family 25 (mitochondrial carrier	6	-1.85
Nedd9	neural precursor cell expressed, developmentally	6	-1.84
Dennd1a	DENN/MADD domain containing 1A	6	-1.83
Nin	ninein isoform 2	6	-1.80
Suv420h2	suppressor of variegation 4-20 homolog 2	6	-1.79
Kit	c-kit	5	-11.33
6330514A18Rik	hypothetical protein LOC216166	5	-8.90
Hist1h3i	histone cluster 1, H3i	5	-6.95
AI851790	TAFA2 protein	5	-6.18
C1ql3	C1q-like 3	5	-5.41
Hspb2	heat shock protein 2	5	-4.93
Ccl4	chemokine (C-C motif) ligand 4	5	-4.74
Sept4	septin 4	5	-4.21
Hist1h2aa	histone cluster 1, H2aa	5	-4.07

Gene Symbol	Gene Name	# TCF binding sites	Fold Change
Usp18	ubiquitin specific peptidase 18	5	-4.06
Isl2	insulin related protein 2 (islet 2)	5	-3.94
Isg15	ISG15 ubiquitin-like modifier	5	-3.84
Ccdc80	steroid-sensitive protein 1	5	-3.56
Slc17a6	solute carrier family 17 (sodium-dependent	5	-3.43
Gng3	guanine nucleotide binding protein (G protein),	5	-3.41
Irf9	interferon regulatory factor 9	5	-3.37
Syt4	synaptotagmin 4	5	-3.30
Calb2	calbindin 2	5	-3.25
Jazf1	expressed sequence AI591476	5	-3.10
Mpnd	MPN domain containing	5	-3.08
Scn3b	voltage-gated sodium channel beta-3 subunit	5	-2.98
Col9a2	collagen, type IX, alpha 2	5	-2.96
Hist1h4m	histone cluster 1, H4m	5	-2.94
Gap43	growth associated protein 43	5	-2.85
S100a4	S100 calcium binding protein A4	5	-2.79
Hist1h2bp	histone cluster 1, H2bp	5	-2.75
Abtb1	ankyrin repeat and BTB (POZ) domain containing	5	-2.58
Impg2	interphotoreceptor matrix proteoglycan 2	5	-2.57
Cd200	Cd200 antigen	5	-2.56
Pde1b	phosphodiesterase 1B, Ca2+-calmodulin dependent	5	-2.50
Hist1h2bk	histone cluster 1, H2bk	5	-2.45
Adck5	aarF domain containing kinase 5	5	-2.40
Dcx	doublecortin isoform c	5	-2.38
Hes6	hairy and enhancer of split 6	5	-2.38

Gene Symbol	Gene Name	# TCF binding sites	Fold Change
Irx6	Iroquois related homeobox 6	5	-2.35
Slc16a3	solute carrier family 16, member 3	5	-2.35
9430010O03Rik	hypothetical protein LOC234023	5	-2.32
Zfp68	zinc finger protein 68 isoform a	5	-2.32
Tk1	thymidine kinase 1	5	-2.27
Dnajc12	DnaJ (Hsp40) homolog, subfamily C, member 12	5	-2.26
Nrm	nurim	5	-2.26
4930488E11Rik	hypothetical protein LOC399591	5	-2.16
Chm	choroidermia	5	-2.13
Fibp	FGF intracellular binding protein	5	-2.11
1110028C15Rik	hypothetical protein LOC68691	5	-2.09
Zfp51	zinc finger protein 51	5	-2.01
Amdhd2	amidohydrolase domain containing 2	5	-1.96
Cntrob	centrobin, centrosomal BRCA2 interacting	5	-1.95
Glcci1	glucocorticoid induced transcript 1 isoform 1	5	-1.93
Cetn3	centrin 3	5	-1.91
Litaf	LPS-induced TN factor	5	-1.90
Rdbp	RD RNA-binding protein	5	-1.89
Dpysl2	dihydropyrimidinase-like 2	5	-1.87
Kcne1l	potassium voltage-gated channel, Isk-related	5	-1.82
Ing4	inhibitor of growth family, member 4	5	-1.76
Hist1h3a	histone cluster 1, H3a	4	-19.93
Ldb2	LIM domain binding 2 isoform 1	4	-13.88
Lrp2bp	LRP2 binding protein	4	-12.44
Athl1	ATH1, acid trehalase-like 1	4	-8.43

Gene Symbol	Gene Name	# TCF binding sites	Fold Change
Fcer1g	Fc receptor, IgE, high affinity I, gamma	4	-5.85
Ctss	cathepsin S preproprotein	4	-4.58
5133400G04Rik	TATA-binding protein-like factor-interacting	4	-4.21
Tusc1	tumor suppressor candidate 1	4	-3.98
2010011I20Rik	hypothetical protein LOC67017	4	-3.85
Espn	espin isoform 1	4	-3.77
Id2	inhibitor of DNA binding 2	4	-3.62
Neurod4	neurogenic differentiation 4	4	-3.55
Selenbp1	selenium binding protein 1	4	-3.50
Tm7sf2	transmembrane 7 superfamily member 2	4	-3.34
H2-Ke6	estradiol 17 beta-dehydrogenase 8	4	-3.00
Flywch2	FLYWCH family member 2	4	-2.98
Insig1	insulin induced gene 1	4	-2.89
Igsf11	immunoglobulin superfamily, member 11	4	-2.88
D030011O10Rik	hypothetical protein LOC320560	4	-2.85
Ndrg2	N-myc downstream regulated gene 2	4	-2.84
Acss2	acyl-CoA synthetase short-chain family member 2	4	-2.81
Ascl1	achaete-scute complex homolog-like 1	4	-2.74
Nrp1	neuropilin 1	4	-2.70
Tcf19	transcription factor 19	4	-2.66
Rassf4	Ras association (RalGDS/AF-6) domain family 4	4	-2.59
Sc4mol	sterol-C4-methyl oxidase-like	4	-2.54
Aacs	acetoacetyl-CoA synthetase	4	-2.53
Hpgd	hydroxyprostaglandin dehydrogenase 15 (NAD)	4	-2.52
Darc	Duffy blood group	4	-2.45

Gene Symbol	Gene Name	# TCF binding sites	Fold Change
Ift20	intraflagellar transport protein IFT20	4	-2.45
Ndrg1	N-myc downstream regulated gene 1	4	-2.42
Fndc4	fibronectin type III domain containing 4	4	-2.40
Ube2l6	ubiquitin-conjugating enzyme E2L 6	4	-2.38
Hist1h4k	histone cluster 1, H4k	4	-2.32
Snn	stannin	4	-2.32
Nxph4	neurexophilin 4	4	-2.27
Abca4	ATP-binding cassette, sub-family A, member 4	4	-2.24
Rac3	RAS-related C3 botulinum substrate 3	4	-2.23
Neil3	putative DNA glycosylase	4	-2.21
Nxnl2	nucleoredoxin	4	-2.21
Loxl2	lysyl oxidase-like 2	4	-2.19
Hist1h2bn	histone cluster 1, H2bn	4	-2.14
Ier5l	immediate early response 5-like	4	-2.11
Tmepai	transmembrane prostate androgen-induced protein	4	-2.08
Stx4a	syntaxin 4A (placental)	4	-2.07
Aqp1	aquaporin 1	4	-2.05
Hist1h4a	histone cluster 1, H4a	4	-2.05
Slc18a2	solute carrier family 18 (vesicular monoamine),	4	-2.04
Slc1a3	solute carrier family 1 (glial high affinity	4	-2.04
Serf1	small EDRK-rich factor 1	4	-2.02
Mvd	mevalonate (diphospho) decarboxylase	4	-1.98
Tyrp1	tyrosinase-related protein 1	4	-1.93
Auh	AU RNA-binding enoyl-coenzyme A hydratase	4	-1.91
Nt5c	5',3'-nucleotidase, cytosolic	4	-1.89

Gene Symbol	Gene Name	# TCF binding sites	Fold Change
Phf1	PHD finger protein 1	4	-1.89
Galntl4	UDP-N-acetyl-alpha-D-galactosamine:polypeptide	4	-1.86
Cirbp	cold inducible RNA binding protein	3	-18.51
Msr2	macrophage scavenger receptor 2	3	-17.13
Aif1	allograft inflammatory factor 1	3	-9.20
Laptm5	lysosomal-associated protein transmembrane 5	3	-7.44
Scd1	stearoyl-Coenzyme A desaturase 1	3	-6.61
Id4	inhibitor of DNA binding 4	3	-5.68
Lpin1	lipin 1 isoform b	3	-5.20
Hspb3	heat shock protein 3	3	-4.46
Ass1	argininosuccinate synthetase	3	-4.42
Rnaseh2c	AYP1 protein	3	-3.62
Pcyt1b	phosphate cytidylyltransferase 1, choline, beta	3	-3.54
C1qc	complement component 1, q subcomponent, gamma	3	-3.43
Gngt2	guanine nucleotide binding protein (G protein),	3	-3.21
2410066E13Rik	hypothetical protein LOC68235	3	-3.16
3110035E14Rik	hypothetical protein LOC76982	3	-3.13
Fdps	farnesyl diphosphate synthetase	3	-3.11
Pou4f3	POU domain, class 4, transcription factor 3	3	-3.02
Ung	uracil DNA glycosylase isoform b	3	-2.86
AI836003	hypothetical protein LOC239650	3	-2.73
Ypel1	yippee-like 1	3	-2.70
Rims2	regulating synaptic membrane exocytosis 2	3	-2.62

Gene Symbol	Gene Name	# TCF binding sites	Fold Change
2600010E01Rik	hypothetical protein LOC72446	3	-2.61
Wdr45	WD repeat domain 45	3	-2.58
Trp53inp2	transformation related protein 53 inducible	3	-2.57
Doc2b	double C2, beta	3	-2.43
Actl6b	actin-like 6B	3	-2.39
Dusp6	dual specificity phosphatase 6	3	-2.39
E430018J23Rik	hypothetical protein LOC101604	3	-2.34
Sh3md4	SH3 multiple domains 4	3	-2.29
Xpa	xeroderma pigmentosum, complementation group A	3	-2.28
Pold4	small subunit DNA polymerase delta p12	3	-2.27
Dnase2b	deoxyribonuclease II beta	3	-2.24
Schip1	schwannomin interacting protein 1	3	-2.21
Serpini1	serine (or cysteine) proteinase inhibitor, clade	3	-2.20
0610037D15Rik	hypothetical protein LOC68394	3	-2.18
Vash2	vasohibin 2	3	-2.18
Idh1	isocitrate dehydrogenase 1 (NADP+), soluble	3	-2.16
BC043118	hypothetical protein LOC224273	3	-2.14
Dut	deoxyuridine triphosphatase	3	-2.13
Wscd1	WSC domain containing 1	3	-2.12
Ctdsp1	CTD (carboxy-terminal domain, RNA polymerase II,	3	-2.10
Tagln3	transgelin 3	3	-2.01
Npdc1	neural proliferation, differentiation and	3	-1.99
Plagl1	pleiomorphic adenoma gene-like 1	3	-1.99
Tax1bp3	Tax1 (human T-cell leukemia virus type I)	3	-1.99

Gene Symbol	Gene Name	# TCF binding sites	Fold Change
Araf	v-raf murine sarcoma 3611 viral oncogene	3	-1.98
Csrp2	cysteine and glycine-rich protein 2	3	-1.96
Pafah1b3	platelet-activating factor acetylhydrolase,	3	-1.96
1810014F10Rik	hypothetical protein LOC69064	3	-1.93
Dll3	delta-like 3	3	-1.92
Cox4i2	cytochrome c oxidase subunit IV isoform 2	3	-1.88
D10Jhu81e	es1 protein	3	-1.88
Pmp22	peripheral myelin protein	3	-1.88
Stmn3	stathmin-like 3	3	-1.88
Apc2	adenomatosis polyposis coli 2	3	-1.87
Mcf2l	mcf.2 transforming sequence-like	3	-1.87
Cd52	CD52 antigen	2	-86.13
Sst	somatostatin	2	-11.12
Dnaic1	dynein, axonemal, intermediate chain 1	2	-9.57
Ccl3	chemokine (C-C motif) ligand 3	2	-8.51
Haghl	hydroxyacylglutathione hydrolase-like	2	-5.85
Mxd3	Max dimerization protein 3	2	-5.77
Dio3	deiodinase, iodothyronine type III	2	-5.08
Cdkn2c	cyclin-dependent kinase inhibitor 2C	2	-4.58
Gp1bb	glycoprotein Ib, beta polypeptide isoform 1	2	-4.37
Hacl1	2-hydroxyacyl-CoA lyase 1	2	-4.33
Fabp7	fatty acid binding protein 7, brain	2	-3.88
Fbxl15	F-box and leucine-rich repeat protein 15	2	-3.69
Sms	spermine synthase	2	-3.59
Bdh1	3-hydroxybutyrate dehydrogenase, type 1	2	-3.52

Gene Symbol	Gene Name	# TCF binding sites	Fold Change
Ppp1r14a	protein phosphatase 1, regulatory (inhibitor)	2	-3.47
Col9a3	procollagen, type IX, alpha 3	2	-3.09
Heyl	hairy/enhancer-of-split related with YRPW	2	-3.05
6330403K07Rik	hypothetical protein LOC103712	2	-2.95
Tmem132e	transmembrane protein 132E	2	-2.94
Nrl	neural retina leucine zipper protein	2	-2.83
Bcl2l2	Bcl2-like 2	2	-2.81
2810408A11Rik	hypothetical protein LOC70419	2	-2.78
Nell2	nel-like 2 homolog	2	-2.72
Id3	inhibitor of DNA binding 3	2	-2.70
Klc3	kinesin light chain 3	2	-2.58
Tcp11	t-complex protein 11 isoform 1	2	-2.58
Vstm2l	V-set and transmembrane domain containing	2	-2.44
Crx	cone-rod homeobox containing	2	-2.43
Irx2	Iroquois related homeobox 2	2	-2.41
Rusc1	RUN and SH3 domain containing 1 isoform 2	2	-2.38
Lrrc4	leucine rich repeat containing 4	2	-2.32
Brwd1	bromodomain and WD repeat domain containing 1	2	-2.28
Tinf2	TRF1-interacting nuclear factor 2	2	-2.28
1500005A01Rik	hypothetical protein LOC85308	2	-2.27
Ensa	endosulfine alpha isoform a	2	-2.23
Osbpl1a	oxysterol binding protein-like 1	2	-2.23
Srr	serine racemase	2	-2.17
A930025D01Rik	hypothetical protein LOC319513	2	-2.15
Pink1	PTEN induced putative kinase 1	2	-2.14

Gene Symbol	Gene Name	# TCF binding sites	Fold Change
Pnck	pregnancy upregulated non-ubiquitously expressed	2	-2.13
Nupr1	p8 protein	2	-2.11
Tiam1	T-cell lymphoma invasion and metastasis 1	2	-2.08
Tnrc4	CUG-BP and ETR-3 like factor 3	2	-2.06
Tbc1d10a	TBC1 domain family, member 10a	2	-2.03
6430598A04Rik	RIKEN cDNA 6430598A04 gene	2	-2.00
Klhl13	kelch-like 13	2	-2.00
Atp1b1	Na+/K+ -ATPase beta 1 subunit	2	-1.99
Dbp	D site albumin promoter binding protein	2	-1.96
Dok4	docking protein 4	2	-1.96
Pgk1	phosphoglycerate kinase 1	2	-1.96
Trafd1	TRAF type zinc finger domain containing 1	2	-1.91
Tyrobp	TYRO protein tyrosine kinase binding protein	1	-5.04
Lyzs	lysozyme	1	-3.64
Sox8	SRY-box containing gene 8	1	-3.48
Tmco6	transmembrane and coiled-coil domains 6	1	-3.12
Jup	junction plakoglobin	1	-3.09
Shd	src homology 2 domain-containing transforming	1	-3.02
Nmnat2	nicotinamide nucleotide adenylyltransferase 2	1	-2.93
Sct	secretin	1	-2.81
Akap7	A-kinase anchor protein 7	1	-2.71
Chrna3	cholinergic receptor, nicotinic, alpha	1	-2.49
Cadps	Ca<2+>dependent activator protein for secretion	1	-2.45
Ptgds	prostaglandin H2 D-isomerase	1	-2.44
Tmem106c	hypothetical protein LOC380967	1	-2.27

Gene Symbol	Gene Name	# TCF binding sites	Fold Change
Gli1	GLI-Kruppel family member GLI1	1	-2.25
Acsf3	acyl-CoA synthetase family member 3	1	-2.24
Fbxo27	F-box only protein 27	1	-2.22
Gnb3	guanine nucleotide-binding protein, beta-3	1	-2.19
Ppp1r13b	apoptosis-stimulating protein of p53, 1	1	-2.14
1110003E01Rik	hypothetical protein LOC68552	1	-2.13
Stau2	staufen (RNA binding protein) homolog 2	1	-2.12
Cbx6	chromobox homolog 6	1	-2.08
Zrsr1	U2 small nuclear ribonucleoprotein auxiliary	1	-2.07
Rph3a	rabphilin 3A	1	-2.04
Llgl1	lethal giant larvae homolog	1	-2.03
Lims1	LIM and senescent cell antigen-like domains 1	1	-1.99
Ypel3	yippee-like 3	1	-1.97
Tcta	T-cell leukemia translocation altered	1	-1.96
Ddx54	DEAD (Asp-Glu-Ala-Asp) box polypeptide 54	1	-1.75

Genes are sorted first by # TCF binding sites then by fold change

Appendix H. Upregulated genes with conserved TCF sites with conservation score >0.7

Gene Symbol	Gene Name	# TCF binding sites	Fold Change
Otx1	orthodenticle 1	7	1.82
Heatr3	HEAT repeat containing 3	6	1.95
Hoxa3	homeobox A3	5	5
Orc1l	origin recognition complex, subunit 1 isoform A	5	2.71
Axin2	axin2	4	2.81
Lix1	limb expression 1	4	2.54
Eif4a2	eukaryotic translation initiation factor 4A2	3	13.64
Slc16a6	solute carrier family 16, member 6 isoform a	3	3.88
Dnajb4	DnaJ (Hsp40) homolog, subfamily B, member 4	3	2.7
Msx1	homeo box, msh-like 1	3	2.34
Commd3	COMM domain containing 3	3	2.16
Med12	mediator of RNA polymerase II transcription,	3	1.99
Tnfrsf19	tumor necrosis factor receptor superfamily,	2	20.85
Dok1	docking protein 1	2	3.48
Aurka	serine/threonine protein kinase 6	2	3.14
Zwilch	Zwilch	2	3.13
Pappa2	pappalysin 2	2	2.93
Usp2	ubiquitin-specific protease 2 isoform Usp2-69	2	2.88
Hnrpdl	heterogeneous nuclear ribonucleoprotein D-like	2	2.86
H2-T22	histocompatibility 2, T region locus 22	2	2.66
Ddx19b	DDX19 homolog	2	2.55
Man2b1	mannosidase 2, alpha B1	2	2.42
Hoxd9	homeo box D9	2	2.4

Gene Symbol	Gene Name	# TCF binding sites	Fold Change
Zfp365	zinc finger protein 365	2	2.36
Ptk7	PTK7 protein tyrosine kinase 7	2	2.3
Cad	carbamoyl-phosphate synthetase 2, aspartate	2	2.24
Celsr2	cadherin EGF LAG seven-pass G-type receptor 2	2	2.24
Tef	thyrotroph embryonic factor isoform 1	2	2.11
Wif1	Wnt inhibitory factor 1	1	29.22
Serpine2	serine (or cysteine) proteinase inhibitor, clade	1	25.12
Lrrc14	leucine rich repeat containing 14	1	19.85
Phlda3	pleckstrin homology-like domain, family A,	1	16.42
Cnn2	calponin 2	1	8.94
Epha2	Eph receptor A2	1	8.36
Tnfrsf10b	tumor necrosis factor receptor superfamily,	1	8.16
Cyr61	cysteine rich protein 61	1	7.61
Plk2	polo-like kinase 2	1	7.12
Npy	neuropeptide Y	1	6.99
Nupl2	nucleoporin like 2	1	6.71
Olfr247	olfactory receptor 247	1	5.66
Raet1a	retinoic acid early transcript 1, alpha	1	5.23
Elmo1	engulfment and cell motility 1 isoform 1	1	4.63
Fyn	protein-tyrosine kinase fyn	1	4.26
Ptp4a3	protein tyrosine phosphatase 4a3	1	4.11
Ogn	osteoglycin	1	3.92
Rap2b	RAP2B, member of RAS oncogene family	1	3.85
Lpp	LIM domain containing preferred translocation	1	3.73
Cpt1c	carnitine palmitoyltransferase 1c	1	3.47

Gene Symbol	Gene Name	# TCF binding sites	Fold Change
Tac2	tachykinin 2	1	3.46
Trp53inp1	transformation related protein 53 inducible	1	3.45
Klf10	Kruppel-like factor 10	1	3.43
Ung	uracil DNA glycosylase isoform b	1	3.38
Ehd4	EH-domain containing 4	1	3.33
Creb3l1	cAMP responsive element binding protein 3-like	1	3.31
Tcf7	transcription factor 7, T-cell specific	1	3.22
Dph2	diptheria toxin resistance protein required for	1	3.1
Gcg	glucagon	1	3.08
Sesn2	sestrin 2	1	2.99
Vcl	vinculin	1	2.98
Tubb6	tubulin, beta 6	1	2.95
P2ry2	purinergic receptor P2Y, G-protein coupled 2	1	2.93
Rsc1a1	regulatory solute carrier protein, family 1,	1	2.91
Mlf1	myeloid leukemia factor 1 isoform a	1	2.82
Mfap3l	microfibrillar-associated protein 3-like	1	2.79
Rrp12	ribosomal RNA processing 12 homolog	1	2.73
Clybl	citrate lyase beta like	1	2.63
Prr11	proline rich 11	1	2.58
Slc44a2	solute carrier family 44, member 2	1	2.47
Galns	galactosamine (N-acetyl)-6-sulfate sulfatase	1	2.42
Pdgfa	platelet derived growth factor, alpha	1	2.4
Tmem43	transmembrane protein 43	1	2.39
Luc7l	Luc7 homolog (S. cerevisiae)-like isoform 2	1	2.34
Plxna1	plexin A1	1	2.34

Gene Symbol	Gene Name	# TCF binding sites	Fold Change
Cox6b2	cytochrome c oxidase subunit VIb polypeptide 2	1	2.33
Recql	RecQ protein-like	1	2.32
Polr2a	polymerase (RNA) II (DNA directed) polypeptide	1	2.31
Ifi30	interferon gamma inducible protein 30	1	2.28
Traf4	Tnf receptor associated factor 4	1	2.27
Exoc6	exocyst complex component 6	1	2.23
Pycrl	pyrroline-5-carboxylate reductase-like	1	2.22
Slc7a3	solute carrier family 7 (cationic amino acid	1	2.17
Pdlim4	PDZ and LIM domain 4	1	2.16
Ube2c	ubiquitin-conjugating enzyme E2C	1	2.13
Lrp4	low density lipoprotein receptor-related protein	1	2.12
Col18a1	procollagen, type XVIII, alpha 1 isoform 2	1	2.07
Mettl1	methyltransferase-like 1	1	2.06
Gpc6	glypican 6 isoform 2	1	2.04
Tcerg1	transcription elongation regulator 1 (CA150)	1	2.04
Col6a1	collagen, type VI, alpha 1	1	1.98
Rap2a	RAP2A, member of RAS oncogene family	1	1.91
Gspt2	G1 to phase transition 2	1	1.9
Pkn3	protein kinase N3	1	1.89
Tmem67	transmembrane protein 67	1	1.88
Tsc22d3	glucocorticoid-induced leucine zipper isoform 2	1	1.88
Slc7a7	solute carrier family 7 (cationic amino acid	1	1.87
Btg3	B-cell translocation gene 3	1	1.86
Cdc25b	cell division cycle 25 homolog B	1	1.86
Sco1	SCO cytochrome oxidase deficient homolog 1	1	1.86

Gene Symbol	Gene Name	# TCF binding sites	Fold Change
Atf5	ativating transcription factor 5	1	1.85
Lenep	lens epithelial protein	1	1.84
Qrsl1	glutaminyl-tRNA synthase	1	1.82
Efna3	ephrin A3	1	1.71

Genes are sorted first by # TCF binding sites then by fold change

Appendix I. Downregulated genes with conserved TCF sites with conservation score >0.7

Gene Symbol	Gene Name	# TCF binding sites	Fold Change
Prdm1	PR domain containing 1, with ZNF domain	7	-2.11
Marcks	myristoylated alanine rich protein kinase C	6	-2.03
Cntf	ciliary neurotrophic factor	6	-1.71
Cd68	CD68 antigen	5	-4
Meis2	homeobox protein Meis2	5	-2.22
Elavl4	ELAV-like 4 isoform a	4	-3.24
S100a4	S100 calcium binding protein A4	4	-2.79
Ap1s2	adaptor-related protein complex 1 sigma 2	4	-2.24
Hist1h3i	histone cluster 1, H3i	3	-6.95
Zfp521	zinc finger protein 521 isoform 1	3	-4.62
Hist1h3b	histone cluster 1, H3b	3	-4.04
Lypd6	LY6/PLAUR domain containing 6	3	-3.75
Ccdc80	steroid-sensitive protein 1	3	-3.56
Irf9	interferon regulatory factor 9	3	-3.37
Hist1h4m	histone cluster 1, H4m	3	-2.94
Hist1h2bp	histone cluster 1, H2bp	3	-2.75
Sncg	synuclein, gamma	3	-2.71
Stmn2	stathmin-like 2	3	-2.5
Rac3	RAS-related C3 botulinum substrate 3	3	-2.23
Tmeff2	transmembrane protein with EGF-like and two	3	-2.19
Etv1	ets variant gene 1	3	-2.18
Nfatc4	cytoplasmic nuclear factor of activated T-cells	3	-2.18
Syt1	synaptotagmin I	3	-2.13

Gene Symbol	Gene Name	# TCF binding sites	Fold Change
Frat2	frequently rearranged in advanced T-cell	3	-2
Rdbp	RD RNA-binding protein	3	-1.89
Nedd9	neural precursor cell expressed, developmentally	3	-1.84
Ing4	inhibitor of growth family, member 4	3	-1.76
Laptm5	lysosomal-associated protein transmembrane 5	2	-7.44
Hist1h4b	histone cluster 1, H4b	2	-4.55
Gsbs	G substrate	2	-4.25
Usp18	ubiquitin specific peptidase 18	2	-4.06
Isg15	ISG15 ubiquitin-like modifier	2	-3.84
Id2	inhibitor of DNA binding 2	2	-3.62
Bdh1	3-hydroxybutyrate dehydrogenase, type 1	2	-3.52
Adcyap1	adenylate cyclase activating polypeptide 1	2	-3.26
Snap25	synaptosomal-associated protein 25	2	-3.25
Ptf1a	pancreas specific transcription factor, 1a	2	-3.17
Hbp1	high mobility group box transcription factor 1	2	-3.13
Zfp524	zinc finger protein 524	2	-3.12
Calb2	calbindin 2	2	-2.9
Ndrg2	N-myc downstream regulated gene 2	2	-2.84
Myt1	myelin transcription factor 1	2	-2.8
Hist1h4i	histone cluster 1, H4i	2	-2.66
Tcf19	transcription factor 19	2	-2.66
Hist1h4f	histone cluster 1, H4f	2	-2.65
Abtb1	ankyrin repeat and BTB (POZ) domain containing	2	-2.58
Hist1h2bj	histone cluster 1, H2bj	2	-2.51
St18	suppression of tumorigenicity 18	2	-2.45

Gene Symbol	Gene Name	# TCF binding sites	Fold Change
Ppap2b	phosphatidic acid phosphatase type 2B	2	-2.4
Dcx	doublecortin isoform c	2	-2.38
Mycl1	lung carcinoma myc related oncogene 1	2	-2.38
Hist1h2bf	histone cluster 1, H2bf	2	-2.36
Nsdhl	NAD(P) dependent steroid dehydrogenase-like	2	-2.28
Hist1h2bh	histone cluster 1, H2bh	2	-2.19
Fibp	FGF intracellular binding protein	2	-2.11
Mxd1	MAX dimerization protein 1	2	-2.02
Nt5c	5',3'-nucleotidase, cytosolic	2	-1.88
Dpysl2	dihydropyrimidinase-like 2	2	-1.87
Dennd1a	DENN/MADD domain containing 1A	2	-1.83
Idi1	isopentenyl-diphosphate delta isomerase isoform	2	-1.83
Kcne1l	potassium voltage-gated channel, Isk-related	2	-1.82
Sri	sorcin isoform 2	2	-1.81
Hist1h3a	histone cluster 1, H3a	1	-19.93
Cirbp	cold inducible RNA binding protein	1	-18.5
Ldb2	LIM domain binding 2 isoform 1	1	-13.88
Aif1	allograft inflammatory factor 1	1	-9.202
Athl1	ATH1, acid trehalase-like 1	1	-8.43
Hist1h3c	histone cluster 1, H3c	1	-7.36
Prickle1	prickle like 1	1	-6.1
Fcer1g	Fc receptor, IgE, high affinity I, gamma	1	-5.85
Mxd3	Max dimerization protein 3	1	-5.78
Mstn	myostatin	1	-5.64
Ccne2	cyclin E2 isoform 1	1	-4.46

Gene Symbol	Gene Name	# TCF binding sites	Fold Change
Hspb3	heat shock protein 3	1	-4.46
Gp1bb	glycoprotein Ib, beta polypeptide isoform 1	1	-4.37
Hist1h2aa	histone cluster 1, H2aa	1	-4.07
Isl2	insulin related protein 2 (islet 2)	1	-3.94
Fbxl15	F-box and leucine-rich repeat protein 15	1	-3.69
Pnrc1	proline-rich nuclear receptor coactivator 1	1	-3.56
Neurod4	neurogenic differentiation 4	1	-3.55
Pcyt1b	phosphate cytidylyltransferase 1, choline, beta	1	-3.54
Slc17a6	solute carrier family 17 (sodium-dependent	1	-3.42
Gng3	guanine nucleotide binding protein (G protein),	1	-3.41
Isl1	ISL1 transcription factor, LIM/homeodomain	1	-3.4
Klhl1	kelch-like 1	1	-3.39
Rgs4	regulator of G-protein signaling 4	1	-3.37
Syt4	synaptotagmin 4	1	-3.3
Col9a3	procollagen, type IX, alpha 3	1	-3.1
Pou4f3	POU domain, class 4, transcription factor 3	1	-3.02
H2-Ke6	estradiol 17 beta-dehydrogenase 8	1	-3
Scn3b	voltage-gated sodium channel beta-3 subunit	1	-2.98
Hist1h4h	histone cluster 1, H4h	1	-2.93
Ung	uracil DNA glycosylase isoform b	1	-2.86
Thsd7b	thrombospondin, type I, domain containing 7B	1	-2.83
Itm2a	integral membrane protein 2A	1	-2.81
Ascl1	achaete-scute complex homolog-like 1	1	-2.74
Hist1h2ba	histone cluster 1, H2ba	1	-2.73
Id3	inhibitor of DNA binding 3	1	-2.7

Gene Symbol	Gene Name	# TCF binding sites	Fold Change
Ypel1	yippee-like 1	1	-2.7
Ccng2	cyclin G2	1	-2.68
Slc10a4	solute carrier family 10 (sodium/bile acid	1	-2.63
Prkar2b	protein kinase, cAMP dependent regulatory, type	1	-2.61
Dab1	disabled homolog 1 isoform 2	1	-2.6
Elmo1	engulfment and cell motility 1 isoform 1	1	-2.6
Hist1h2bb	histone cluster 1, H2bb	1	-2.59
Cd200	Cd200 antigen	1	-2.56
Pacsin3	protein kinase C and casein kinase substrate in	1	-2.5
Hist1h4c	histone cluster 1, H4c	1	-2.49
Pde1b	phosphodiesterase 1B, Ca2+-calmodulin dependent	1	-2.49
Vstm2l	V-set and transmembrane domain containing	1	-2.44
Irx2	Iroquois related homeobox 2	1	-2.41
Fndc4	fibronectin type III domain containing 4	1	-2.4
Hes6	hairy and enhancer of split 6	1	-2.38
Rusc1	RUN and SH3 domain containing 1 isoform 2	1	-2.38
Hist1h4k	histone cluster 1, H4k	1	-2.32
Lrrc4	leucine rich repeat containing 4	1	-2.32
Zfp593	zinc finger protein 593	1	-2.32
Zfp68	zinc finger protein 68 isoform a	1	-2.32
Pold4	small subunit DNA polymerase delta p12	1	-2.27
Mtap2	microtubule-associated protein 2 isoform 2	1	-2.26
Ccdc28b	coiled coil domain containing 28B	1	-2.25
Gng2	guanine nucleotide binding protein (G protein),	1	-2.2
Nxnl2	nucleoredoxin	1	-2.2

Gene Symbol	Gene Name	# TCF binding sites	Fold Change
Serpini1	serine (or cysteine) proteinase inhibitor, clade	1	-2.2
Crabp1	cellular retinoic acid binding protein I	1	-2.18
Loxl2	lysyl oxidase-like 2	1	-2.18
Vash2	vasohibin 2	1	-2.18
Srr	serine racemase	1	-2.17
Hist1h2bn	histone cluster 1, H2bn	1	-2.14
Pftk1	PFTAIRE protein kinase 1	1	-2.14
BC043118	hypothetical protein LOC224273	1	-2.13
Chm	choroidermia	1	-2.13
P2ry5	purinergic receptor P2Y, G-protein coupled, 5	1	-2.13
Ctdsp1	CTD (carboxy-terminal domain, RNA polymerase II,	1	-2.1
Tax1bp3	Tax1 (human T-cell leukemia virus type I)	1	-2.1
Tk1	thymidine kinase 1	1	-2.08
Tmepai	transmembrane prostate androgen-induced protein	1	-2.08
Pex3	peroxisomal biogenesis factor 3	1	-2.07
Pex7	peroxisome biogenesis factor 7	1	-2.07
Spon1	spondin 1, (f-spondin) extracellular matrix	1	-2.06
Tnrc4	CUG-BP and ETR-3 like factor 3	1	-2.06
Hist1h4a	histone cluster 1, H4a	1	-2.05
Hist1h4d	histone cluster 1, H4d	1	-2.04
Slc1a3	solute carrier family 1 (glial high affinity	1	-2.04
Bbs2	Bardet-Biedl syndrome 2 homolog	1	-2.03
Serf1	small EDRK-rich factor 1	1	-2.02
Araf	v-raf murine sarcoma 3611 viral oncogene	1	-1.98
Entpd5	ectonucleoside triphosphate diphosphohydrolase 5	1	-1.98

Gene Symbol	Gene Name	# TCF binding sites	Fold Change
Ypel3	yippee-like 3	1	-1.97
Dbp	D site albumin promoter binding protein	1	-1.96
Khdrbs2	KH domain-containing, RNA-binding, signal	1	-1.96
Glcci1	glucocorticoid induced transcript 1 isoform 1	1	-1.93
Cox4i2	cytochrome c oxidase subunit IV isoform 2	1	-1.88
Apc2	adenomatosis polyposis coli 2	1	-1.87
Rbpms	RNA binding protein gene with multiple splicing	1	-1.86
Nin	ninein isoform 2	1	-1.8
Dusp4	dual specificity phosphatase 4	1	-1.79

Genes are sorted first by # TCF binding sites then by fold change